



Technical Report

ESSA RESEARCH LABORATORIES

ERL 79-ITS 67

Prediction of Tropospheric Radio Transmission Loss Over Irregular Terrain

A Computer Method-1968

GPO PRICE \$ _____
CFSTI PRICE(S) \$ _____

Hard copy (HC) 3.00
Microfiche (MF) -65

ff 653 July 65

FACILITY FORM 602	N 68 - 37023	
	(ACCESSION NUMBER)	(THRU)
	<u>139</u> (PAGES)	<u>1</u> (CODE)
	<u>CR 97275</u> (NASA CR OR TMX OR AD NUMBER)	<u>07</u> (CATEGORY)

JULY 1968

Boulder, Colorado 80302

ESSA RESEARCH LABORATORIES

The mission of the Research Laboratories is to study the oceans, inland waters, the lower and upper atmosphere, the space environment, and the earth, in search of the understanding needed to provide more useful services in improving man's prospects for survival as influenced by the physical environment. Laboratories contributing to these studies are:

Earth Sciences Laboratories: Geomagnetism, seismology, geodesy, and related earth sciences; earthquake processes, internal structure and accurate figure of the Earth, and distribution of the Earth's mass.

Atlantic Oceanographic Laboratories and Pacific Oceanographic Laboratories: Oceanography, with emphasis on ocean basins and borders, and oceanic processes; sea-air interactions; and land-sea interactions. (Miami, Florida)

Atmospheric Physics and Chemistry Laboratory: Cloud physics and precipitation; chemical composition and nucleating substances in the lower atmosphere; and laboratory and field experiments toward developing feasible methods of weather modification.

Air Resources Laboratories: Diffusion, transport, and dissipation of atmospheric contaminants; development of methods for prediction and control of atmospheric pollution. (Silver Spring, Maryland)

Geophysical Fluid Dynamics Laboratory: Dynamics and physics of geophysical fluid systems; development of a theoretical basis, through mathematical modeling and computer simulation, for the behavior and properties of the atmosphere and the oceans. (Washington, D. C.)

National Hurricane Research Laboratory: Hurricanes and other tropical weather phenomena by observational, analytical, and theoretical means; hurricane modification experiments to improve understanding of tropical storms and prediction of their movement and severity. (Miami, Florida)

National Severe Storms Laboratory: Tornadoes, squall lines, thunderstorms, and other severe local convective phenomena toward achieving improved methods of forecasting, detecting, and providing advance warnings. (Norman, Oklahoma)

Space Disturbances Laboratory: Nature, behavior, and mechanisms of space disturbances; development and use of techniques for continuous monitoring and early detection and reporting of important disturbances.

Aeronomy Laboratory: Theoretical, laboratory, rocket, and satellite studies of the physical and chemical processes controlling the ionosphere and exosphere of the earth and other planets.

Wave Propagation Laboratory: Development of new methods for remote sensing of the geophysical environment; special emphasis on propagation of sound waves, and electromagnetic waves at millimeter, infrared, and optical frequencies.

Institute for Telecommunication Sciences: Central federal agency for research and services in propagation of radio waves, radio properties of the earth and its atmosphere, nature of radio noise and interference, information transmission and antennas, and methods for the more effective use of the radio spectrum for telecommunications.

Research Flight Facility: Outfits and operates aircraft specially instrumented for research; and meets needs of ESSA and other groups for environmental measurements for aircraft. (Miami, Florida)

ENVIRONMENTAL SCIENCE SERVICES ADMINISTRATION

BOULDER, COLORADO 80302



U. S. DEPARTMENT OF COMMERCE

C. R. Smith, Secretary

ENVIRONMENTAL SCIENCE SERVICES ADMINISTRATION

Robert M. White, Administrator

ESSA RESEARCH LABORATORIES

George S. Benton, Director

ESSA TECHNICAL REPORT ERL 79-ITS 67

Prediction of Tropospheric Radio Transmission Loss Over Irregular Terrain

A Computer Method—1968

A. G. LONGLEY

P. L. RICE

Tropospheric Telecommunications Laboratory

INSTITUTE FOR TELECOMMUNICATION SCIENCES
BOULDER, COLORADO 80302
July 1968

For sale by the Superintendent of Documents, U.S. Government Printing Office, Washington, D.C. 20402
Price 70 cents.

TABLE OF CONTENTS

	Page
1. INTRODUCTION	1
2. ATMOSPHERIC AND TERRAIN PARAMETERS	3
2.1 Atmospheric Effects	3
2.2 Description of Terrain	6
2.3 Parameters Required to Compute Transmission Loss	7
2.4 Effective Antenna Heights, Horizon Distances, and Elevation Angles	9
3. TRANSMISSION LOSS CALCULATIONS	14
3.1 To Compute A_{cr} Within Radio Line of Sight	15
3.2 To Compute Diffraction Attenuation A_d	17
3.3 To Compute Forward Scatter Attenuation A_s	18
4. ACKNOWLEDGMENTS	26
5. REFERENCES	27
ANNEX 1. VARIABILITY IN TIME AND WITH LOCATION, PREDICTION ERROR, AND SERVICE PROBABILITY	1-1
1-1 Variability in Time	1-2
1-1.1 Adjustment Function $V(0.5, d_e)$	1-2
1-1.2 Long-Term Variability About the Median	1-8
1-1.3 Computer Method for Estimating Long-Term Variability	1-12
1-2 Variability with Location	1-15
1-3 Prediction Error and Service Probability	1-16
1-4 List of Symbols	1-22
ANNEX 2. STUDIES OF TERRAIN PROFILES	2-1
2-1 Introduction	2-1
2-2 The Terrain Parameter Δh	2-3
2-3 The Horizon Distance d_L	2-15
2-4 The Elevation Angle θ_e	2-21

TABLE OF CONTENTS (cont'd.)

	Page
2-5 Terrain Parameters for Colorado Plains, Mountains, and Northeastern Ohio	2-33
2-6 Location Variability	2-38
2-7 The Terrain Roughness Factor σ_h	2-41
ANNEX 3. EQUATIONS AND METHODS FOR COMPUTING THE REFERENCE ATTENUATION A_{cr}	3-1
3-1 Two-Ray Optics Formulas for Computing A_o and A_l	3-2
3-2 Formulas for Computing Diffraction At- tenuation A_d	3-8
3-3 Formulas for Computing Scatter Atten- uation A_s	3-13
3-4 List of Symbols	3-17
3-5 Computer Program Listing and Sample Output	3-24

PREDICTION OF TROPOSPHERIC RADIO TRANSMISSION LOSS OVER IRREGULAR TERRAIN

A COMPUTER METHOD - 1968

by

A. G. Longley and P. L. Rice

This report describes a computer method for predicting long-term median transmission loss over irregular terrain. The method is applicable for radio frequencies above 20 MHz and may be used either with detailed terrain profiles for actual paths or with profiles that are representative of median terrain characteristics for a given area. Estimates of variability in time and with location, and a method for computing service probability, are included.

KEY WORDS: transmission loss, tropospheric propagation, irregular terrain, time availability, service probability

1. INTRODUCTION

This report describes a computer method for predicting long-term median radio transmission loss over irregular terrain. The method is based on well-established propagation theory and has been tested against a large number of propagation measurements. It is applicable for radio frequencies above 20 MHz and may be used either with detailed terrain profiles for actual paths or with profiles that are representative of median terrain characteristics for a given area. Estimates of median terrain characteristics are based on a large number of terrain profiles for several types of terrain, including plains, desert, rolling hills, foothills, and rugged mountains.

Given radio frequency, antenna heights, and an estimate of terrain irregularity, median reference values of attenuation relative to the transmission loss in free space are calculated as a function of distance. For

radio line-of-sight paths, the calculated reference is based on two-ray theory and an extrapolated value of diffraction attenuation. For trans-horizon paths, the reference value is either diffraction attenuation or forward scatter attenuation, whichever is smaller.

This prediction method was developed for use with a digital computer and has been made sufficiently general to provide estimates of transmission loss expected over a wide range of frequencies, path lengths, and antenna height combinations, over smooth to highly rugged terrain, and for both vertical and horizontal polarization. The method is described in complete detail in annex 3. Shortcuts appropriate for limited applications are indicated throughout the body of the report. Familiarity with other propagation models, such as those described by Rice et al. (1967) is not essential for using the prediction method described here.

Predictions have been tested against data for wide ranges of frequency, antenna height and distance, and for all types of terrain from very smooth plains to extremely rugged mountains. The data base includes more than 500 long-term recordings throughout the world in the frequency range 40 to 10,000 MHz, and several thousand mobile recordings in the United States at frequencies from 20 to 1000 MHz. The method is intended for use within the following ranges:

<u>Parameter</u>	<u>Range</u>
frequency	20 to 40,000 MHz
antenna heights	0.5 to 3,000 m
distance	1 to 2,000 km
surface refractivity	250 to 400 N-units

In applying this prediction method to specific paths for which detailed profiles are available, certain limitations on antenna siting are desirable. For example, the angle of elevation of each horizon ray above the horizontal should not exceed 12° , and the distance from each

antenna to its horizon should not be less than $1/10$, or more than three times, the corresponding smooth-earth distance.

Section 2 discusses atmospheric and terrain parameters, and section 3 explains how transmission loss is calculated. The topics treated in the annexes are as follows:

Annex 1 shows how the computed reference values, A_{cr} , are adjusted to provide long-term median estimates, $A(0.5)$, of attenuation relative to free space for any given set of data. This annex also gives estimates of the variability in time and with location and shows how to estimate prediction errors.

Annex 2 shows how various path parameters have been derived from studies of terrain profiles.

Annex 3 gives detailed formulas and procedures required to calculate the median reference attenuation A_{cr} . A computer program listing, flow diagram, and sample computations are included.

Annexes 1 and 3 each contain a list of symbols used in that annex, with their definitions.

2. ATMOSPHERIC AND TERRAIN PARAMETERS

2.1 Atmospheric Effects

Radio transmission loss in tropospheric propagation depends on characteristics of the atmosphere and of terrain. For predicting a long-term median reference value of transmission loss, the refractive index gradient near the earth's surface is the most important atmospheric parameter. This surface gradient largely determines the bending of a radio ray as it passes through the atmosphere. Rays may be represented as straight lines, within the first kilometer above the earth's surface, if an "effective earth's radius", a , is defined as a function of the refractivity gradient or of the mean surface refractivity, N_s . In

calculating the long-term reference value, the minimum monthly mean value of N_s is chosen to characterize average atmospheric conditions.

The effective earth's radius, which allows for regional differences in average atmospheric conditions, is defined as

$$a = 6370 [1 - 0.04665 \exp(0.005577 N_s)]^{-1} \text{ km}, \quad (1)$$

where the actual radius of the earth is taken to be 6370 km.

The minimum monthly mean value of surface refractivity may be obtained from measurements or from maps showing a related parameter, N_o . The refractivity, N_o , represents surface refractivity reduced to sea level. Figure 1, reproduced from Bean, Horn, and Ozanich (1960) shows minimum monthly mean values of N_o throughout the world. The corresponding surface refractivity N_s is then

$$N_s = N_o \exp(-0.1057 h_s), \quad (2)$$

where h_s is the elevation of the earth's surface in kilometers above mean sea level. The elevation h_s is determined at the base of the lower antenna for line-of-sight paths. For a transhorizon path, N_s is taken as the average of two values computed by substituting the heights of the horizon obstacles, h_{L1} and h_{L2} , in (2). If an antenna is more than 150 m below its horizon, h_s and N_o should be determined at the antenna location. A commonly used value of N_s is 301 with an effective earth's radius $a = 8497$ km, which corresponds to $4/3$ of the actual radius.

Other atmospheric effects, such as changes in the refractive index, changes in the amount of turbulence or stratification, as well as absorption by oxygen, water vapor, clouds, and precipitation, are allowed for by empirical adjustments. Adjustments to the median, allowing for differences in climate, and estimates of variability relative to the median are described in annex 1.

MINIMUM MONTHLY SURFACE REFRACTIVITY VALUES REFERRED TO MEAN SEA LEVEL

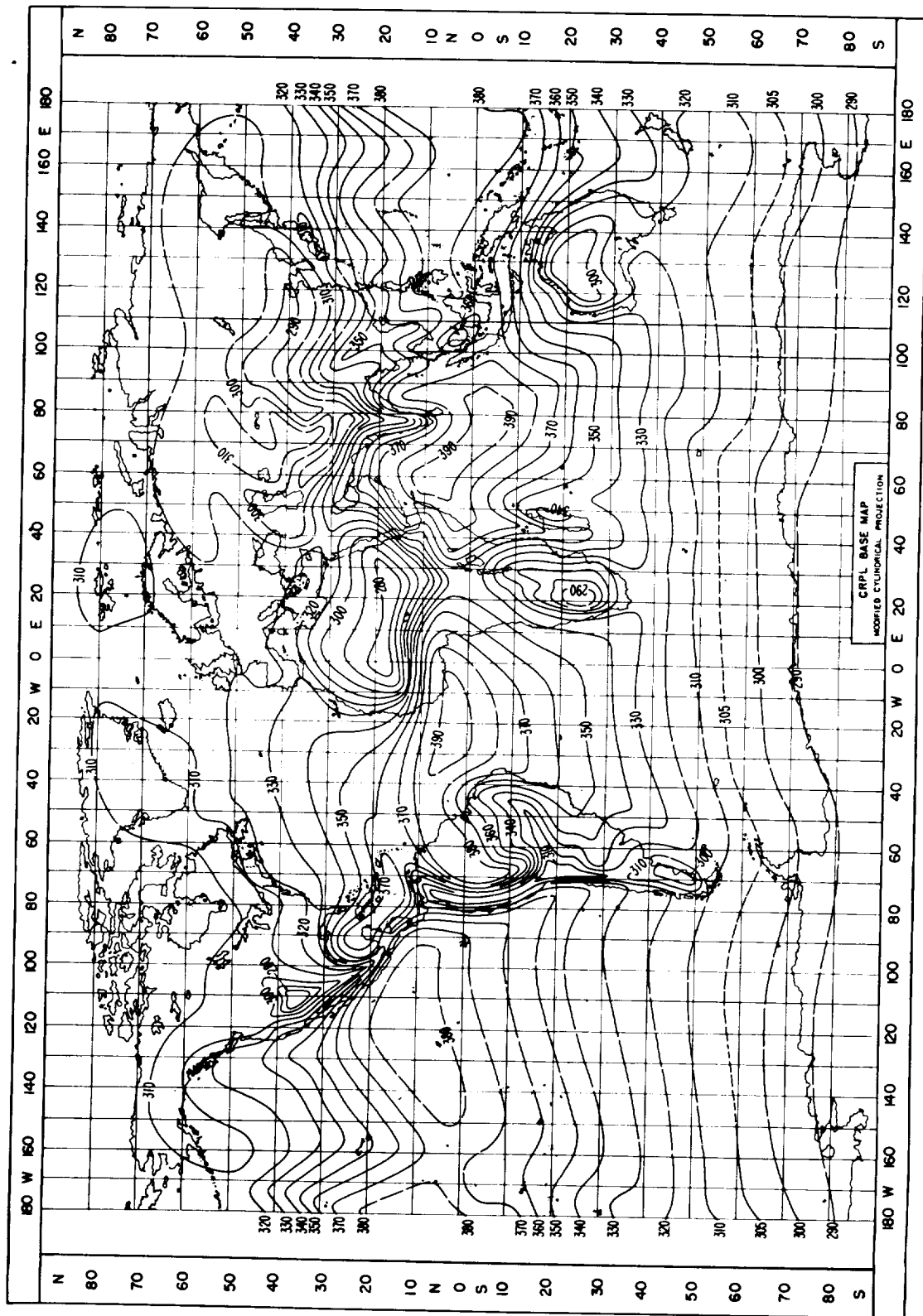


Figure 1

2.2 Description of Terrain

Transmission loss may be calculated for specific paths where detailed profiles are available, but the prediction method is particularly useful when little is known of the details of terrain for actual paths. To characterize terrain, profiles may be read at regular intervals in both N-S and E-W directions, forming a uniform grid over an area. Or an actual or proposed deployment of propagation paths, representing a wide variety of terrain conditions, may be combined to provide a single set of profiles for which an estimate of median propagation conditions is desired. The interdecile range, $\Delta h(d)$, of terrain heights above and below a straight line fitted to elevations above sea level, is calculated at fixed distances. Usually median values of $\Delta h(d)$ increase with path length to an asymptotic value, Δh , which is used to characterize the terrain.

When terrain profiles are not available, estimates of Δh may be obtained from table 1.

Table 1. Estimates of Δh .

<u>Type of Terrain</u>	<u>Δh in Meters</u>
Water or very smooth plains	0 - 5
Smooth plains	5 - 20
Slightly rolling plains	20 - 40
Rolling plains	40 - 80
Hills	80 - 150
Mountains	150 - 300
Rugged mountains	300 - 700
Extremely rugged mountains	>700

Median estimates of $\Delta h(d)$ at desired distances may be obtained from the following relationship, which is based on a study of a large number of profiles:

$$\Delta h(d) = \Delta h [1 - 0.8 \exp(- 0.02 d)] \text{ m}, \quad (3)$$

where $\Delta h(d)$ and Δh are in meters and the distance d is in kilometers. Studies of terrain are described in annex 2.

2.3 Parameters Required to Compute Transmission Loss

For any specific application, a minimum of four essential parameters must be supplied in order to calculate reference values of transmission loss. These are the carrier frequency f in megahertz, the path distance d in kilometers, and the transmitting and receiving antenna heights above ground h_{g1} and h_{g2} in meters. Other path parameters used in the computations, such as horizon distances and elevation angles, may be derived from these values and available terrain information as described in the next subsection. When detailed profiles for individual paths are available one may compute these additional path parameters using the methods outlined in annex 3.

In addition to estimates of surface refractivity N_s and the terrain parameter Δh , previously discussed, the ground constants applicable to the intervening terrain should be considered. The conductivity, σ , of the earth's surface and its permittivity or relative dielectric constant, ϵ , enter into the calculations for line-of-sight and diffraction attenuation. When these constants are not known for a given path or area the following values may be assumed:

Table 2. Typical Ground Constants

Type of surface	σ mho/ m	ϵ
Poor ground	0.001	4
Average ground	0.005	15
Good ground	0.02	25
Sea water	5	81
Fresh water	0.01	81

At sufficiently low frequencies, the effect of the conductivity σ is dominant, while at sufficiently high frequencies, the dielectric constant ϵ has the dominant effect. For oversea transmission, this transition occurs between 300 and 3000 MHz, while over "average" ground, the transition is between 5 and 50 MHz. For propagation over irregular terrain, at frequencies above 100 MHz, and with antennas more than 5 m above ground, the effects of the ground constants are slight, and the results for horizontal and vertical polarization are nearly the same. Under these conditions the method may be simplified considerably by assuming the magnitude of the theoretical reflection coefficient $R_{h,v} \approx 0.95$ and the phase shift $c \approx 0$. For many applications this results in an estimate of the effective reflection coefficient $R_e \approx 0.9$, and the attenuation A in (3.2) may be calculated directly, bypassing the calculations shown in equations (3.5) through (3.15) in annex 3. These approximations are not applicable for transmission over the sea. For oversea transmission $R_{h,v}$ and c may be computed using the equations given in annex 3 or estimated from figure III. 1 or figure III. 5 of annex III, volume II of the report by Rice et al. (1967).

The parameters required for computing reference values of transmission loss L_{cr} , or the corresponding attenuation below free space A_{cr} , are then: frequency f in megahertz, distance d in kilometers, antenna heights above ground h_{g1} and h_{g2} in meters, as well as

estimates of surface refractivity N_s , the terrain irregularity Δh in meters, the conductivity σ mho/m, and the relative dielectric constant ϵ of the ground.

The next subsection shows how additional path parameters are obtained from these basic parameters.

2.4 Effective Antenna Heights, Horizon Distances, and Elevation Angles

Additional path parameters that must be known or estimated to calculate long-term reference values of transmission loss are the effective antenna heights h_{e1} and h_{e2} , the horizon distances d_{L1} and d_{L2} , and the horizon elevation angles θ_{e1} and θ_{e2} . Horizon distances and elevation angles are shown in figure 2. When a detailed terrain profile is available for a given path, these parameters may be computed by the methods described by Rice et al. (1967) and outlined in annex 3 of this report. Otherwise, estimates of effective antenna heights and of horizon distances and angles must be calculated. Such estimates are based on the terrain factor Δh , on the antenna heights above ground h_{g1} and h_{g2} , and on the method used for selecting antenna sites.

When antennas are high and the terrain is relatively smooth, the actual horizon distances d_{L1} and d_{L2} are approximately equal to the smooth-earth horizon distances d_{Ls1} and d_{Ls2} . When antennas are low and randomly located with respect to hills or other obstructions, as with many tactical communication nets, the actual horizon distances will vary greatly and their median values may be less than the corresponding smooth-earth values. When sites are chosen to take advantage of hill-tops, with propagation across valleys, as for radio relays, the horizon distances and effective antenna heights may be greatly increased. Consequently the following estimates are used:

GEOMETRY OF A TRANSHORIZON RADIO PATH

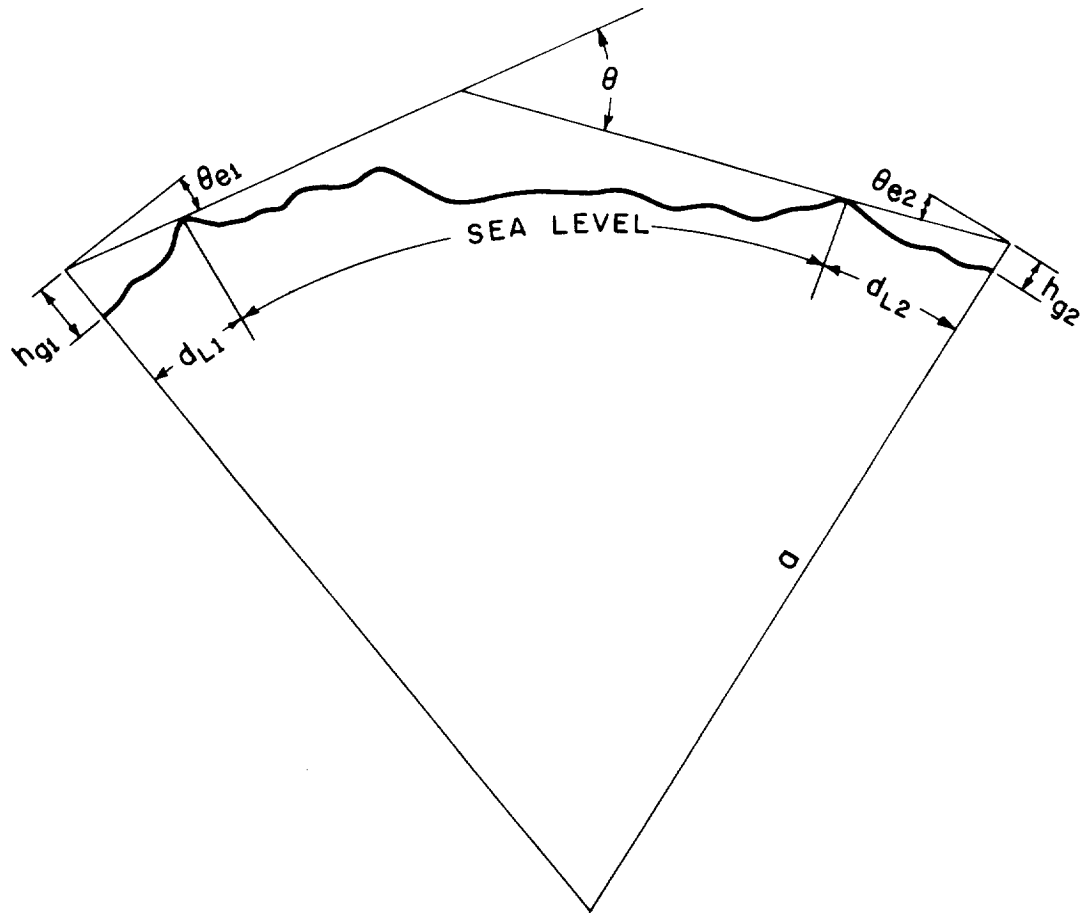


Figure 2

a) For net-type communications, with random antenna siting, the effective antenna heights h_{e1} and h_{e2} are assumed to be equal to the structural heights above ground:

$$h_{e1,2} = h_{g1,2} \text{ m.} \quad (4a)$$

b) For radio relay links, with antennas located on or near hilltops, the effective heights are larger than the structural heights by an amount whose median value depends on the structural heights and the terrain irregularity Δh :

$$h_{e1,2} = h_{g1,2} + k \exp(-2 h_{g1,2} / \Delta h) \text{ m.} \quad (4b)$$

Studies of terrain have shown that the maximum difference to be expected between median values of structural and effective height is 50 m, in which case k would be equal to 50. But in most situations such a difference would be unrealistic, especially with low antennas and limited freedom in site selection. Over moderately hilly to mountainous terrain, with structural antenna heights less than or equal to 10 m, the following estimates of k may be used:

When antenna sites are rather carefully selected in an area of limited extent,

$$k = \begin{cases} 1 + 4 \sin(\pi h_{g1,2} / 10) & \text{if } 0 \leq h_{g1,2} \leq 5, \\ 5 & \text{otherwise.} \end{cases} \quad (4c)$$

When antenna sites are still more carefully selected,

$$k = \begin{cases} 1 + 9 \sin(\pi h_{g1,2} / 10) & \text{if } 0 \leq h_{g1,2} \leq 5, \\ 10 & \text{otherwise.} \end{cases} \quad (4d)$$

For each application the question of a suitable allowance for effective antenna height should be carefully considered. The improved propagation conditions that can be obtained by careful site selection may be highly significant. Further study of definitions of effective antenna height appears to be the most urgent requirement for improving these predictions for low antenna heights over irregular terrain. Different definitions of $h_{e1,2}$ may be found appropriate for line-of-sight and diffraction formulas.

When individual path profiles are not available, median values of the horizon distances d_{L1} and d_{L2} are estimated as functions of the median effective antenna heights h_{e1} and h_{e2} determined above, the terrain irregularity factor Δh , and the smooth-earth horizon distances d_{Ls1} and d_{Ls2} . The distance from each antenna to its horizon over a smooth earth is defined as

$$d_{Ls1,2} = \sqrt{0.002a h_{e1,2}} \text{ km}, \quad (5a)$$

where the effective antenna heights $h_{e1,2}$ are in meters and the effective earth's radius a is in kilometers, as defined by (1). The sum of the smooth-earth horizon distances is

$$d_{Ls} = d_{Ls1} + d_{Ls2} \text{ km}. \quad (5b)$$

Median values of horizon distances over irregular terrain are estimated as

$$d_{L1,2} = d_{Ls1,2} \exp(-0.07 \sqrt{\Delta h / h_e}) \text{ km}, \quad (5c)$$

where

$$h_e = \begin{cases} h_{e1,2} & \text{for } h_{e1,2} \geq 5 \text{ m,} \\ 5 & \text{otherwise.} \end{cases}$$

The total distance, d_L , between the antennas and their horizons is

$$d_L = d_{L1} + d_{L2} \text{ km.} \quad (5d)$$

For paths whose antennas are within radio line of sight of each other, estimates of transmission loss depend on the particular effective antenna heights that define the dominant reflecting plane between the antennas. Even for known line-of-sight paths an estimate of the sum of the horizon distances, $d_L \geq d$, is required to compute a reference value of attenuation relative to free space A_{cr} , or of transmission loss L_{cr} , as described in annex 3, subject to the restriction

$$d_{Ls} \geq d_L \geq d. \quad (5e)$$

If this condition is not met, a non-line-of-sight path is implied, the estimates of $h_{e1,2}$ are too low, and both should be multiplied by the smallest factor that will satisfy (5e).

The horizon elevation angles θ_{e1} and θ_{e2} , shown in figure 2, are the angles by which the horizon rays are elevated, or depressed, relative to the horizontal at each antenna. When detailed profiles for individual paths are not available, median values of $\theta_{e1,2}$ may be estimated as

$$\theta_{e1,2} = \frac{0.0005}{d_{Ls1,2}} \left[1.3 \left(\frac{d_{Ls1,2}}{d_{L1,2}} - 1 \right) \Delta h - 4 h_{e1,2} \right] \text{ radians.} \quad (6a)$$

The sum of the elevation angles is

$$\theta_e = \theta_{e1} + \theta_{e2} \quad \text{or} \quad -d_L/a \text{ radians,} \quad (6b)$$

whichever is larger algebraically. In (6) all distances are in kilometers and heights are in meters.

For transhorizon paths the path length d is equal to or greater than the sum of the horizon distances d_L . The angular distance for a transhorizon path is always positive and is defined as

$$\theta = \theta_e + d/a \text{ radians,} \quad (7)$$

where d is the path length and a is the effective earth's radius, both in kilometers.

These additional path parameters, $h_{e1,2}$, $d_{L1,2}$, $\theta_{e1,2}$, and θ , are used in computing reference values of attenuation relative to free space A_{cr} , or transmission loss L_{cr} . When only the basic parameters are supplied, estimates of these additional parameters are calculated using equations (4) through (7). When detailed profiles are available for desired paths, these additional parameters are obtained as described by Rice et al. (1967) and outlined in annex 3.

3. TRANSMISSION LOSS CALCULATIONS

This section describes how the various parameters discussed in section 2 are used to compute transmission loss. Median reference values A_{cr} of attenuation below free space are computed first. The reference values L_{cr} of transmission loss are then the sum of the free space basic transmission loss, L_{bf} , and the reference attenuation relative to free space, A_{cr} :

$$L_{cr} = L_{bf} + A_{cr} \text{ dB.} \quad (8)$$

The free-space basic transmission loss is

$$L_{bf} = 32.45 + 20 \log_{10} f + 20 \log_{10} d \text{ dB}, \quad (9)$$

where the radio frequency f is in megahertz, and the distance d is in kilometers.

The reference attenuation A_{cr} is computed using methods based on different propagation mechanisms for three distance ranges. Well within radio line of sight, the formulas of two-ray optics are used to compute attenuation relative to free space. Just beyond line of sight, diffraction is the dominant mechanism. The prediction method computes a weighted average, A_d , of estimates of diffraction attenuation over a double knife edge, and over irregular terrain. At greater distances, well beyond the radio horizon, the dominant propagation mechanism is usually forward scatter. The prediction method for this distance range is a modification of the scatter computations described by Rice et al. (1967). The reference attenuation A_{cr} for transhorizon paths is either the diffraction attenuation A_d or the scatter attenuation A_s , whichever is smaller. The distance at which diffraction and scatter losses are equal is defined as d_x .

To provide a continuous curve of the computed reference attenuation A_{cr} as a function of distance the following methods are used.

3.1 To Compute A_{cr} Within Radio Line of Sight

When transmitting and receiving antennas are within radio line of sight, the two-ray optics formulas described in annex 3 are used to compute attenuations A_0 and A_1 at specified distances d_0 and d_1 that are well within the horizon. The distance d_0 is chosen to approximate the greatest distance at which the attenuation below free space is zero. The

distance d_1 is greater than d_o but well within the range for which two-ray optics formulas are valid. The methods described in the next subsection are used to compute the diffraction attenuation A_{Ls} at the smooth earth horizon distance d_{Ls} . These three values of attenuation, A_o , A_1 , and A_{Ls} , computed at the distances d_o , d_1 , and d_{Ls} , respectively, are used to determine the slopes k_1 and k_2 of a smooth curve of A_{cr} versus distance for the range $1 \leq d \leq d_{Ls}$:

$$A_{cr} = A_o + k_1 (d - d_o) + k_2 \log_{10} (d/d_o) \text{ dB.} \quad (10)$$

Note that the smooth-earth horizon distance d_{Ls} may be greater than the actual horizon distance d_L .

Equation (10) may be simplified by defining a term A_e :

$$A_e = A_o - k_1 d_o - k_2 \log_{10} d_o \text{ dB.} \quad (11)$$

Then for all distances greater than one and less than d_{Ls} , reference attenuation is defined as

$$A_{cr} = A_e + k_1 d + k_2 \log_{10} d \text{ dB.} \quad (12)$$

Detailed methods for computing k_1 and k_2 are given in annex 3. Whenever the value of A_{cr} computed from (12) is less than zero, it is assumed that $A_{cr} = 0$. This prediction method does not attempt to describe the lobery within line of sight over irregular terrain.

3.2 To Compute Diffraction Attenuation A_d

The diffraction attenuation is computed by combining estimates of knife-edge diffraction, based on Fresnel-Kirchhoff theory, with a modification of the method for computing diffraction over smooth terrain

developed by Vogler (1964). Vogler's method estimates the diffraction attenuation, A_r , over the bulge of the earth in the far diffraction region, and is applicable for smooth terrain. Knife-edge diffraction theory is used to estimate attenuation over an isolated hill or ridge. In this application the knife-edge attenuation, A_k , is computed as though the radio path crossed two sharp, isolated ridges. In general, for irregular terrain, the diffraction attenuation, A_d , is computed as a weighted average of the two estimates A_r and A_k :

$$A_d = (1 - w) A_k + w A_r \text{ dB}, \quad (13)$$

where the weighting factor, w , is determined empirically as a function of radio frequency and terrain parameters and is defined in annex 3.

The diffraction attenuation A_d is calculated at distances d_3 and d_4 in the far diffraction region using the formulas given in annex 3. A straight line through these points (A_3, d_3) and (A_4, d_4) is then defined by the intercept, A_{ed} , and slope, m_d , as follows:

$$m_d = (A_4 - A_3) / (d_4 - d_3) \text{ dB/km}, \quad (14)$$

and

$$A_{ed} = A_{fo} + A_4 - m_d d_4 \text{ dB}, \quad (15)$$

where A_{fo} is a clutter factor defined in annex 3.

The reference attenuation A_{cr} at any distance d greater than the smooth earth horizon distance d_{Ls} and less than the distance d_x where diffraction and scatter attenuation are equal is

$$A_{cr} = A_d = A_{ed} + m_d d \text{ dB}, \quad \text{for } d_{Ls} \leq d \leq d_x. \quad (16)$$

3.3 To Compute Forward Scatter Attenuation A_s

When the path length d or the angular distance θ is large, the forward scatter attenuation A_s may be less than the diffraction attenuation A_d . Therefore, when the product of the distance in kilometers and the angular distance in radians exceeds 0.5 ($\theta d > 0.5$), forward scatter attenuation A_s is computed for comparison with A_d .

For large values of θd , the scatter attenuation A_s is assumed to have a linear dependence on distance; therefore, A_s is computed at two large distances d_5 and d_6 . A straight line through the points (A_5, d_5) and (A_6, d_6) is then defined by the intercept A_{es} and the slope m_s as follows:

$$A_{es} = A_5 - m_s d_5 \text{ dB}, \quad (17a)$$

and

$$m_s = (A_6 - A_5) / (d_6 - d_5) \text{ dB}. \quad (17b)$$

The reference attenuation A_{cr} at any distance d greater than the distance d_x where diffraction and scatter attenuations are equal is given by

$$A_{cr} = A_s = A_{es} + m_s d \text{ dB}, \quad \text{for } d \geq d_x. \quad (18)$$

The detailed equations and techniques required to compute the reference attenuation A_{cr} as a function of distance are given in annex 3.

Figures 3 through 8 show computed and measured values of attenuation below free space plotted as a function of distance. The data were obtained in a measurement program described by Johnson et al. (1967). Measurements were made at frequencies of 20, 50, and 100 MHz in three areas. Figures 3 and 4 show data from northeastern Ohio, with corresponding predicted values. Figure 3 shows medians of data recorded at distances of 10, 20, 30, and 50 km from the transmitter, using both vertical and horizontal polarization at 100 MHz, and with receiver heights of 3, 6, and 9 m. The number of measurements at each distance is tabulated, and corresponding medians of point-to-point predictions based on individual profiles for each of the measurement paths are shown. The lines represent computed reference values A_{cr} , based on frequency, antenna heights, and the asymptotic value of terrain irregularity Δh . Figure 4 shows data and predicted values at frequencies of 20 and 50 MHz.

Figures 5 and 6 show measured and predicted values of attenuation below free space for an area in the plains near Boulder, Colorado. Measurements were made at distances of 5 to 80 km from the transmitter. Medians of data and the number of measurements made at each distance are shown, with corresponding point-to-point predictions. The lines represent computed reference values A_{cr} , based on the asymptotic value of terrain irregularity Δh .

Figures 7 and 8 show measured and predicted values of attenuation below free space in the Colorado mountains west of Boulder. The computed values of A_{cr} represented by lines assume $\Delta h = 650$ m. Actually the shorter paths extend only into the foothills. For the 5-km paths the median value of $\Delta h(d)$ is 100 m. The triangles on figures 7 and 8 show values computed using these estimates of Δh .

COMPUTED AND MEASURED VALUES OF ATTENUATION BELOW FREE SPACE
 NORTHEASTERN, OHIO
 $f=100$ MHz, $\Delta h=90$ m, $N_s=312$

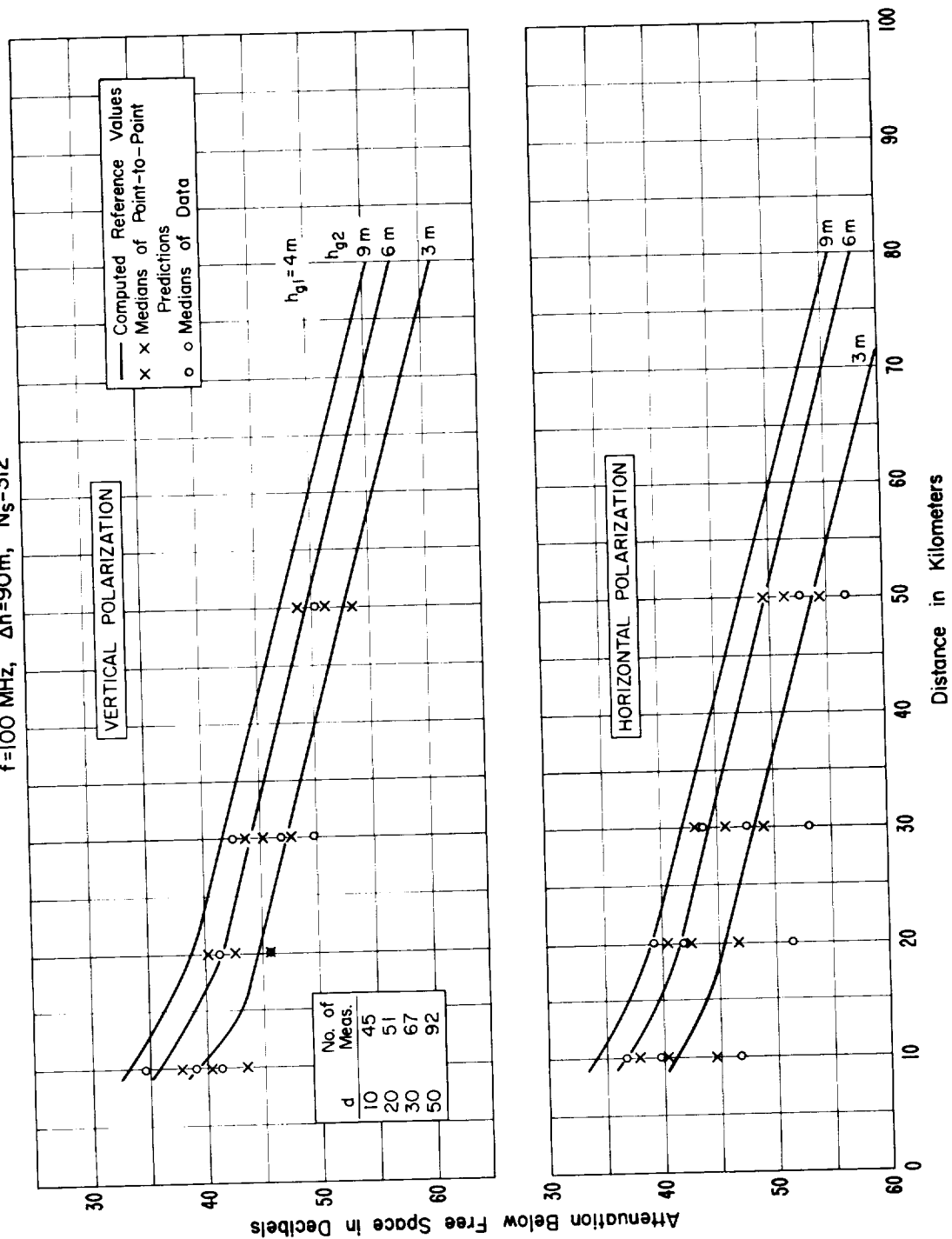


Figure 3

COMPUTED AND MEASURED VALUES OF ATTENUATION BELOW FREE SPACE NORTHEASTERN, OHIO

$f=50$ and 20 MHz, $\Delta h=90$ m, $N_s=312$

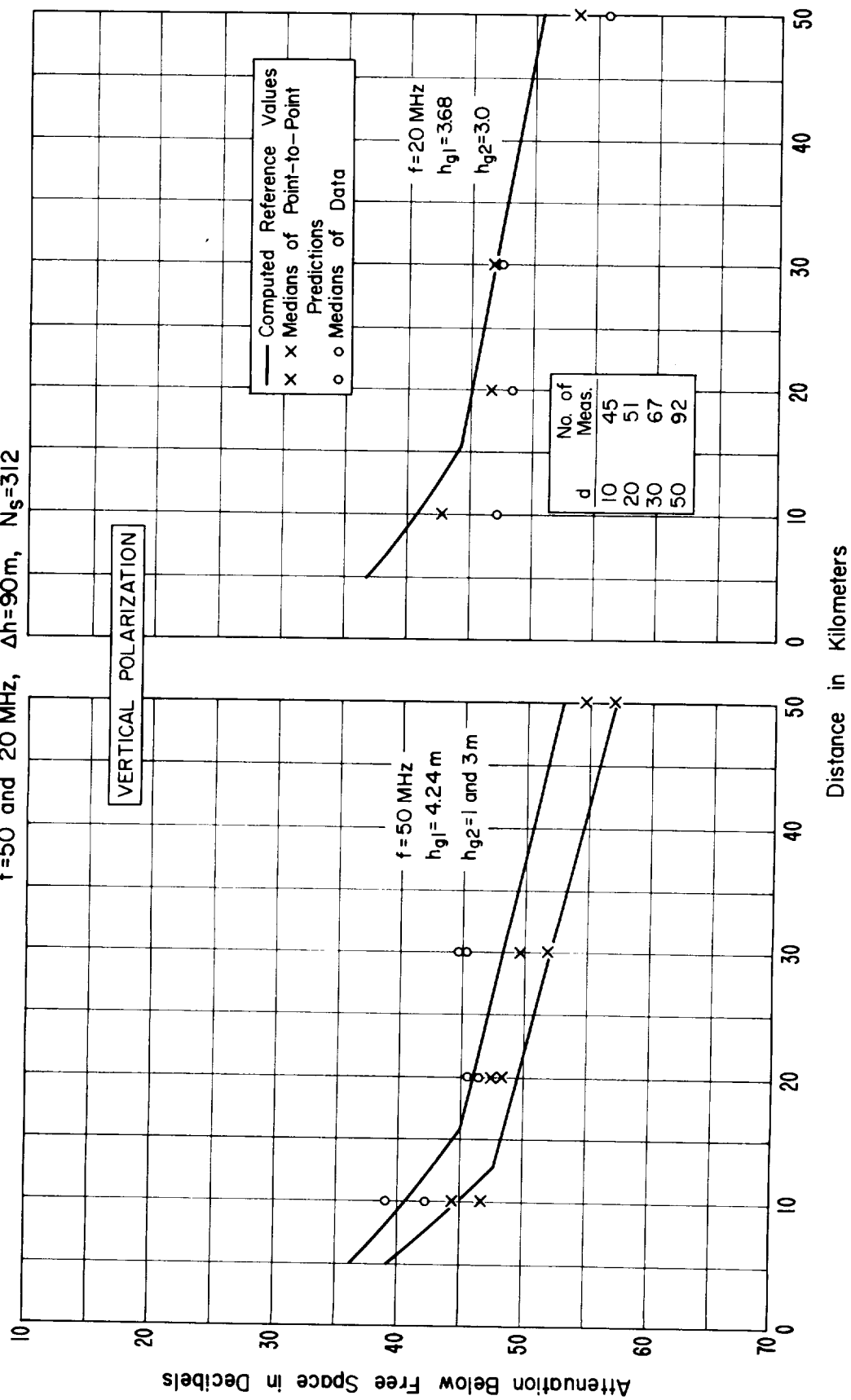


Figure 4

COMPUTED AND MEASURED VALUES OF ATTENUATION BELOW FREE SPACE COLORADO PLAINS

$f=100$ MHz, $\Delta h=90$ m, $N_s=290$

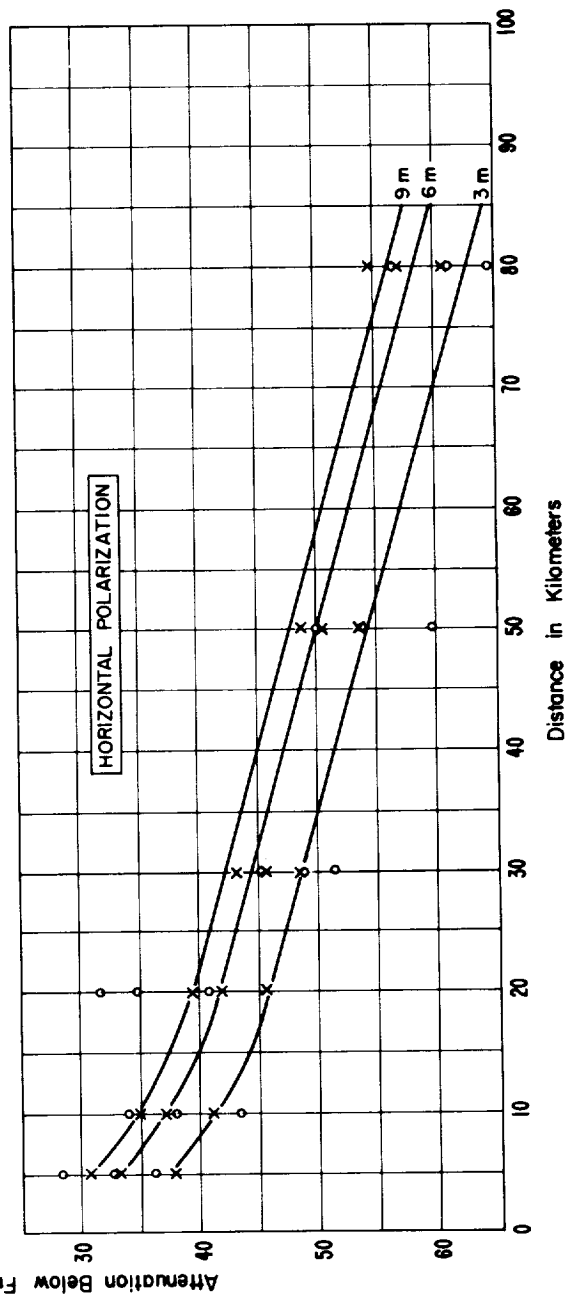
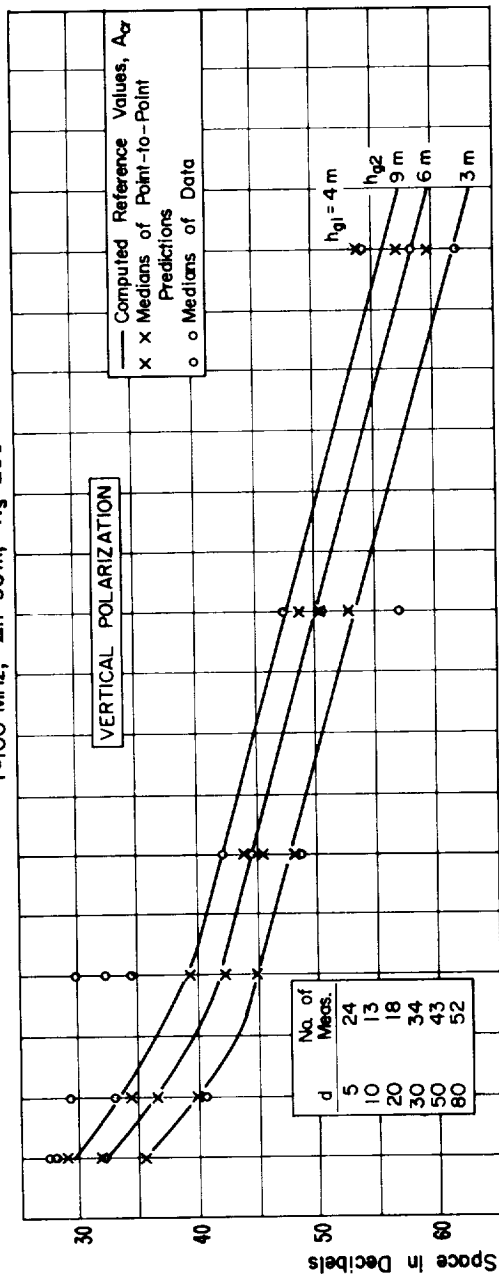


Figure 5

COMPUTED AND MEASURED VALUES OF ATTENUATION BELOW FREE SPACE COLORADO PLAINS

$f=50$ and 20 MHz, $\Delta h=90$ m, $N_s=290$

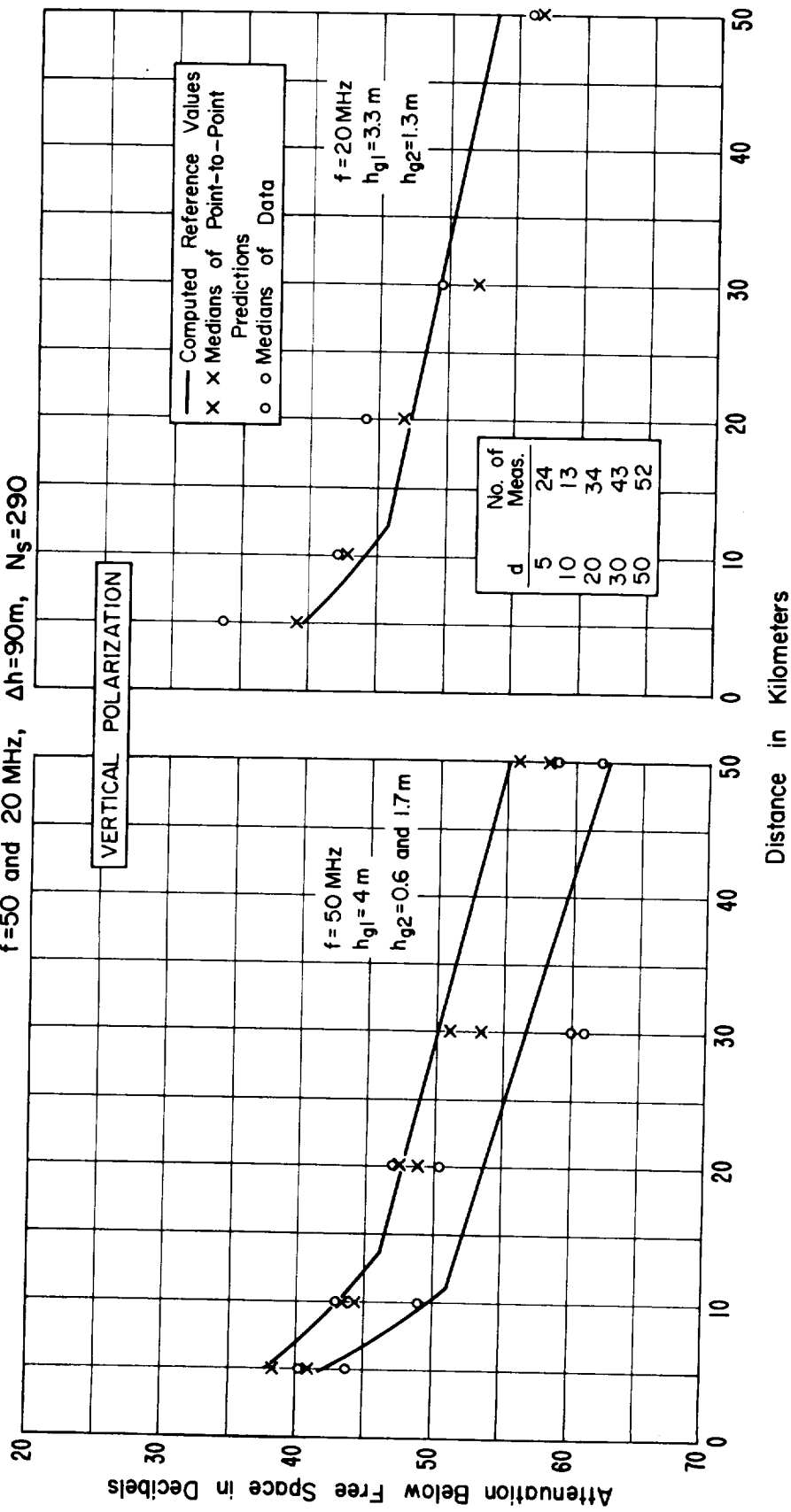


Figure 6

COMPUTED AND MEASURED VALUES OF ATTENUATION BELOW FREE SPACE
 COLORADO MOUNTAINS
 $f=100$ MHz, $\Delta h=650$ m, $N_s=290$

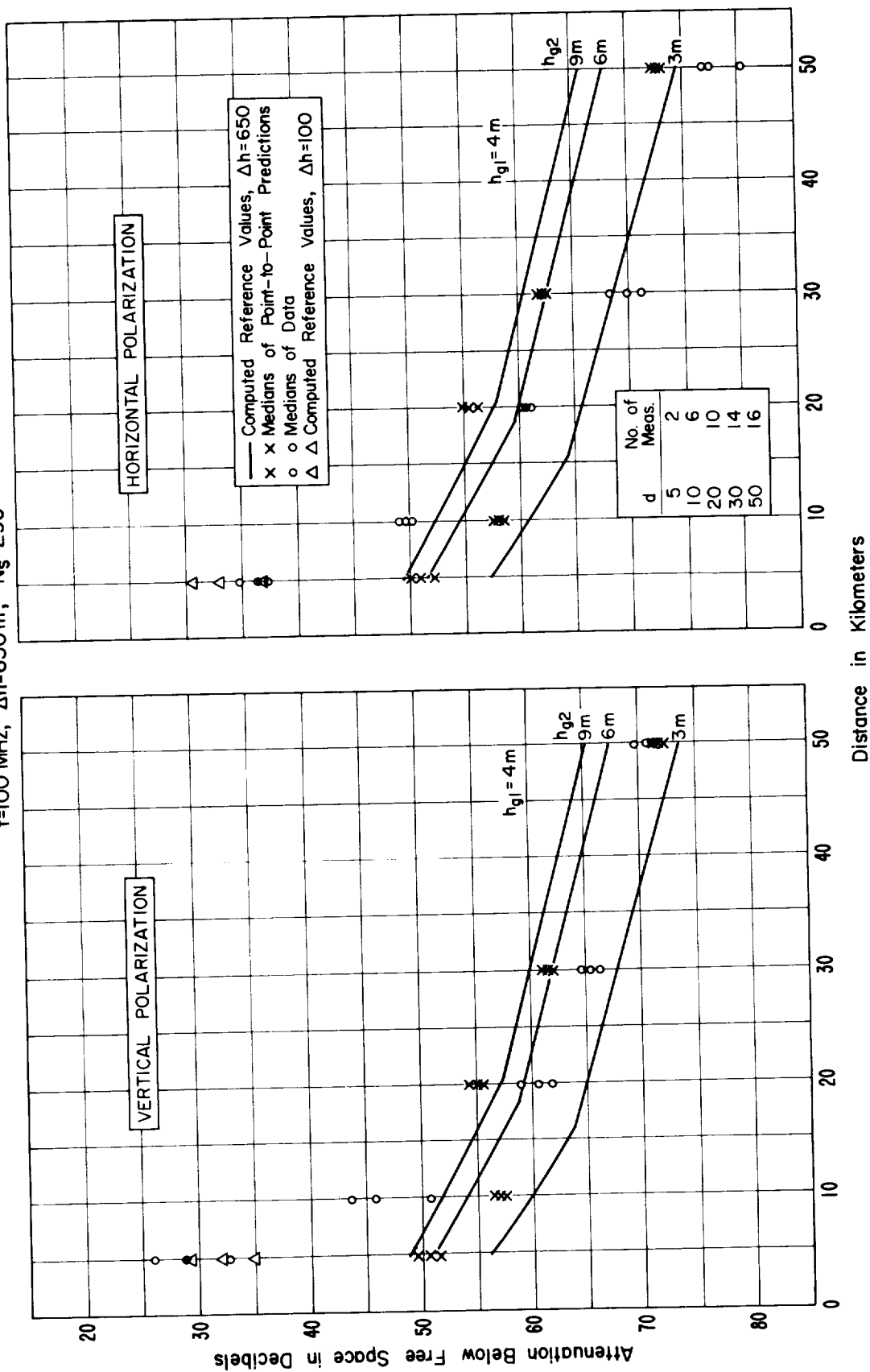


Figure 7

COMPUTED AND MEASURED VALUES OF ATTENUATION BELOW FREE SPACE COLORADO MOUNTAINS

$f=50$ and 20 MHz, $\Delta h=650$ m, $N_s=290$

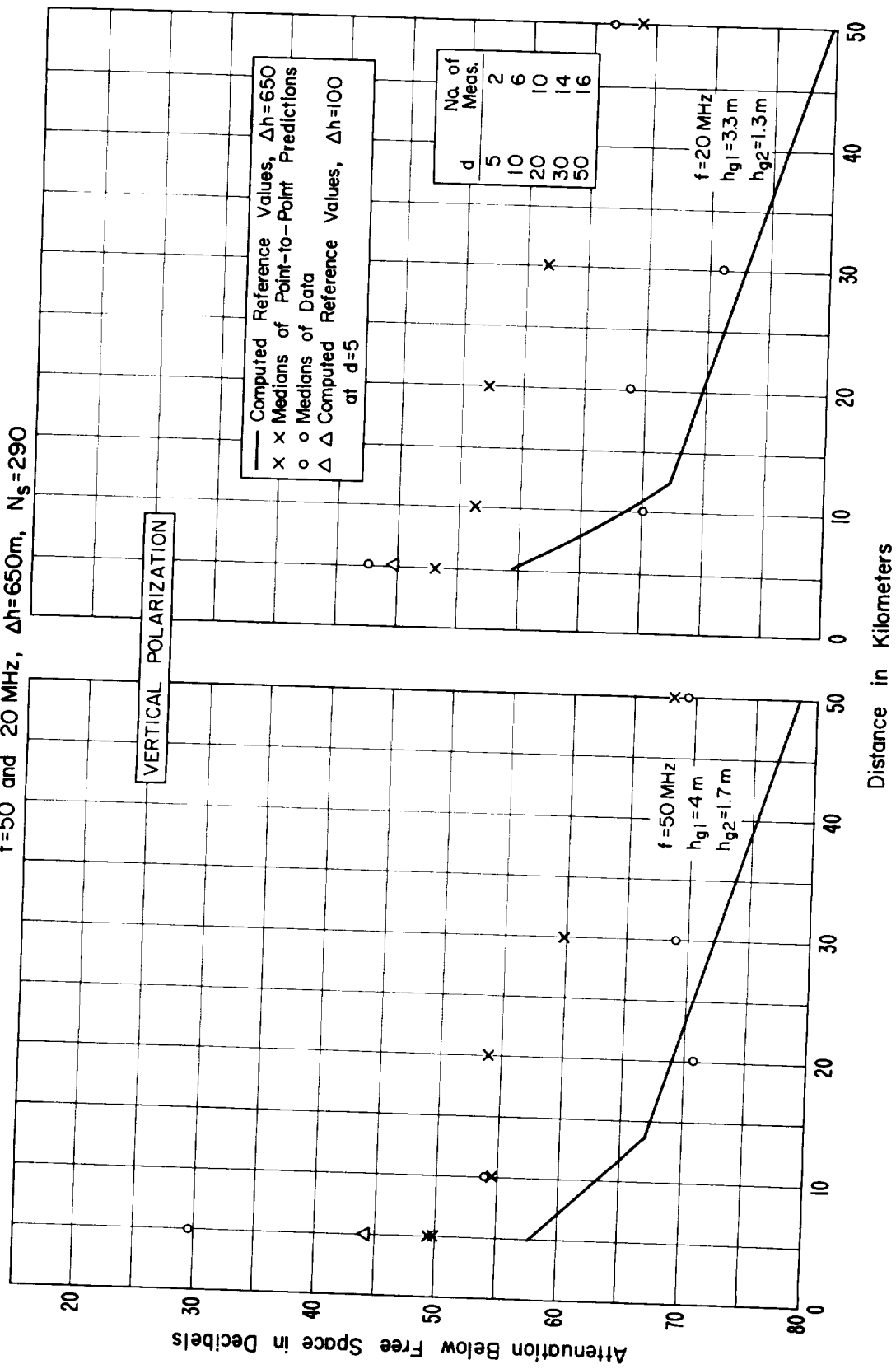


Figure 8

4. ACKNOWLEDGMENT

This computer method summarizes much of the work done at ESSA in predicting tropospheric transmission loss over irregular terrain. We particularly wish to acknowledge the work done by R. K. Reasoner in programming and testing the prediction method, and that of J. L. Montgomery, V. L. Fuller, C. Moncure, P. C. Whittaker, M. M. Coyle, and P. G. Ratcliffe in summarizing propagation data and preparing and analyzing terrain profiles. Data from an extended program of measurements were furnished by A. P. Barsis, who also provided a critical evaluation of the method and many valuable suggestions.

The work was sponsored by the U. S. Army Electronics Command, Fort Monmouth, New Jersey, under Contract No. 67-95863.

5. REFERENCES

- Bean, B.R., J.D. Horn, and A.M. Ozanich, Jr. (1960, "Climatic charts and data of the radio refractive index for the United States and the world," NBS Monograph No. 22 (U.S. Government Printing Office, Washington, D.C.).
- CCIR (1966), Rept. 244-1, Vol. 2, Doc. 11th Plenary Assembly, Oslo.
- Johnson, M.E., M.J. Miles, P.L. McQuate, and A.P. Barsis (1967), "Tabulations of VHF propagation data obtained over irregular terrain, at 20, 50 and 100 MHz," ESSA Tech. Rept. IER 38-ITSA 38-1, 38-2, and 38-3.
- Miles, M.J., and A.P. Barsis (1966), "Summary of 20-100 MHz propagation measurement results over irregular terrain using low antenna heights," ESSA Tech. Rept. IER 10-ITSA 10.
- Rice, P.L., A.G. Longley, K.A. Norton, and A.P. Barsis (1967), "Transmission loss predictions for tropospheric communication circuits," NBS Tech. Note 101, Vols. I and II (revised).
- Vogler, L.E. (1964), "Calculation of groundwave attenuation in the far diffraction region," Radio Sci. J. Res. NBS 68D, No. 7, 819-826.

ANNEX 1

VARIABILITY IN TIME AND WITH LOCATION, PREDICTION ERROR, AND SERVICE PROBABILITY

This annex deals with definitions of satisfactory service for any radio communication system, the variability of service with time and location, and ways of allowing for random errors of prediction. A specified grade of service, g , from a wanted signal in the presence of unwanted signals, and rapid or fine-grained variations of these signal levels with time or receiving location, is assumed to depend only upon whether a required wanted-to-unwanted signal ratio $R_r(g_r)$ is exceeded. If increasing values of available grades represent better grades of service, $R_r(g)$ must increase with g . For any reasonable selection of a receiving system, the probability of power-independent distortion is assumed negligible, or at least minimized.

Let $R(q_T)$ represent the available wanted-to-unwanted signal exceeded for a fraction q_T of a specified period of time. With R_r and q_T fixed, satisfactory service exists if $R(q_T) > R_r$. Data normalized to correspond with the given conditions can be used to predict $R(q_T)$. The service probability, Q , is defined as the expected fraction of normalized data for which $R(q_T) > R_r$.

To avoid accepting an unsatisfactory system, a high service probability is required, while there should be a low service probability for any system that is rejected, other things being equal. Service probability can also be used as a weighting factor in cost-benefit studies or in studying complex netting and multiple access problems. For some applications, such as broadcasting or relay networks with many receivers and/or transmitters, it may be worthwhile to describe variations from location to location statistically instead of examining every possible propagation link. Then the quantity $R(q_T, q_L, Q)$ is defined as the

wanted-to-unwanted signal ratio exceeded for at least a fraction q_T of a specified period of time, for a fraction q_L of all receiving antenna locations or propagation paths in a statistically homogeneous area or group, and with a probability Q .

Interference probability is the complement, $P \equiv 1 - Q$, of the service probability. Harmful interference may be said to exist at the antenna terminals of a particular receiving system if the service probability is less than 0.95, i.e., the interference probability is greater than 0.05.

The first section of this annex discusses the time variability of propagation attenuation, the next section describes variability with location, and the last section deals with the statistics of R .

1-1. Variability in Time

1-1.1 Adjustment Function $V(0.5, d_e)$

Adjustments to the calculated long-term reference value A_{cr} of attenuation relative to free space may be required to provide long-term median estimates of $A(0.5)$ for given sets of data. Adjustments described here provide estimates of $A(0.5)$ for specific periods of time and for various climatic regions. Climatic regions are distinguished on the basis of meteorological data as described by the CCIR (1966) and by Rice et al. (1967).

The calculated long-term reference value A_{cr} represents the median attenuation to be expected, assuming minimum monthly mean values of surface refractivity N_s (see sec. 2.1). Therefore, differences are to be expected between the reference value A_{cr} and the long-term median $A(0.5)$ that represents all hours of the year. In the northern temperate zone, for example, minimum monthly mean values of N_s occur during the winter months.

The all-year median attenuation $A(0.5)$ differs from the computed value A_{cr} by an amount $V(0.5)$ dB:

$$A(0.5) = A_{cr} - V(0.5) \text{ dB.} \quad (1.1)$$

This difference $V(0.5)$ between the all-year median attenuation and A_{cr} is shown in figure 1.1 for several climatic regions as a function of an effective distance, d_e , expressed in kilometers.

The effective distance d_e depends on the distance at which diffraction and forward scatter losses are approximately equal over a smooth earth, and on d_{Lo} , which is the sum of the smooth-earth horizon distances for an effective earth's radius $a = 9000$ km. Define θ_{s1} as the angular distance where diffraction and scatter losses are approximately equal over a smooth earth of effective radius $a = 9000$ km. Then,

$$d_{s1} = a \theta_{s1} = 65(100/f)^{\frac{1}{3}} \text{ km, and} \quad (1.2a)$$

$$d_{Lo} = 3(\sqrt{2 h_{e1}} + \sqrt{2 h_{e2}}) \text{ km,} \quad (1.2b)$$

where f is the frequency in megahertz and $h_{e1,2}$ are the effective antenna heights in meters, defined in section 2.4 (4). The effective distance d_e is then defined as follows:

$$\text{For } d \leq (d_{Lo} + d_{s1}) \text{ km,} \quad d_e = 130 d / (d_{Lo} + d_{s1}) \text{ km} \quad (1.3a)$$

$$\text{For } d > (d_{Lo} + d_{s1}) \text{ km,} \quad d_e = 130 + d - (d_{Lo} + d_{s1}) \text{ km.} \quad (1.3b)$$

In each climatic region the calculated reference value should be adjusted by the amount $V(0.5, d_e)$ to obtain the predicted all-year median value of attenuation.

The curves shown in figure 1.1 represent $V(0.5, d_e)$ for all hours of the day throughout the entire year. For some applications it is important to know something about the diurnal and seasonal changes that

THE ADJUSTMENT FACTOR $V(0.5, d_e)$ FOR 8 CLIMATIC REGIONS

$$A(0.5) = A_{cr} - V(0.5, d_e) \text{ dB}$$

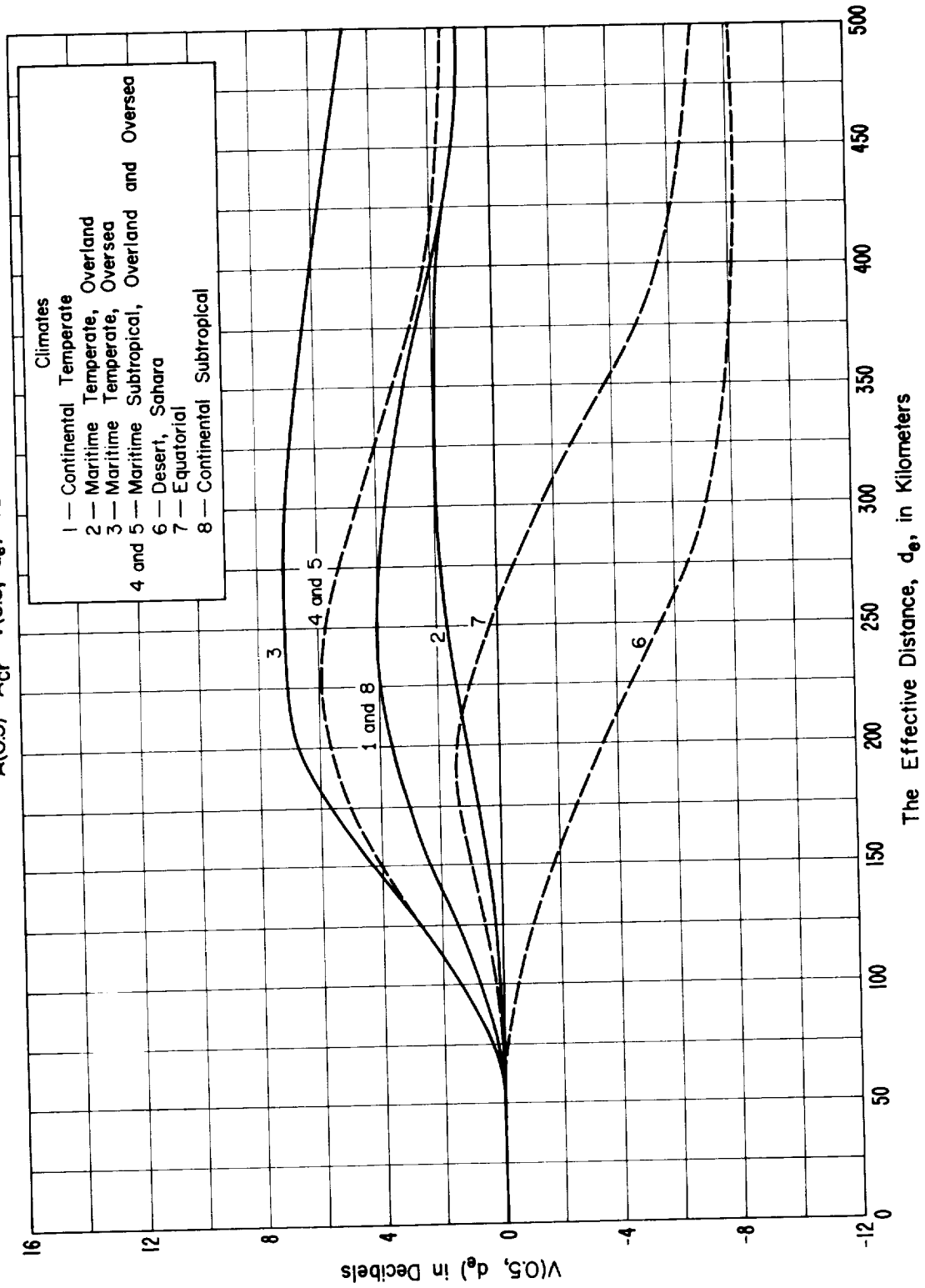


Figure 1.1

may be expected. Such changes have been studied in the continental United States where a large amount of data, recorded for periods of at least a year, is available. The variation of long-term median levels with season usually shows maximum attenuation in midwinter, especially on winter afternoons, and minimum attenuation during the summer months, particularly during the morning hours.

The data were divided into summer and winter periods, May through October, and November through April, and the hours of the day were divided into four groups providing the following eight time blocks:

<u>No.</u>	<u>Months</u>	<u>Hours</u>
1	Nov - Apr	0600 - 1300
2	Nov - Apr	1300 - 1800
3	Nov - Apr	1800 - 2400
4	May - Oct	0600 - 1300
5	May - Oct	1300 - 1800
6	May - Oct	1800 - 2400
7	May - Oct	0000 - 0600
8	Nov - Apr	0000 - 0600

The data for time blocks 1, 2, 3, and 8 were combined to form a winter all-hours group and the data for time blocks 4, 5, 6, and 7 were combined to form a summer all-hours group. The adjustment factor $V(0.5)$ for each of these periods of time is shown in figure 1.2 for the United States, which is typical of a continental temperate climate.

For other climatic regions an indication of the seasonal variation to be expected may be obtained from the annual range of monthly mean N_s shown in figure 1.3. Much of the data in the United States was recorded where the annual range of monthly mean N_s is 40 to 50 N-units. In regions where the annual range is less than 20 N-units, seasonal variations

THE FUNCTION $V(0.5, d_e)$ FOR VARIOUS PERIODS OF TIME IN THE U.S.A.

$$A(0.5) = A_{cr} - V(0.5, d_e) \text{ dB}$$

TIME BLOCK	
WINTER	SUMMER
1. NOV. - APR. 0600 - 1300	4. MAY - OCT. 0600 - 1300
2. NOV. - APR. 1300 - 1800	5. MAY - OCT. 1300 - 1800
3. NOV. - APR. 1800 - 2400	6. MAY - OCT. 1800 - 2400
8. NOV. - APR. 0000 - 0600	7. MAY - OCT. 0000 - 0600

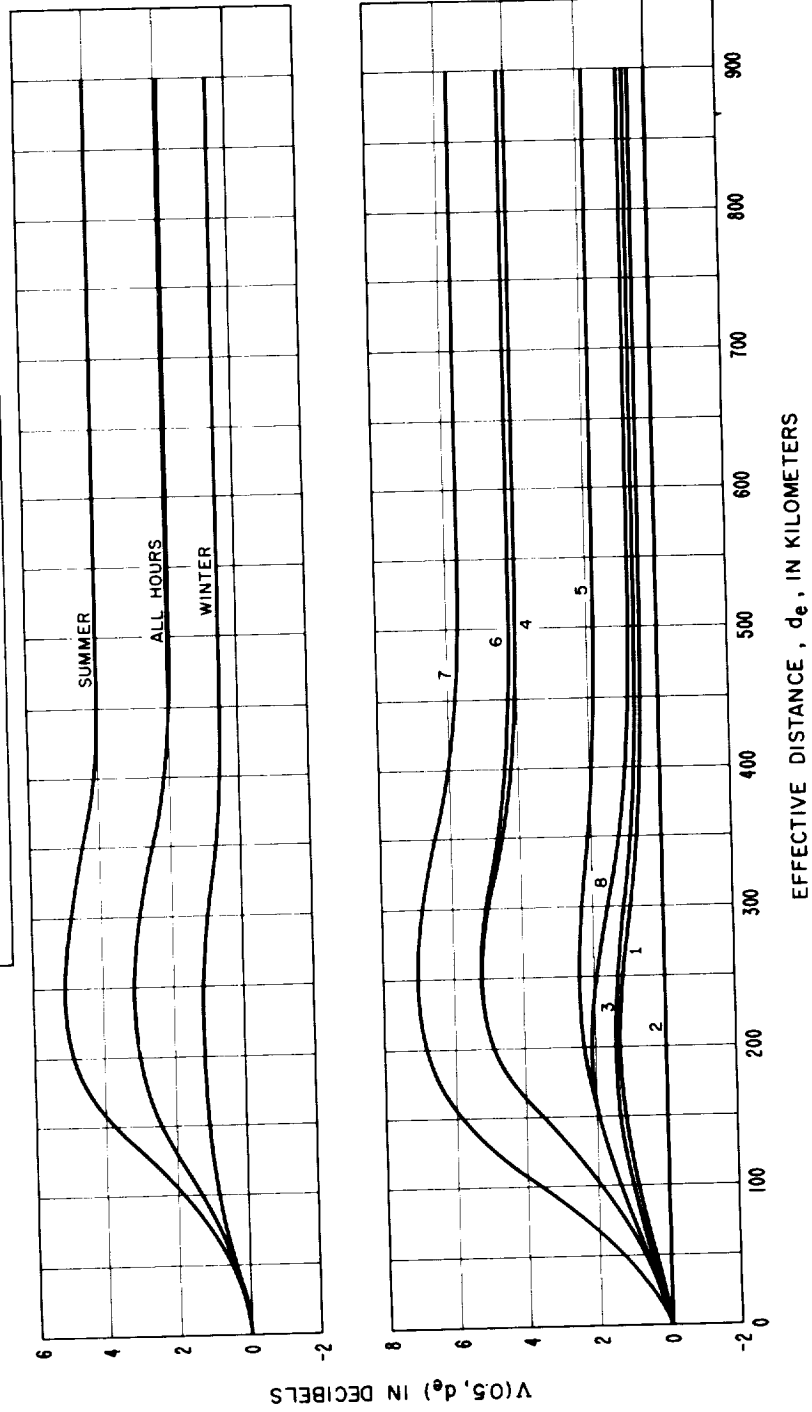


Figure 1.2

ANNUAL RANGE OF MONTHLY MEAN N_s

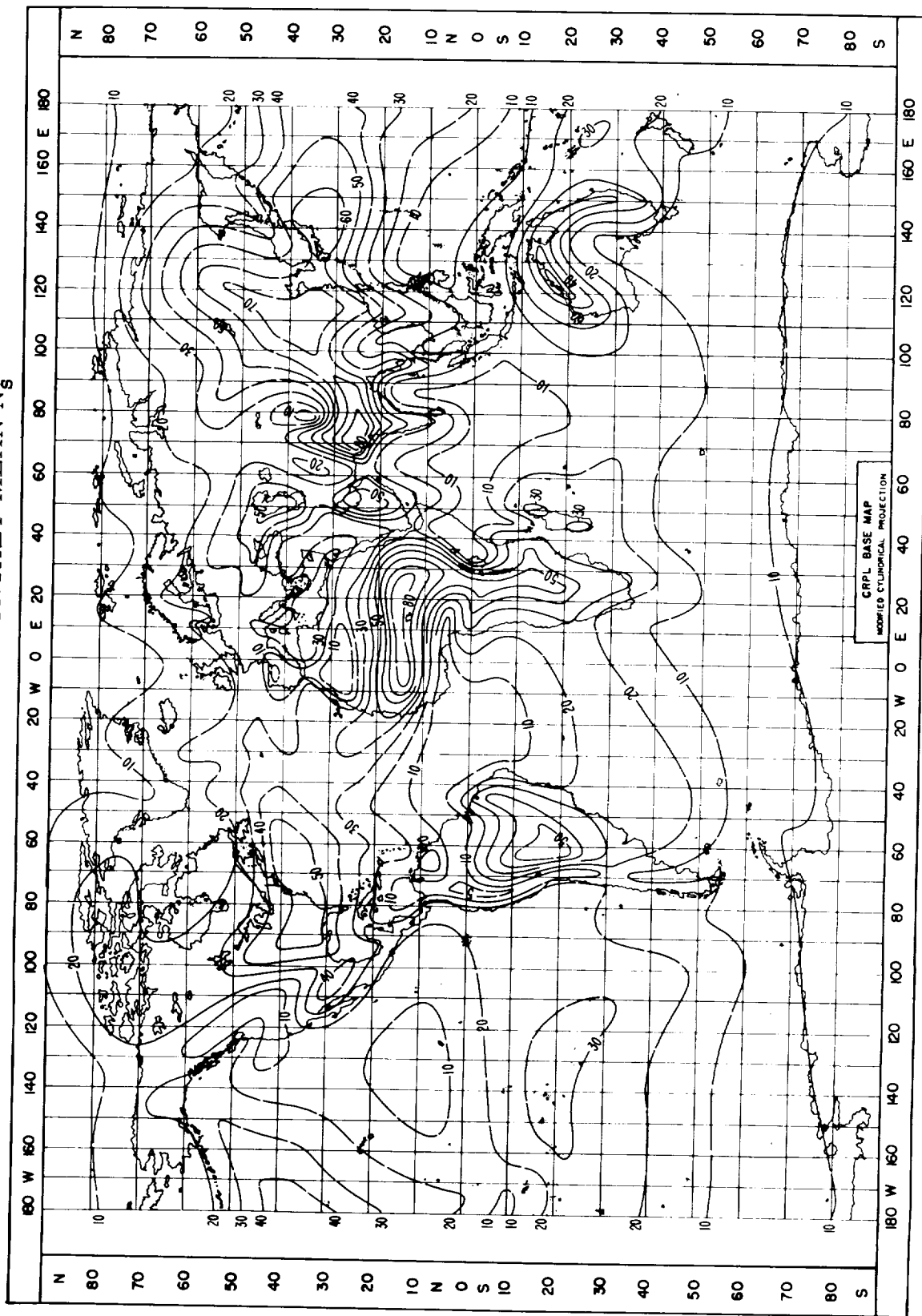


Figure 1.3

are expected to be negligible. One would also expect less diurnal change, for example, in a maritime temperate climate where changes in temperature during the day are less extreme. In climates where the surface refractivity N_s changes considerably throughout the year, the consecutive 4-to 6-month period when the monthly mean value of N_s is lowest is assumed to correspond to "winter", whatever months are involved.

1-1.2 Long-Term Variability About the Median

Long-term variability, identified with the variability of hourly median values of attenuation, usually results from slow changes in average atmospheric refraction, in the degree of atmospheric stratification, or in the intensity of atmospheric turbulence. Estimates of long-term variability to be expected are important to insure adequate service and to avoid possible interference between services operating on the same or adjacent frequencies.

Estimates of variability in time about the long-term median attenuation are based on measurements. Hourly median values of transmission loss recorded for a long period of time over a single path may show wide variations, especially in areas where marked seasonal changes occur in the surface refractivity N_s and in the refractive index gradient.

Figure 1.4 shows the variability expected at 100 MHz in a continental temperate climate for all hours of the year, for the summer hours, and for the winter hours. The curves show the interdecile range of attenuation as a function of the effective distance d_e . They were drawn through medians of a large amount of data recorded in the frequency range 88 to 108 MHz. The curve $Y_o(0.1)$ is the difference between the median attenuation $A(0.5)$ and the attenuation $A(0.1)$ not exceeded 10 percent of the time. Similarly, the curve $Y_o(0.9)$ represents the difference between the median attenuation and the attenuation $A(0.9)$ not exceeded 90 percent of the time:

$$Y_o(0.1) = A(0.5) - A(0.1) \equiv L_b(0.5) - L_b(0.1) \text{ dB} \quad (1.4a)$$

$$Y_o(0.9) = A(0.5) - A(0.9) \equiv L_b(0.5) - L_b(0.9) \text{ dB} \quad (1.4b)$$

The variability in time of attenuation over a given path also depends on frequency-related effects. The frequency factors $g(0.1, f)$ and $g(0.9, f)$ shown in figure 1.5 adjust the predicted variability for 100 MHz, shown in figure 1.4 for use at other frequencies:

$$Y(0.1) = Y_o(0.1) g(0.1, f) \text{ dB} \quad (1.5a)$$

$$Y(0.9) = Y_o(0.9) g(0.9, f) \text{ dB} . \quad (1.5b)$$

The empirical curves $g(q, f)$ should not be regarded as an estimate of the dependence of long-term variability on frequency; they represent only an average of many effects, some of which are frequency-sensitive. The apparent frequency dependence is a function of the relative dominance of various propagation mechanisms, which in turn depends on climate, time of day, season and the particular types of terrain profiles for which data are available. An allowance for year-to-year variability is included in $g(q, f)$.

The estimates of A_{cr} , $V(0.5)$, $Y(0.1)$ and $Y(0.9)$ may be used to predict an entire cumulative distribution of attenuation relative to free space using the following ratios:

$Y(0.0001) = 3.33 Y(0.1)$	$Y(0.9999) = 2.90 Y(0.9)$
$Y(0.001) = 2.73 Y(0.1)$	$Y(0.999) = 2.41 Y(0.9)$
$Y(0.01) = 2.00 Y(0.1)$	$Y(0.99) = 1.82 Y(0.9)$

LONG-TERM POWER-FADING FUNCTION $Y_0(q, d_e)$
CONTINENTAL TEMPERATE CLIMATE

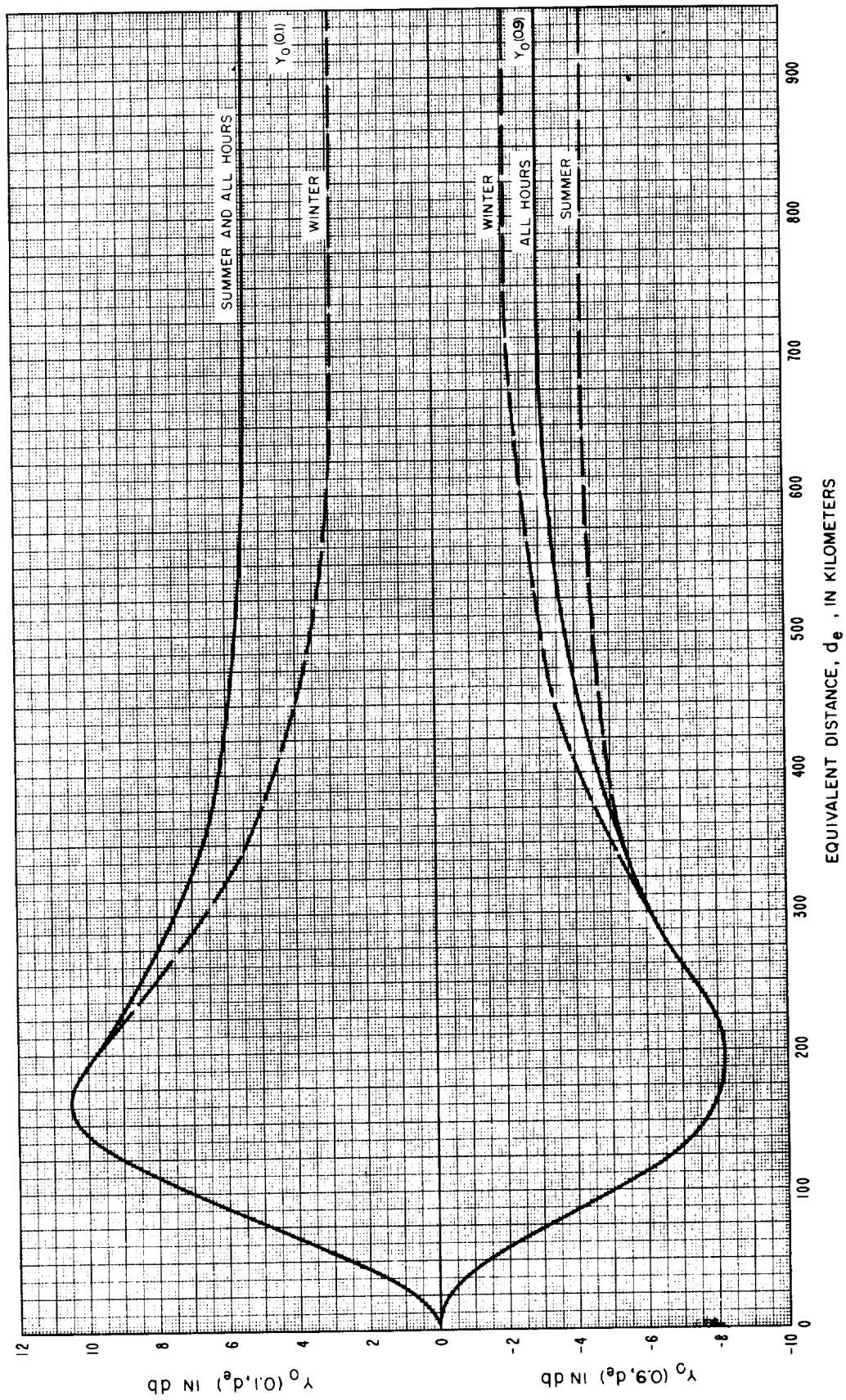


Figure 1.4

THE FREQUENCY FACTOR $g(q,f)$
BASED ON U.S. OVERLAND DATA

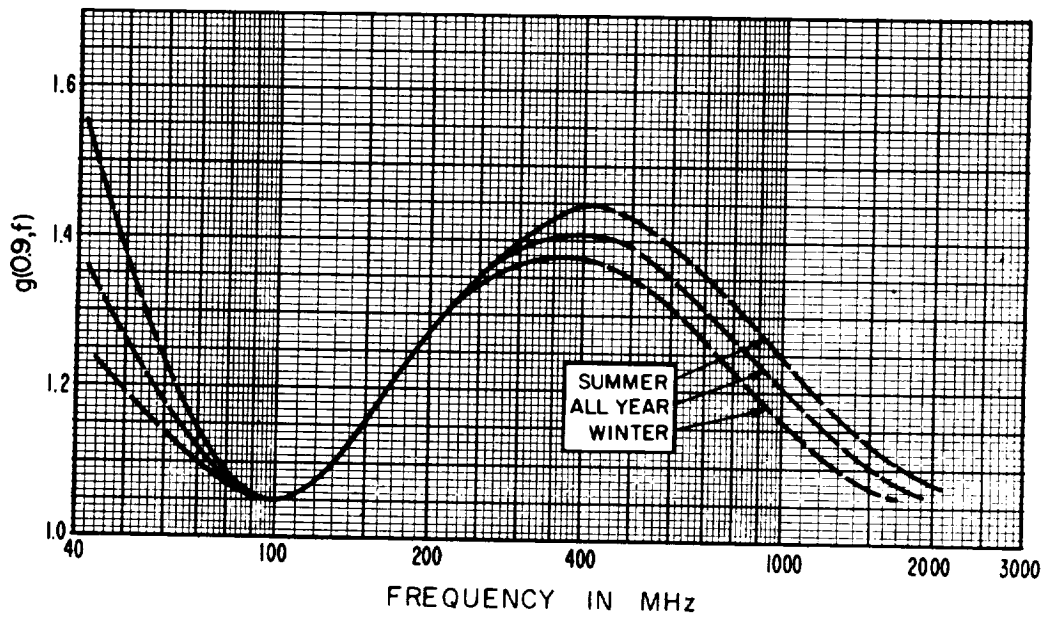
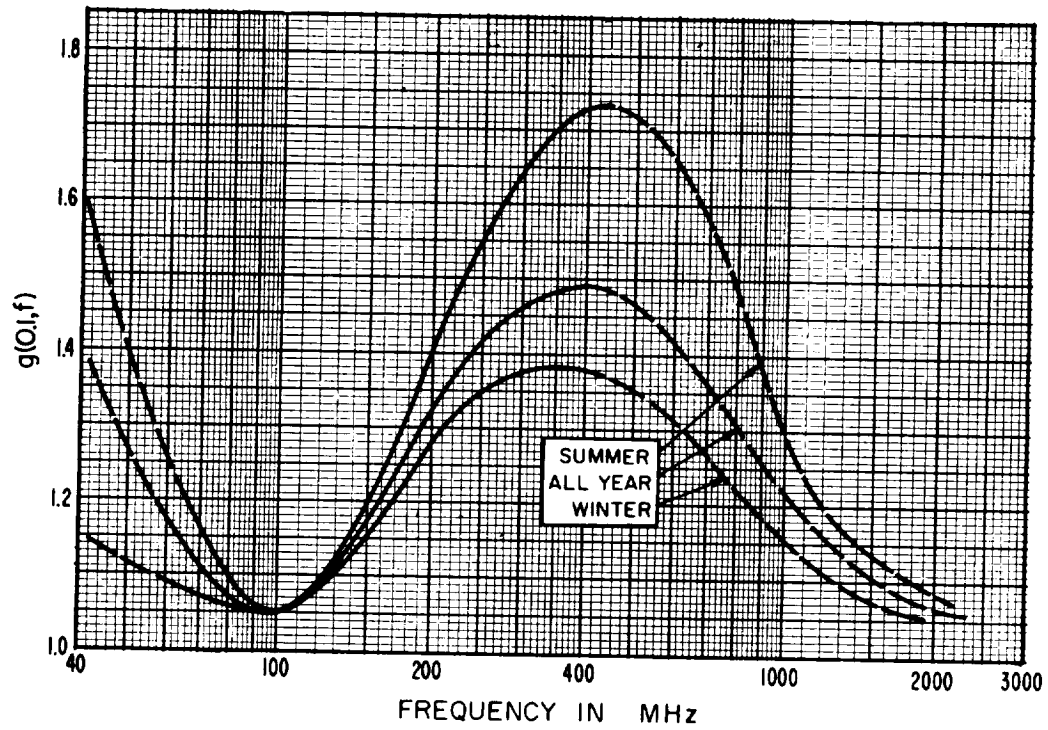


Figure 1.5

Figure 1.6 shows such a predicted distribution compared with values measured over a path for more than 2 years. The figure shows the bi-variate distribution that is typical of a continental temperate climate.

The preceding discussion and figures 1.2, 1.4, and 1.5 are for a continental temperate climate and are based largely on data from measurements made in the United States and in West Germany. Data from other geographical regions were used to develop curves for other climates, notably data from the British Isles and the west coastal areas of Europe that characterize the maritime temperate overland and maritime temperate overseas curves. The curves presented by Rice et al. (1967) for other climatic regions are based on relatively few measurements.

1-1.3 Computer Method for Estimating Long-Term Variability

Long-term variability about the median attenuation may be estimated in terms of a standard deviation, σ_{Ta} , and a standard normal deviate, $z_o(q)$. The symbol q , representing any fraction between 0 and 1, and the standard normal deviate $z_o(q)$ may be expressed in terms of the error function, $\text{erf } x$, and its inverse, $\text{erf}^{-1} x$.

$$q = 0.5 + 0.5 \text{ erf}(z_o / \sqrt{2}) \quad (1.6a)$$

$$z_o(q) = \sqrt{2} \text{ erf}^{-1}(2q-1). \quad (1.6b)$$

Then the long-term variability about the median exceeded at least a fraction q_T of the time may be expressed as

$$Y(q_T) = - \sigma_{Ta} z_o(q_T) \text{ dB}, \quad (1.7)$$

where q_T is any desired fraction of time and $Y(q_T)$ is the difference between the median attenuation $A(0.5)$ and the attenuation not exceeded a fraction q_T of the time.

COMPARISON OF MEASURED AND PREDICTED ATTENUATION, OVER A PATH FROM CHICAGO TO URBANA, ILLINOIS

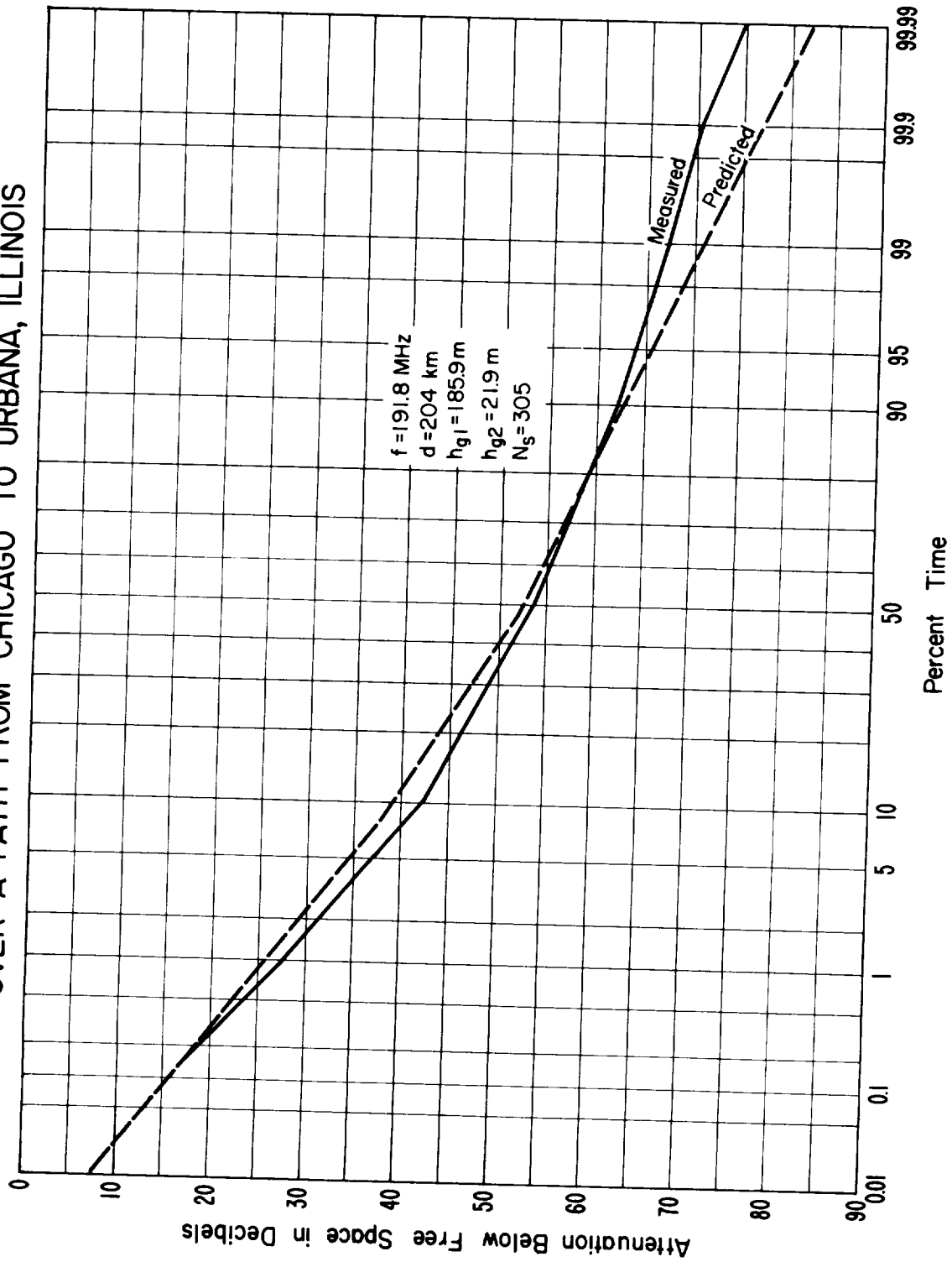


Figure 1.6

For a continental temperate climate, $Y(0.1)$ is not equal to $Y(0.9)$. The cumulative distribution may be considered as consisting of two parts, represented by standard deviations $\sigma_{Ta}(0.1)$ and $\sigma_{Ta}(0.9)$, where

$$Y(0.1) = 1.282 \sigma_{Ta}(0.1), \text{ and} \quad (1.8a)$$

$$Y(0.9) = -1.282 \sigma_{Ta}(0.9). \quad (1.8b)$$

Define $x = d_e / 100$.

For $d_e \leq 200$:

$$\sigma_{Ta}(0.1) = 8 x^2 g(0.1, f) \exp(-0.36 x^2). \quad (1.9a)$$

For $d_e > 200$:

$$\sigma_{Ta}(0.1) = g(0.1, f) [4.2 + 16.5 \exp(-0.77 x)]. \quad (1.9b)$$

For $d_e \leq 250$:

$$\sigma_{Ta}(0.9) = 4.6 x^2 g(0.9, f) \exp(-0.26 x^2). \quad (1.10a)$$

For $d_e > 250$:

$$\sigma_{Ta}(0.9) = g(0.9, f) [2.3 + 15 \exp(-0.6 x)]. \quad (1.10b)$$

For $60 \leq f \leq 1600$ MHz:

$$g(0.1, f) = 0.21 \sin \left[5.22 \log_{10}(f/200) \right] + 1.28, \quad (1.11a)$$

$$g(0.9, f) = 0.18 \sin \left[5.22 \log_{10} (f/200) \right] + 1.23. \quad (1.11b)$$

For $f > 1600$:

$$g(0.1, f) = g(0.9, f) = 1.05. \quad (1.11c)$$

Equations (1.11a-c) represent approximations to the empirical estimates of $g(0.1)$ and $g(0.9)$ plotted in figure 1.5 for all year.

1-2. Variability with Location

There is a path-to-path variation in the available wanted signal power that may be referred to as location variability. Such random variations from location to location for any given q_T may be assumed to be normally distributed with a standard deviation σ_{La} dB. Then $A(q_L)$ is the attenuation below free space not exceeded for at least a fraction q_L of all randomly chosen paths for which other parameters, such as frequency, antenna heights, and path length, are fixed. A value $q_L = 0.5$ would represent median conditions, while $q_L = 0.1$ would mean that the antennas are assumed to be located at sites selected to be among the best 10 percent of all possible locations within a given area. For low antennas, over irregular terrain, the best estimate from presently available data indicates a value of $\sigma_{La} \approx 10$ dB, as shown in annex 2. The location variability $Y(q_L)$ for any fraction q_L may be expressed in terms of the standard deviation σ_{La} and a standard normal deviate $z_o(q_L)$,

$$Y_L \equiv Y(q_L) = - \sigma_{La} z_o(q_L) \text{ dB}, \quad (1.12a)$$

where

$$z_o(q_L) = \sqrt{2} \operatorname{erf}^{-1} (2q_L - 1). \quad (1.12b)$$

1-3. Prediction Error and Service Probability

A communication link is assumed to provide satisfactory service of a given grade g_r if the available signal-to-noise ratio R exceeds the required protection ratio $R_r(g_r)$ for at least a fraction q_T of the time and a fraction q_L of all similar links. The noise-limited service requirement may be written as

$$R(q_T, q_L, Q) = R_o + Y_T + Y_L + Y_c \text{ dB}, \quad (1.13a)$$

where R_o is the median available signal-to-noise ratio and the symbols Y_T , Y_L , and Y_c represent biases or safety factors required to achieve protection for at least the desired fraction q_T of the time, the desired fraction q_L of locations, and with a probability Q . These biases are considered in the order given, allowing first for time availability q_T , then for location variability q_L , with q_T fixed, and finally for service probability Q , with both q_T and q_L fixed. That is, we may write (1.13a) as

$$R(q_T, q_L, Q) = R_o + Y_T(q_T) + Y_L(q_T, q_L) + Y_c(q_T, q_L, Q) \text{ dB}. \quad (1.13b)$$

In this discussion we consider interference due to noise at the terminals of the receiving antenna, including both internal system noise and externally generated unwanted signals whose effect can be represented by an equivalent noise power whenever the probability of power-independent distortion is negligible. Further discussion of interference from unwanted signals may be found in annex V of the report by Rice et al. (1967).

The biases Y_T , Y_L , and Y_c expressed in decibels are assumed to be normally distributed in time and with location, with errors of prediction also normally distributed. The biases may then be expressed in

terms of a standard normal deviate $z_o(q)$, and the variance of the available signal-to-noise ratio in time, σ_T^2 , with location, σ_L^2 , and with prediction error, σ_c^2 . The variance σ_T^2 is defined in terms of variances in time σ_{Ta}^2 and σ_{Tn}^2 associated with the available wanted signal power W_a and the noise power W_n , respectively, and of ρ_T , the coefficient of correlation between them:

$$\sigma_T^2 = \sigma_{Ta}^2 + \sigma_{Tn}^2 - 2\rho_T \sigma_{Ta} \sigma_{Tn} \text{ dB}^2, \quad (1.14a)$$

where σ_{Ta} is defined by (1.9) and (1.10).

Similarly the path-to-path variance σ_L^2 of the available signal-to-noise ratio may be expressed as:

$$\sigma_L^2 = \sigma_{La}^2 + \sigma_{Ln}^2 - 2\rho_L \sigma_{La} \sigma_{Ln} \text{ dB}^2, \quad (1.14b)$$

where σ_{La} and σ_{Ln} are the location-to-location standard deviations of the available wanted signal power W_a and the noise power W_n , respectively, and ρ_L is the normalized coefficient of correlation between them. For service limited by a background of man-made noise, a study of available data indicates that $\sigma_{Tn} \simeq 4$ dB and $\sigma_{Ln} \simeq 4$ dB, while $\sigma_{La} \simeq 10$ dB, as previously stated. The correlation coefficients ρ_T and ρ_L are usually assumed to be positive because when the received signal is high as a result of good propagation conditions the noise level is likely to be high also.

The estimated standard error of prediction σ_c may be defined in terms of the variance σ_{ca}^2 associated with the received power exceeded at least a fraction q_T of the time at a fraction q_L of the locations, the variance σ_{cn}^2 associated with the corresponding noise power, and the correlation ρ_c between them, with additional allowances for time and location variability:

$$\sigma_c^2 = \sigma_{ca}^2 + \sigma_{cn}^2 - 2\rho_c \sigma_{ca} \sigma_{cn} + 0.12 \sigma_T^2 z_o^2(q_T) + 4 z_o^2(q_L) + \sigma_x^2 \text{ dB}^2, \quad (1.15)$$

$$\text{where } \sigma_{ca} = 5 [1 + 0.6 \exp(-d_e/100)] \text{ dB}. \quad (1.16)$$

The estimated prediction error σ_c includes an allowance σ_x for errors in predicting the required signal-to-noise ratio $R_r(g_r)$. The coefficients 0.12 and 4 in (1.15) and 5 and 0.6 in (1.16) represent the best empirical estimates presently available.

Estimates of $\sigma_{cn} \simeq 4 \text{ dB}$, $\sigma_x \simeq 5 \text{ dB}$ are probably adequate, and the standard deviation σ_{ca} is computed using (1.16) as a function of the effective distance d_e , defined by (1.3). Little information is available regarding the correlation ρ_c between prediction errors for wanted signals and noise. The correlation is expected to be positive and less than unity.

The safety factors or biases shown in (1.13) may be allowed for separately in the order given. The bias Y_T , assuming $q_T = 0.99$, is the difference between an available signal-to-noise ratio $R(0.99, q_L) \text{ dB}$ exceeded at least 99 percent of the time at any location and the median-time value $R(0.5, q_L)$. Then the bias Y_L , assuming $q_T = 0.99$ and $q_L = 0.1$, is the difference between the ratio $R(0.99, 0.1)$ exceeded at least 99 percent of the time at 10 percent of the locations and the median-time, median-location value $R(0.5, 0.5)$:

$$Y_T = -\sigma_T(\rho_T) z_o(q_T) \text{ dB}, \quad (1.17a)$$

$$Y_L = -\sigma_L(\rho_L) z_o(q_L) \text{ dB}, \quad (1.17b)$$

where ρ_T is the time correlation and ρ_L is the path-to-path correlation between wanted signals and noise.

The bias or safety margin,

$$Y_c = -\sigma_c(\rho_c) z_o(Q) \text{ dB}, \quad (1.17c)$$

required to achieve a given signal-to-noise ratio with a service probability Q depends in turn on the correlation ρ_c assumed between prediction errors for wanted signals and noise in (1.15).

The available wanted signal power is

$$W_a = W_t + G_p - L_b \text{ dBW}, \quad (1.18)$$

where W_t is the total radiated power in dBW, G_p is the path antenna gain in dB, and L_b is the basic transmission loss in dB. The path antenna gain may be expressed as

$$G_p = G_1 + G_2 - L_{gp} \text{ dB}, \quad (1.19)$$

where G_1 and G_2 are the free space antenna gains in decibels relative to an isotropic radiator. The loss in path antenna gain, L_{gp} , may be approximated as follows:

$$\text{For } G_1 + G_2 \leq 50 \text{ dB} \quad L_{gp} \leq 1 \text{ dB}, \quad (1.20a)$$

$$\text{For } 50 \leq G_1 + G_2 \leq 100 \text{ dB}$$

$$L_{gp} \approx 0.07 \exp[0.055 (G_1 + G_2)] \text{ dB}. \quad (1.20b)$$

In most situations we assume that free-space gains are realized. Where the loss in gain may be appreciable, other methods for estimating G_p are described in the report by Rice et al. (1967). The approximation in (1.20b) tends to give substantially larger values of L_{gp} for large $G_1 + G_2$ than the methods reported by Rice et al. Experience with actual communication links at 4500 MHz using 10 m parabolic reflectors suggests that (1.20b) may provide more realistic estimates of link performance. However, more theoretical and experimental studies are needed to resolve this problem.

The available signal to noise ratio R is

$$R = W_a - W_n \text{ dB}, \quad (1.21)$$

where W_n is the total equivalent r-f noise power in dBW. It is often convenient to express W_a and W_n as power spectral densities, in dB(W/kHz), rather than expressing the total power in the r-f passband of the receiver in dBW.

The powers, or power spectral densities, W_a and W_n and the basic transmission loss L_b are assumed to be normally distributed in time and from path to path. The median values of W_a , W_n , and L_b may be denoted as W_o , W_{no} , and L_{bo} . Then the median available signal-to-noise ratio R_o is

$$R_o = W_o - W_{no} = W_t + G_p - L_{bo} - W_{no} \text{ dB}, \quad (1.22)$$

and the signal-to-noise ratio R may be expressed in terms of its median value R_o and the biases Y_T , Y_L and Y_c :

$$R = R_o + Y_T + Y_L + Y_c \text{ dB}, \quad (1.23)$$

where

$$Y_c = -\sigma_c z_o(Q) \text{ dB}.$$

The grade of service at any receiving location is satisfactory if the available wanted signal-to-noise ratio R exceeds the ratio R_r required for satisfactory service in the presence of fine-grained time and space variations of signals and noise, that is, if $R - R_r > 0$, where

$$R - R_r = R_o + Y_T + Y_L - R_r - \sigma_c z_o(Q) \text{ dB}. \quad (1.24)$$

Substituting (1.22) in (1.24) and defining

$$S_o = W_t + G_p - R_r - W_{no} + Y_T + Y_L \text{ dB}, \quad (1.25)$$

we can write

$$R - R_r = S_o - L_{bo} - \sigma_c z_o(Q). \quad (1.26)$$

The service probability Q is calculated by setting $R - R_r$ equal to zero and solving for Q in terms of the error function:

$$\sigma_c z_o(Q) = S_o - L_{bo} \text{ dB}, \quad (1.27a)$$

$$Q = 0.5 + 0.5 \operatorname{erf}[(S_o - L_{bo})/(\sigma_c \sqrt{2})]. \quad (1.27b)$$

Or, for a given value of Q , such as $Q_o = 0.95$, (1.27a) may be solved for the value of S_o required to achieve this service probability.

1-4 List of Symbols and Abbreviations

In the following list the English alphabet precedes the Greek alphabet and lower case letters precede upper case letters. In general, upper case letters are used for quantities expressed in decibels.

a an effective earth's radius that allows for average refraction of radio rays near the surface of the earth, (1.2a).

A_{cr} a predicted reference value of attenuation below free space, expressed in decibels, (1.1).

$A(q_L)$ attenuation below free space not exceeded for at least a fraction q_L of all randomly chosen paths for which other parameters, such as frequency, antenna heights, and path length, are fixed.

$A(0.5)$ long-term median value of attenuation below free space for a specified period of time, climatic region, etc. (1.1).

$A(0.1)$, $A(0.9)$ attenuation below free space not exceeded for 10 percent and 90 percent of the time, respectively, (1.4).

d great circle distance in kilometers

dB abbreviation for decibel.

d_e an effective distance in kilometers, defined by (1.3).

d_{Lo} the sum of the smooth-earth horizon distances for an effective earth's radius $a = 9000$ km, (1.2).

d_{s1} the distance between horizons for which diffraction and forward scatter losses are approximately equal over a smooth earth, (1.2a).

$\text{erf } x$ the error function of x , (1.6), defined as $H(x) = \frac{2}{\sqrt{\pi}} \int_0^x e^{-\alpha^2} d\alpha$.

$\text{erf}^{-1} x$ the inverse error function of x , (1.6).

- f radio wave frequency, expressed in megahertz, (1.2).
- $g(q, f)$ frequency factors used to adjust the predicted variability in time at 100 MHz for use at other frequencies, (1.5) and figure 1.4.
- $g(0.1, f)$, $g(0.9, f)$ frequency factors used to adjust $Y_o(0.1)$ and $Y_o(0.9)$, respectively, (1.5) and figure 1.4.
- G_p path antenna gain in decibels above the unit gain of an isotropic radiator, (1.19).
- G_1, G_2 free-space antenna gains, in decibels relative to an isotropic radiator, of the transmitting and receiving antennas, respectively, (1.19).
- h_{e1} , h_{e2} effective heights in meters of the transmitting and receiving antennas, respectively, (1.2b).
- L_b basic transmission loss in decibels, (1.18).
- L_{bo} , $L_b(0.5)$ long-term median value of basic transmission loss in decibels, (1.4) and (1.22).
- $L_b(0.1)$, $L_b(0.9)$ basic transmission loss not exceeded for fractions 0.1 and 0.9 of hourly medians, (1.4).
- L_{gp} loss in path antenna gain, (1.19) and (1.20).
- N_s atmospheric refractivity at the surface of the earth.
- q a symbol that represents any fraction between 0 and 1, (1.6).
- q_L any desired fraction of all randomly chosen paths for which such parameters as frequency, antenna heights, and path length are fixed, (1.12).
- q_T any desired fraction of time, (1.7).
- Q a symbol that represents service probability, (1.17) and (1.27).

- R the available signal-to-noise ratio expressed in decibels, (1.21).
- R_r the signal-to-noise ratio required to provide satisfactory service in the presence of fine-grained time and space variations of signals and noise, (1.24).
- R_o median value of the available signal-to-noise ratio expressed in decibels, (1.22).
- $R(q_T, q_L, Q)$ the signal-to-noise ratio available for at least a desired fraction q_T of the time at a desired fraction q_L of locations, with a probability Q , (1.13).
- $R(0.5, q_L)$ the median time value of the available signal-to-noise ratio at any location.
- $R(0.99, q_L)$ the available signal-to-noise ratio exceeded at least 99 percent of the time at any location.
- $R(0.99, 0.1)$ the available signal-to-noise ratio exceeded at least 99 percent of the time at 10 percent of the locations.
- S_o a term defined by (1.25).
- $V(0.5)$ the difference in decibels between a computed reference value A_{cr} and the median attenuation $A(0.5)$ expected for a specified climate, season, time of day, or desired group of paths, (1.1).
- $V(0.5, d_e)$ the adjustment factor $V(0.5)$ as a function of the effective distance d_e , figure 1.1.
- W_a radio frequency signal power or power spectral density that would be available from an equivalent loss-free receiving antenna, (1.18).
- W_n the total equivalent r-f noise power or power spectral density at the terminals of a loss-free receiving antenna, including

both internal system noise referred to these terminals and externally generated unwanted signals whose effect can be represented by an equivalent noise power, (1.21).

W_t the total power radiated from a transmitting antenna in a given band of radio frequencies, (1.18).

W_{no} the median value of W_n , (1.22).

W_o the median value of W_a , (1.22).

x a parameter defined as $x = d_e / 100$ used in (1.9) and (1.10).

Y_c an allowance in decibels for prediction error, (1.13) and (1.17).

Y_L an allowance in decibels for random variations in transmission loss from location to location, (1.13) and (1.17).

Y_T an allowance in decibels for long-term variability in time, (1.13) and (1.17).

$Y(q_L)$ the location variability for any fraction q_L of all randomly chosen paths for which other parameters, such as frequency, path length and antenna heights, are fixed, (1.12a).

$Y(q_T)$ the variability in time about the long-term median exceeded at least a fraction q_T of the time, (1.7).

$Y(0.1), Y(0.01)$ the difference between the long-term median at $Y(0.9), Y(0.99)$ and that not exceeded for fractions 0.1, 0.01, 0.9, and 0.99 of the time, respectively, (1.5) and following discussion.

$Y_o(0.1), Y_o(0.9)$ values of $Y(0.1)$ and $Y(0.9)$, respectively, expected at 100 MHz in a continental temperate climate, plotted versus an effective distance d_e , figure 1.4 and (1.4).

z_o a standard normal deviate, (1.6).
 $z_o(q)$ a standard normal deviate where the symbol q represents any fraction between zero and unity, (1.6).
 $z_o(q_L)$ a standard normal deviate where the symbol q_L represents any desired fraction of all randomly chosen paths for which such parameters as frequency, distance, and antenna heights are fixed, (1.12) and (1.17).
 $z_o(q_T)$ a standard normal deviate where the symbol q_T represents any desired fraction of time, (1.7) and (1.17).
 $z_o(Q)$ a standard normal deviate where the symbol Q represents the desired service probability, (1.17).

θ_{s1} the angular distance at which scatter and diffraction transmission losses are approximately equal over a smooth earth of effective radius $a = 9000$ km, (1.2).

ρ_c the cross-correlation coefficient between the variations of the received signal power exceeded at least a fraction q_T of the time at a fraction q_L of locations and variations of the corresponding noise power, (1.15).

ρ_L the coefficient of correlation between the location-to-location variations of the available wanted signal power and the noise power, (1.14b).

ρ_T the coefficient of correlation in time between the available wanted signal power and the noise power, (1.14a).

σ_c estimated prediction error, defined by (1.15).

σ_{ca}, σ_{cn} the standard deviations of the received wanted signal power and noise power, respectively, exceeded at least a

fraction q_T of the time at a fraction q_L of the locations,
 (1.15); σ_{ca} is defined by (1.16), $\sigma_{cn} \approx 4$ dB.

$\sigma_c(\rho_c)$ a value of σ_c computed using a specified value of ρ_c , (1.17c).

σ_L, σ_L^2 the standard deviation and variance, respectively, from
 location to location of the available signal-to-noise ratio,
 (1.14b).

σ_{La}, σ_{Ln} the location-to-location standard deviations of the avail-
 able wanted signal power and noise power respectively,
 (1.14b); available data indicate $\sigma_{La} \approx 10$ dB and $\sigma_{Ln} \approx$
 4 dB.

$\sigma_L(\rho_L)$ the location-to-location standard deviation of the available
 signal-to-noise ratio assuming a specified value of ρ_L ,
 (1.17b).

σ_T, σ_T^2 the standard deviation and variance, respectively, of the
 available wanted signal-to-noise ratio in time, (1.14a).

σ_{Ta}, σ_{Tn} the standard deviation in time of the available wanted
 signal power and noise power, respectively, (1.14a); σ_{Ta}
 is computed using (1.9) and (1.10); available data indicate
 $\sigma_{Tn} \approx 4$ dB.

$\sigma_{Ta}(0.1), \sigma_{Ta}(0.9)$ standard deviations representing the bi-normal
 time distribution of attenuation relative to free space, illus-
 trated in figure 1.6, (1.9), and (1.10).

$\sigma_T(\rho_T)$ the standard deviation in time of the available signal-to-
 noise ratio assuming a specified value of ρ_T , (1.17a).

σ_x a term used in estimating prediction error that allows for
 errors in predicting the required signal-to-noise ratio, $\sigma_x \approx$
 5 dB, (1.15).

ANNEX 2

STUDIES OF TERRAIN PROFILES

2-1 Introduction

Radio transmission loss over irregular terrain, for the frequencies and distances considered in this report, depends mainly on the profile characteristics of a great circle path between transmitting and receiving antennas. Some allowance is made for vegetation and man-made clutter, while large buildings and dense vegetation are treated in the same way as features of the terrain itself.

For point-to-point transmission loss calculations for a given terrain profile and antenna locations, the parameters of interest, in order of their usual importance, are the sum of horizon ray elevation angles θ_e , the effective antenna heights $h_{e1,2}$, the path distance d , the interdecile range of terrain elevations $\Delta h(d)$, the horizon distances $d_{L1,2}$, and the effective dielectric constant ϵ , and conductivity σ , for a terrain or sea surface. The definition, use, and importance of these parameters are explained in the body of the report.

To obtain calculated reference values of propagation attenuation for specified sets of terrain profiles and antenna locations, or to obtain estimates of variability from location to location with several or all of the above parameters fixed, within limits, and to estimate prediction errors, statistical descriptions of these parameters are needed, especially estimates of median values for commonly occurring situations. Terrain statistics were developed for selected areas by reading a large number of terrain profiles. Each profile is represented by discrete elevations at uniform distances of half a kilometer. The areas

selected for terrain study include one in the tree-covered rolling hills of northeastern Ohio, and one in the plains and foothills of Colorado, where an exhaustive transmission loss measurement program was carried out (Miles and Barsis, 1966). About 100 paths, each 60 km in length, were selected at random throughout the continental United States to provide an estimate of "average" terrain statistics. Two limited regions, one entirely in the mountains crossing the Continental Divide and the other entirely in the plains, were chosen for an intensive study of correlation along and between profiles.

Within each region selected for intensive study, 36 profiles, 60 km in length, were read in each of six directions separated in azimuth by 30° , providing a total of 216 profiles that form a rather closely spaced "grid" over a 100 km square area. The 101 "random" paths throughout the continental United States were so chosen that they would not approach or cross each other. The separation between adjacent paths ranges from 60 to 320 km with a median separation of about 200 km. These "random" paths lie chiefly in four directions, N-S, E-W, NE-SW, and NW-SE. None are located in Colorado which is well represented by the "plains" and "mountains" grids and the area over which radio propagation measurements were made.

In the measurement program antenna sites were located randomly on or near roads without regard to the proximity of natural or man-made obstacles. To correspond with these measurements the path profiles were also selected arbitrarily, without regard to the location of hills or other obstacles. Each of the 60 km profiles in the mountains, plains, and random U. S. samples was considered in lengths of 5, 10, 20, 30, 40, 50, and 60 km, starting from one end of each profile, to study the effect

of path length on various terrain parameters. A further statistical terrain study, assuming antenna sites placed advantageously on hilltops, should be carried out to show the improvement in radio transmission to be expected by increasing the effective height of one or both antennas.

2-2 The Terrain Parameter Δh

The path profiles described above were used to obtain estimates of several terrain parameters for paths of a given length. Of these the interdecile range $\Delta h(d)$ of terrain heights, above and below a straight line fitted by least squares to elevations above sea level, was calculated at fixed distances. Usually the median values of $\Delta h(d)$, for a specified group of profiles, increase with path length to an asymptotic value, Δh . As explained in detail in the body of the report, this parameter Δh is used to characterize nondeterministic aspects of terrain irregularity.

Figures 2.1 and 2.2 show cumulative distributions of $\Delta h(d)$ for the random U.S. mountain, and plains paths. Each distribution represents 101 profiles for random terrain and 216 profiles each for mountain and plains terrain. These distributions show a consistent increase in the median value of $\Delta h(d)$ with increasing path length. As one would expect, the variance of $\Delta h(d)$ for the randomly chosen paths is much greater than that for the more homogeneous terrain included in the plains and mountain areas.

Distributions of $\Delta h(d)$ for the area in Colorado where radio measurements were made are shown in figure 2.3. These paths are located in an area that includes plains, foothills, and mountains, but were considered in only two groups. For these much smaller groups of profiles, the same trends are observed, the median value of $\Delta h(d)$ increasing consistently with increasing path length. This trend was not observed in the

CUMULATIVE DISTRIBUTIONS OF $\Delta h(d)$
U.S. Random Paths

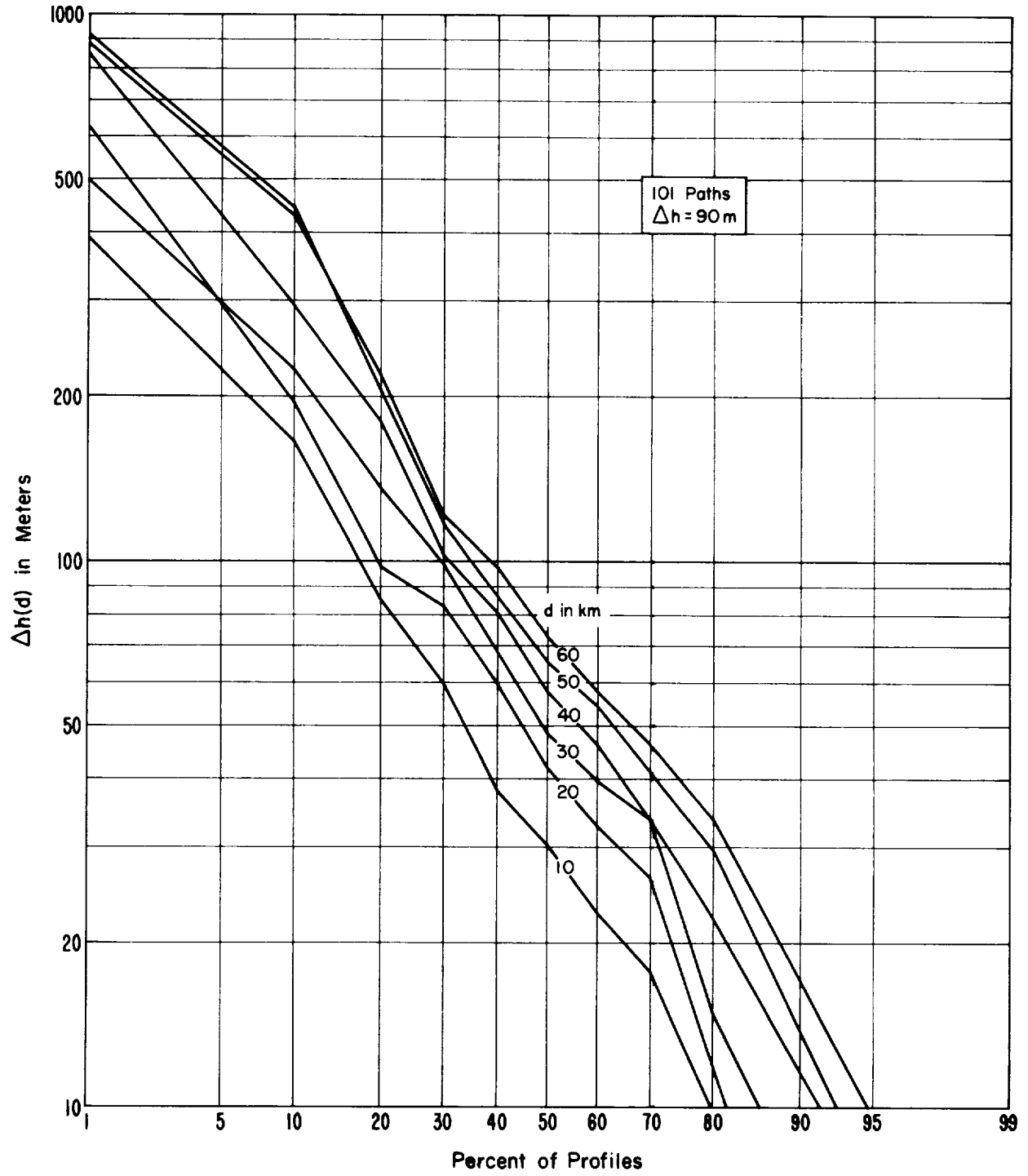
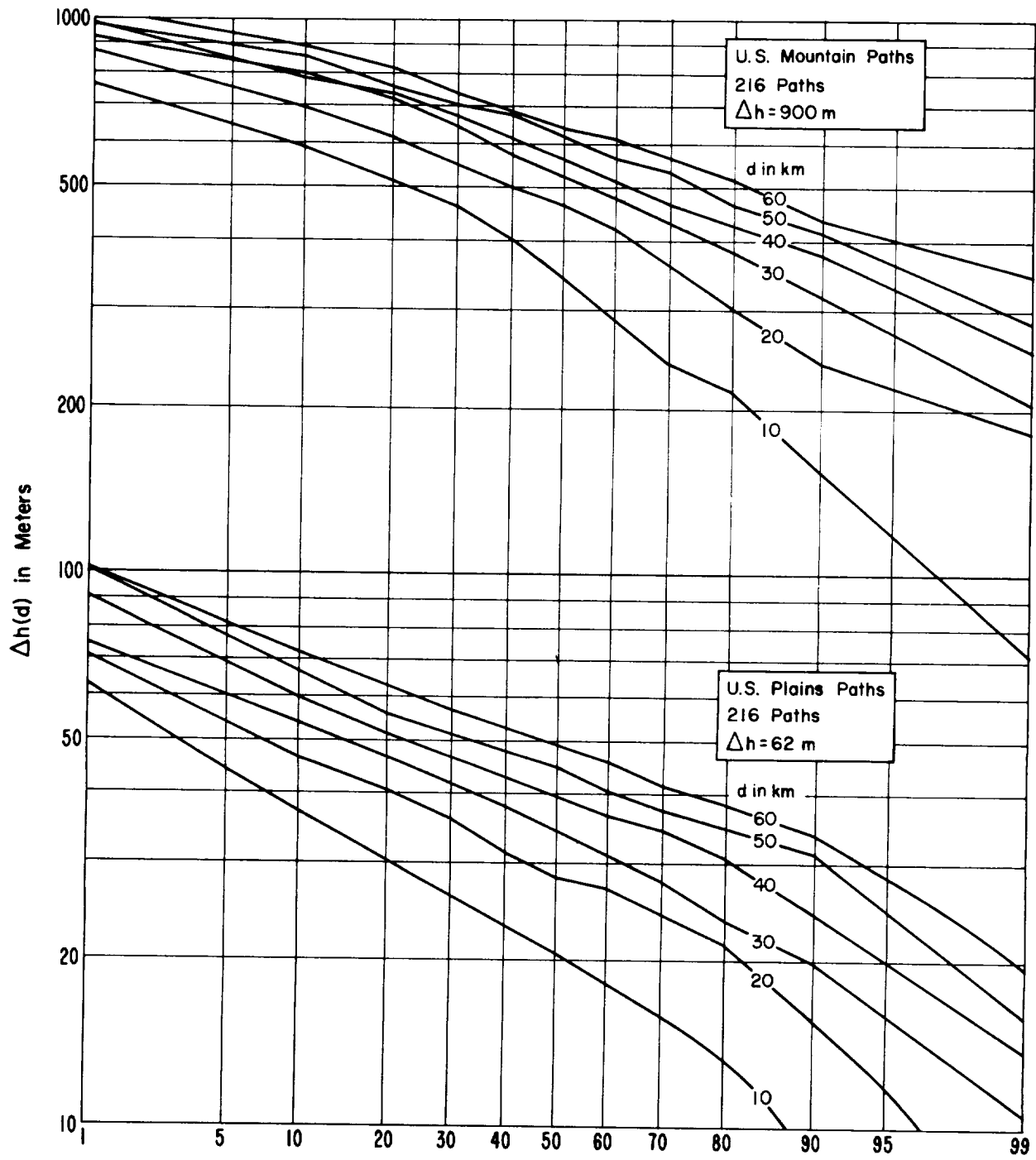


Figure 2.1

CUMULATIVE DISTRIBUTIONS OF $\Delta h(d)$



Percent of Profiles
Figure 2.2

CUMULATIVE DISTRIBUTIONS OF $\Delta h(d)$

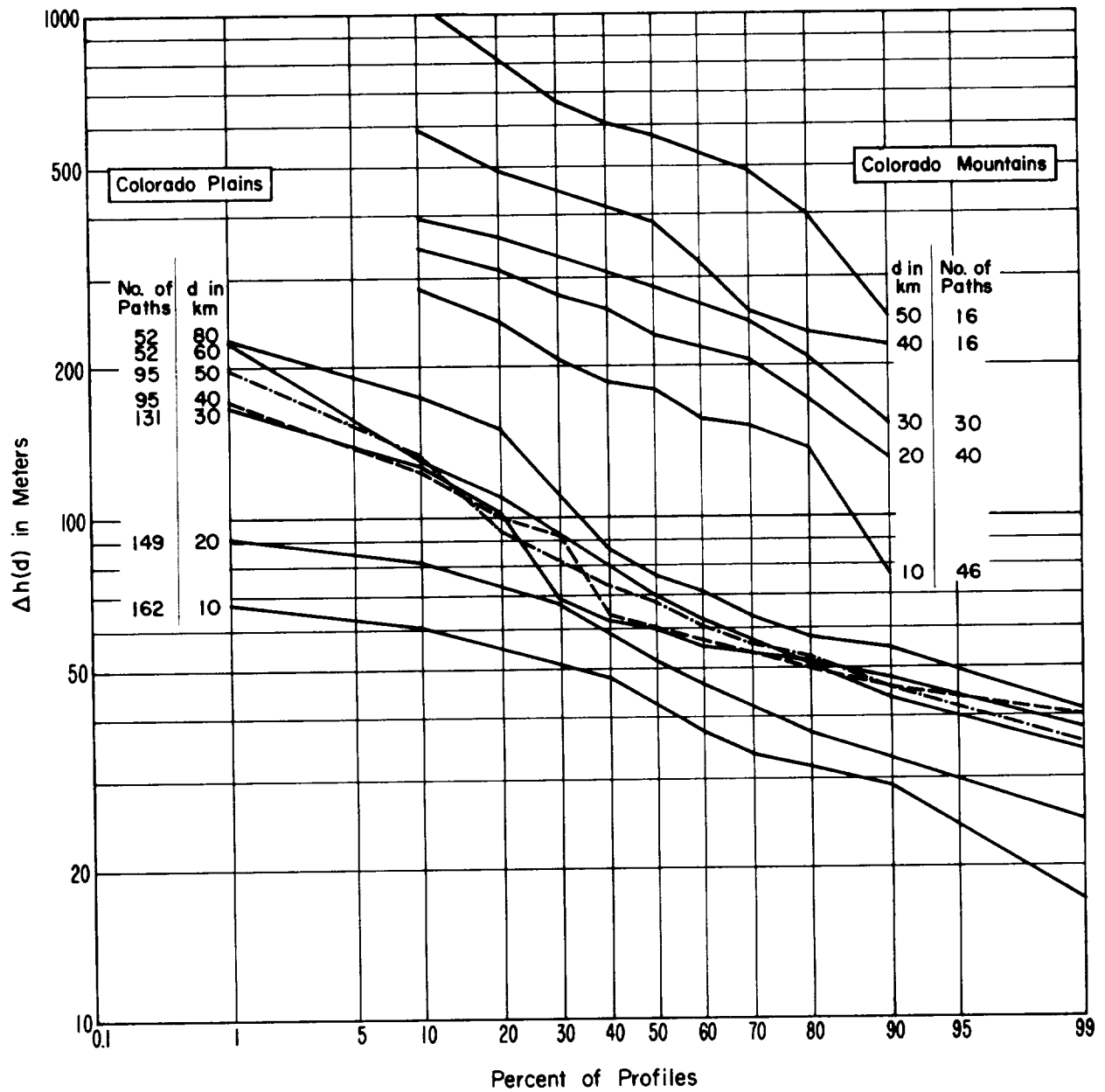


Figure 2.3

CUMULATIVE DISTRIBUTIONS OF $\Delta h(d)$ Northeastern Ohio

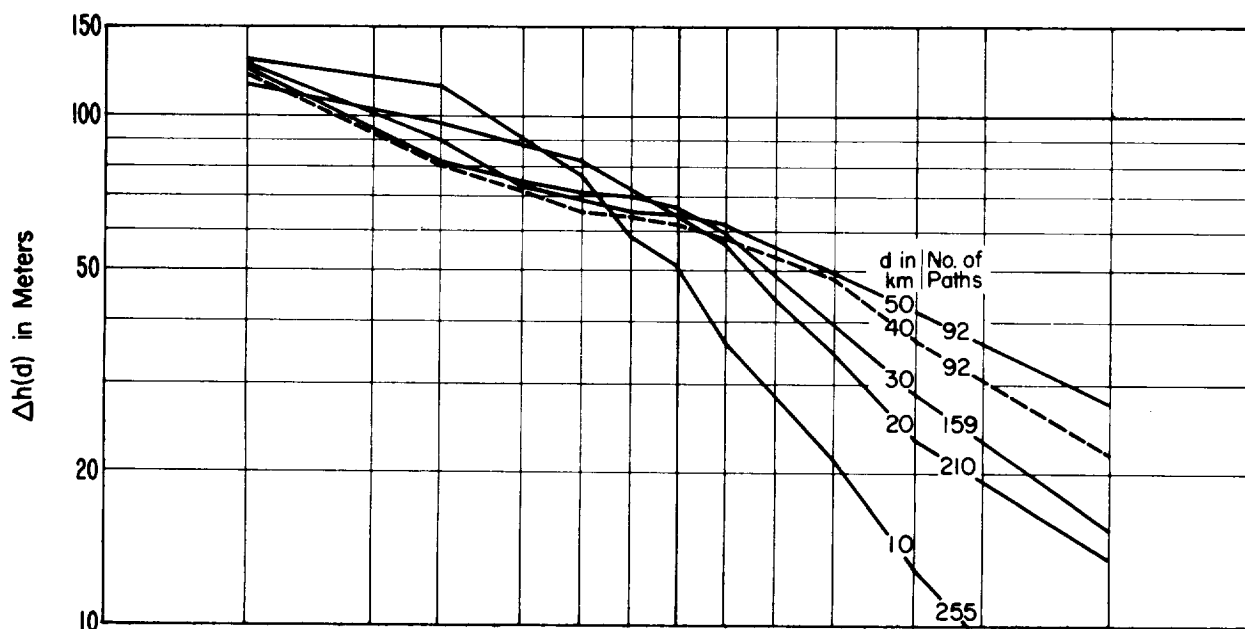


Figure 2.4 a

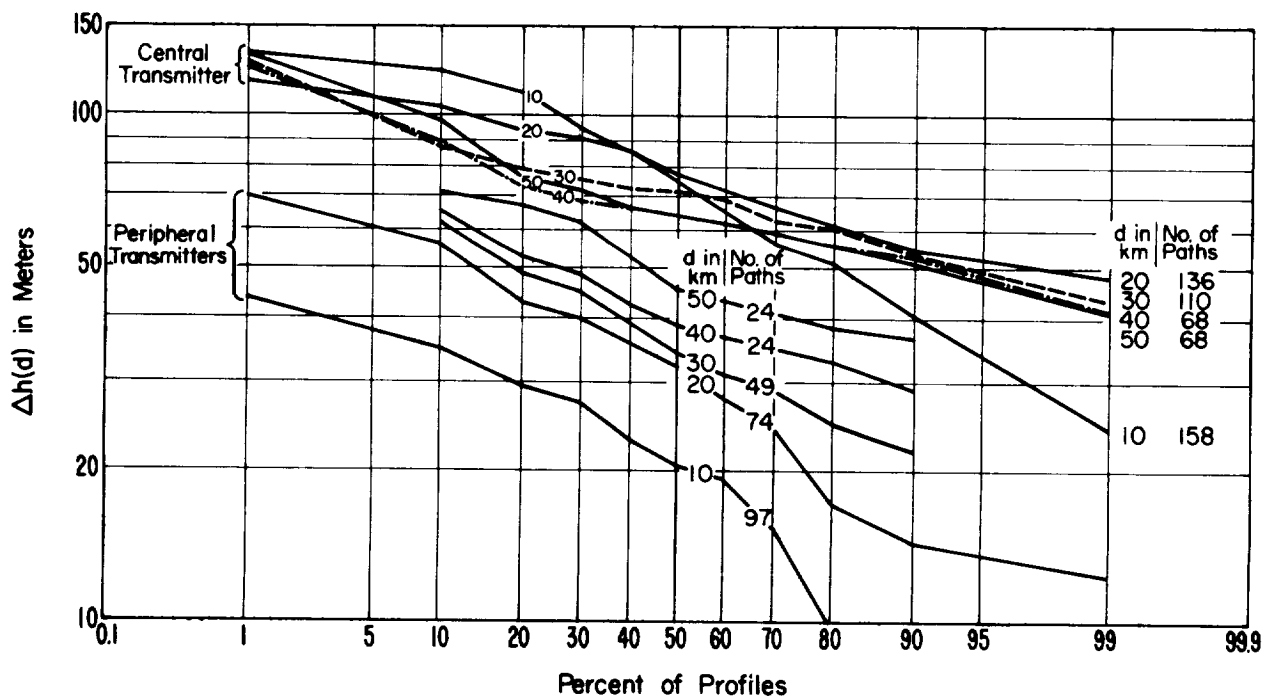


Figure 2.4 b

distribution of $\Delta h(d)$ for northeastern Ohio, as shown in figure 2.4a, where for path lengths from 20 to 50 km no consistent increase in $\Delta h(d)$ is shown. These data include a group of profiles that form radials from the location of the "central transmitter", and a smaller group of profiles that radiate from each of 5 peripheral transmitter locations. When the profiles from each of the peripheral transmitter locations are grouped together, the usual trend is observed, with the median $\Delta h(d)$ increasing consistently with path length, as shown in figure 2.4b. For the groups of paths from the location of the central transmitter the median $\Delta h(d)$ is higher at all distances but particularly for the 10- and 20-km profiles. This indicates that the terrain is more rugged in the vicinity of the central transmitter than in the remainder of the area.

Median values of $\Delta h(d)$ are plotted versus distance in figures 2.5, 2.6, and 2.7 for random, plains, and mountain paths. For each median $\Delta h(d)$, an estimate of the asymptotic value Δh was calculated using (3) of the main body of this report:

$$\Delta h(d) = \Delta h [1 - 0.8 \exp(-0.02 d)] \text{ m}, \quad (3)$$

where $\Delta h(d)$ and Δh are in meters and the distance d is in kilometers. Choosing appropriate values of Δh from these calculations, the smooth curves on the figures were plotted. Figure 2.5 shows for the 101 randomly chosen paths how the medians of data at each distance compare with a curve computed assuming the asymptotic value, $\Delta h = 90 \text{ m}$. In the plains and mountain areas 36 profiles, 60 km in length, were read in each of 6 directions. To determine whether the terrain changes in a predictable way from one direction to another the paths in each direction were considered separately. In figures 2.6 and 2.7 each symbol

THE PARAMETER $\Delta h(d)$ VERSUS DISTANCE

U.S. Random Paths

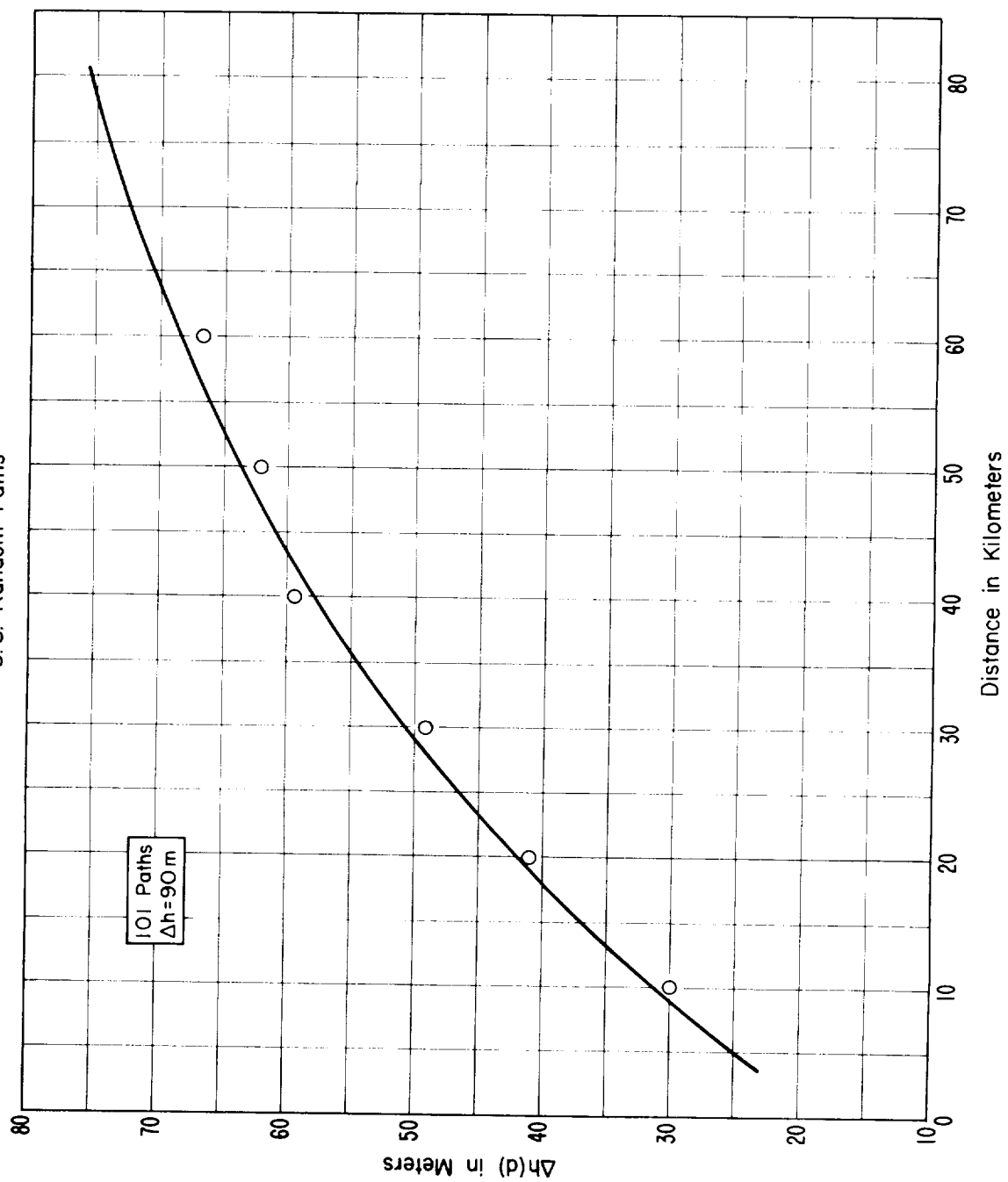


Figure 2.5

THE PARAMETER $\Delta h(d)$ VERSUS DISTANCE U.S. Plains Paths

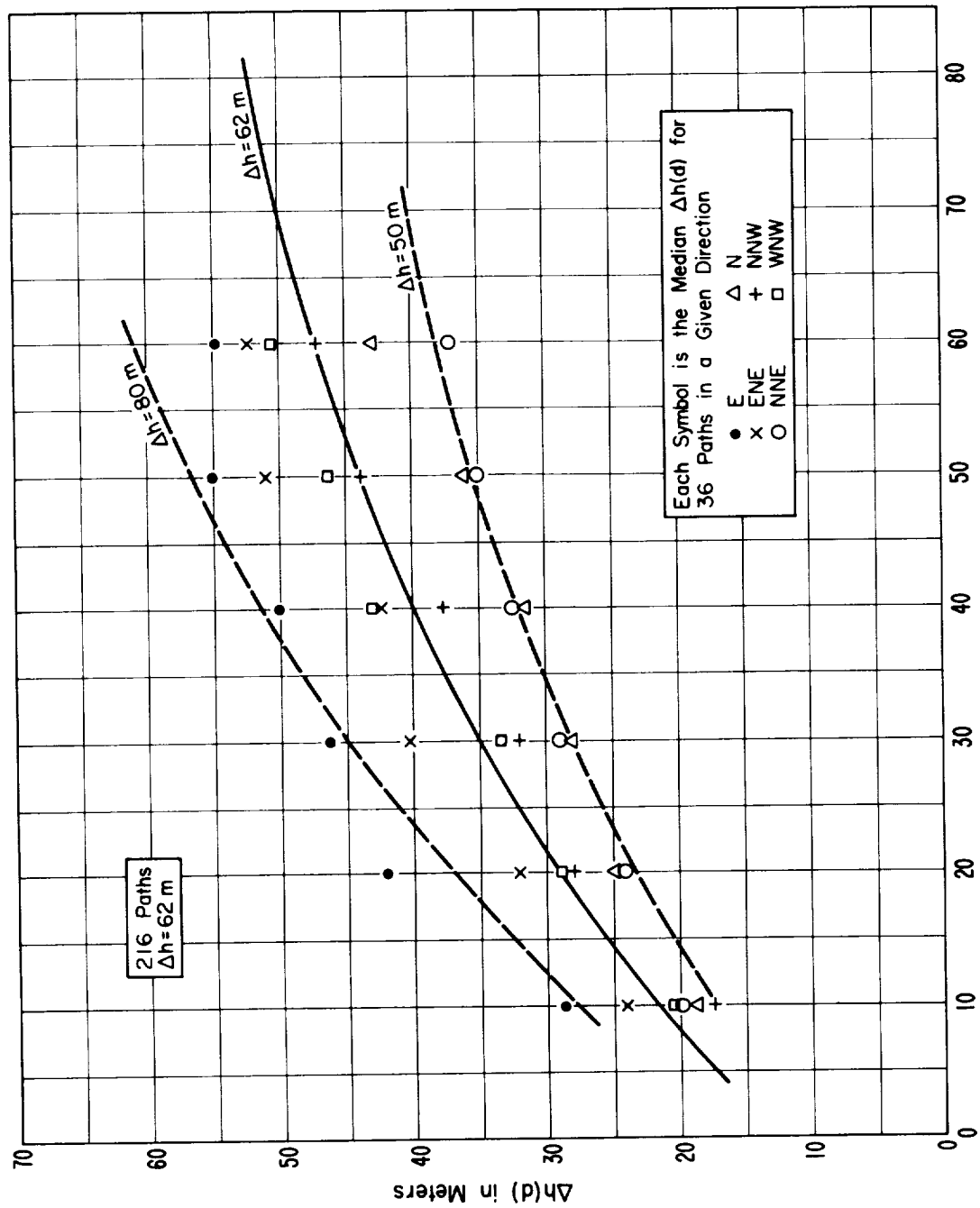
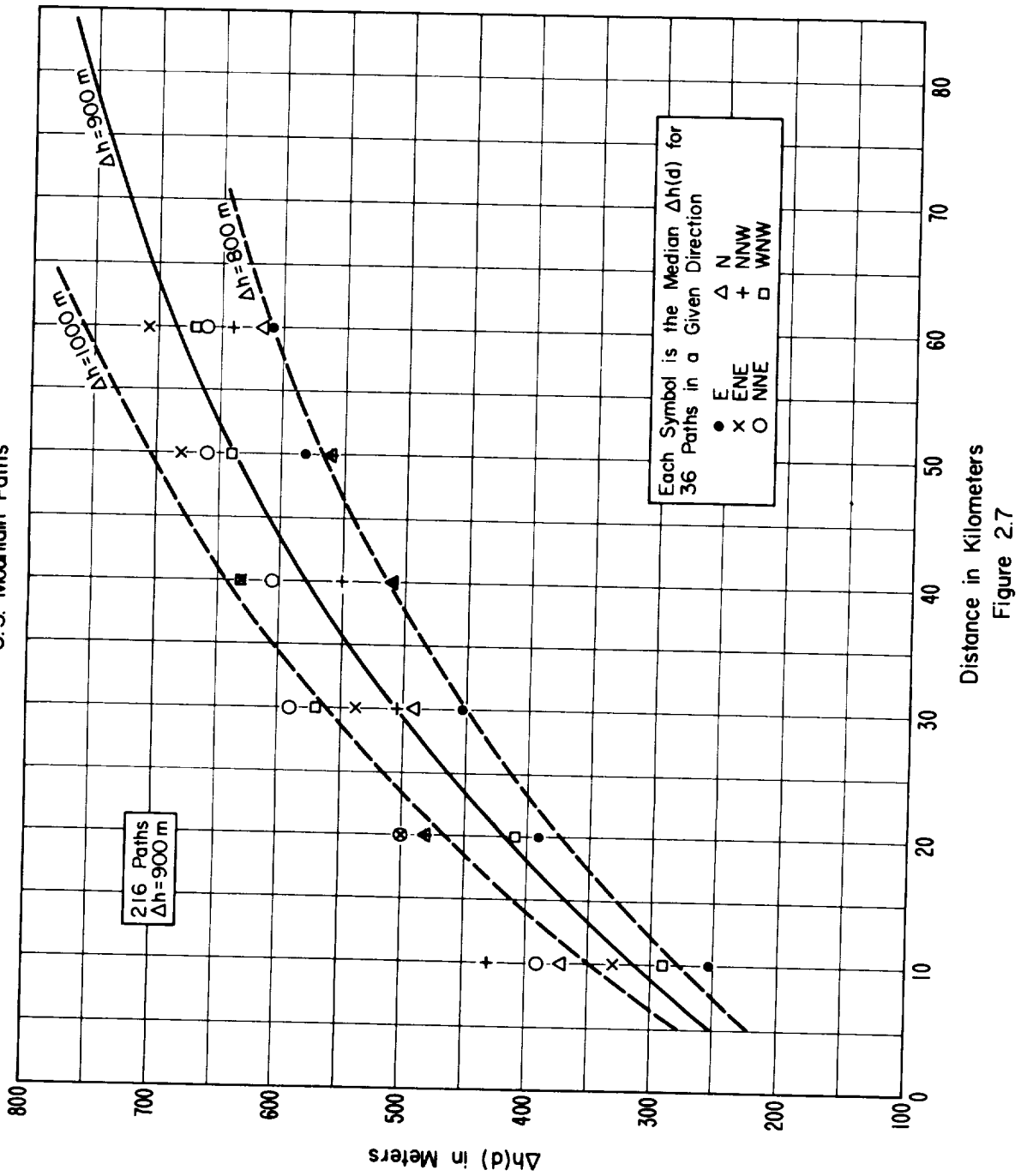


Figure 2.6

THE PARAMETER $\Delta h(d)$ VERSUS DISTANCE U.S. Mountain Paths

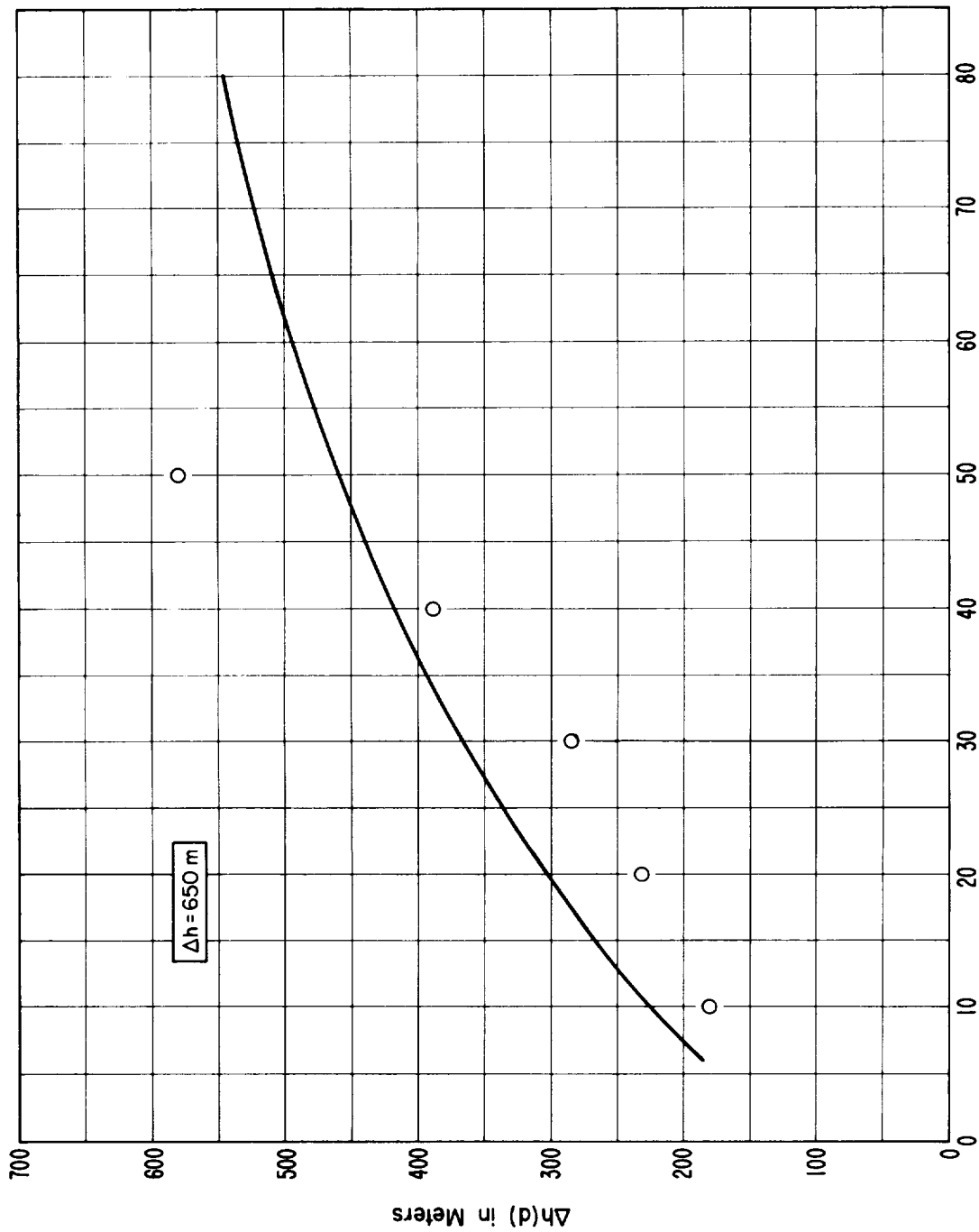


represents the median value of $\Delta h(d)$ for 36 paths in a specified direction. Figure 2.6 shows that paths in an east-west direction consistently show a larger interdecile range of terrain heights than those in a north-south direction. Data from the E-W paths suggest an asymptotic value $\Delta h = 80$ m, while those from the N-S paths suggest $\Delta h = 50$ m. The median value for paths in all six directions is $\Delta h = 62$ m. In the figure smooth curves calculated from (3) for $\Delta h = 50$, 62 and 80 m are compared with medians from profiles in each direction. The data for the mountain profiles do not show as consistent a directional trend, but in this case the east-west paths show the smallest values and the east-northeast paths tend to yield the largest values of $\Delta h(d)$ as shown on figure 2.7. The data for the most part fall between the limits $\Delta h = 800$ m and $\Delta h = 1000$ m, and the terrain is represented by the asymptotic value $\Delta h = 900$ m.

Figure 2.8 shows median values of $\Delta h(d)$ for the few Colorado mountain paths over which measurements were made, and a curve of $\Delta h(d)$ for $\Delta h = 650$ m. The value $\Delta h = 650$ m was assumed in calculating transmission loss to be expected over these paths. For the shorter paths this value is too large, as indicated in the figure. For the paths in Ohio and those in the Colorado plains, the value $\Delta h = 90$ m was assumed in calculating expected transmission losses. Figure 2.9 shows the corresponding smooth curve of $\Delta h(d)$ versus d compared with median values of $\Delta h(d)$ from path profiles. The symbol x , representing median values of $\Delta h(d)$ for Colorado plains paths, shows good agreement with the curve especially at the greater distances where most of the radio data were recorded. The square symbol represents median values of $\Delta h(d)$ for all Ohio paths at each distance, the circle represents values

THE PARAMETER $\Delta h(d)$ VERSUS DISTANCE

Colorado Mountains



Distance in Kilometers
Figure 2.8

THE PARAMETER $\Delta h(d)$ VERSUS DISTANCE N.E. Ohio and Colorado Plains

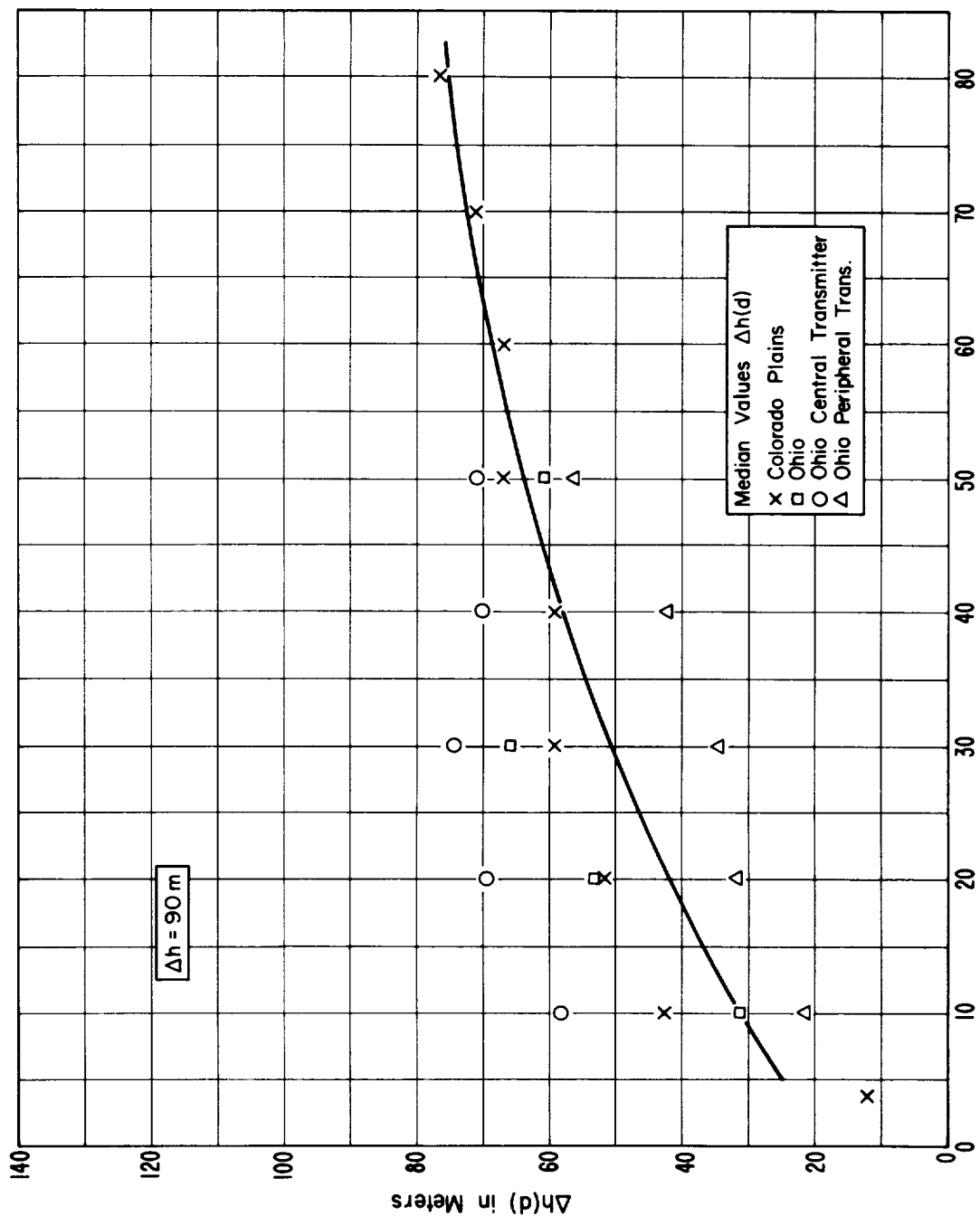


Figure 2.9

for the central transmitter, and the triangle those for the peripheral transmitters at each distance. Although the terrain in this Ohio area is obviously not homogeneous, the value $\Delta h = 90$ m was chosen as being representative of the terrain.

The following values of Δh were chosen as representative of the terrain in each of the areas for which terrain statistics were obtained:

<u>Area</u>	<u>Δh in m</u>
U.S. random	90
Plains grid	62
Mountain grid	900
Colorado plains (meas. paths)	90
Colorado mountains (meas. paths)	650
NE Ohio (meas. paths)	90

These figures provided most of the basis for the values of Δh listed in table 1 of the main body of the report.

2-3 The Horizon Distance, d_L

When a detailed terrain profile is available for a given path, the horizon distances d_{L1} and d_{L2} and their sum d_L may be obtained directly from the profile information and an estimate of the effective earth's radius. When individual path profiles are not available, median values of d_{L1} and d_{L2} are estimated as functions of the median effective antenna heights, the terrain irregularity factor Δh , and the corresponding distances to the horizon over a smooth earth.

The estimates d_{L1} and d_{L2} computed using equation (5c) of the main body of the report,

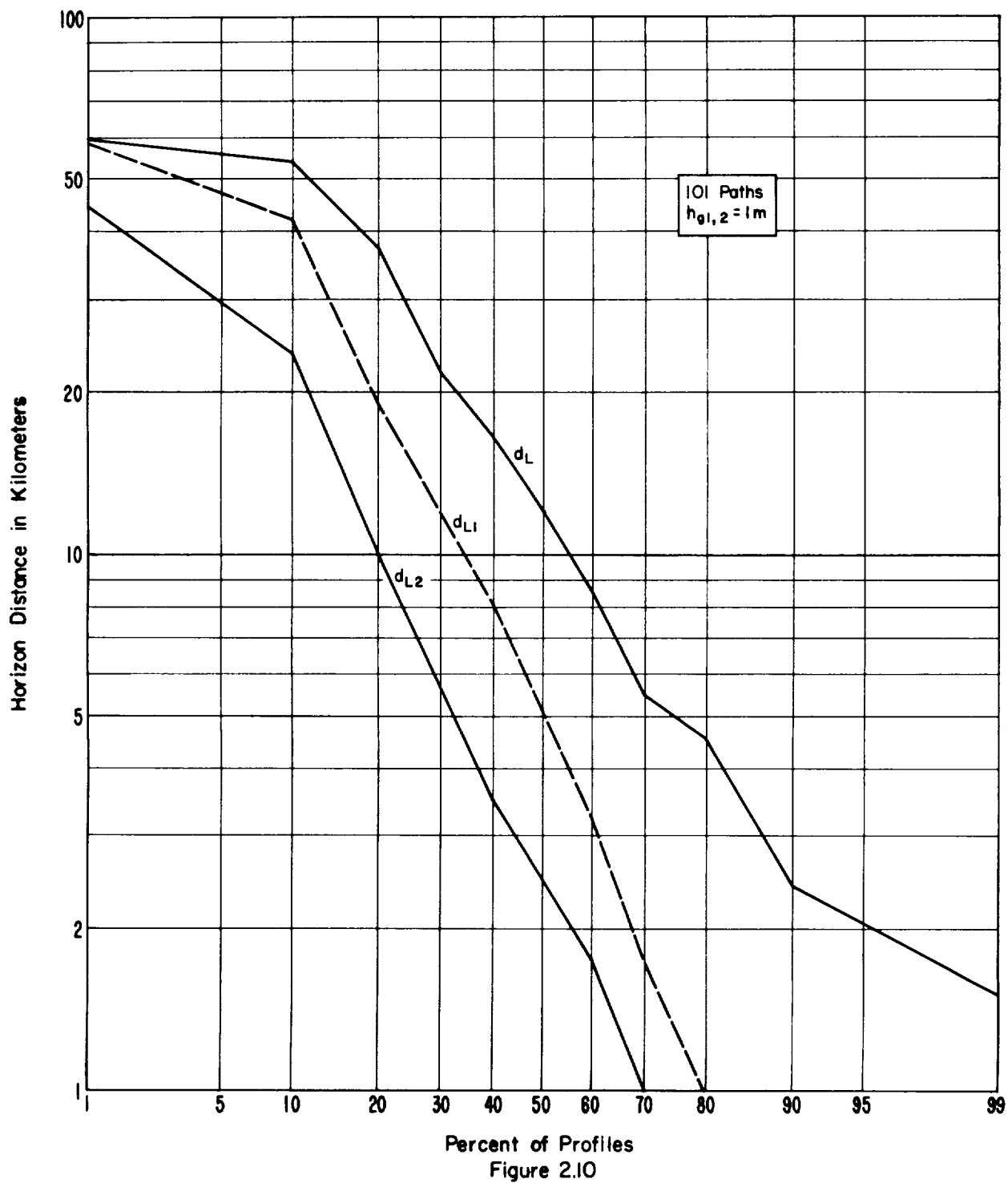
$$d_{L1,2} = d_{Ls1,2} \exp(-0.07 \sqrt{\Delta h/h_e}) \text{ km}, \quad (5c)$$

approach the smooth-earth values d_{Ls1} and d_{Ls2} as the terrain factor Δh approaches zero or as the antenna heights become very large. To determine the constant in (5c), horizon distances were obtained for the sets of U. S. random, plains, and mountains profiles with pairs of antenna heights above ground, h_{g1} and h_{g2} , chosen as follows:

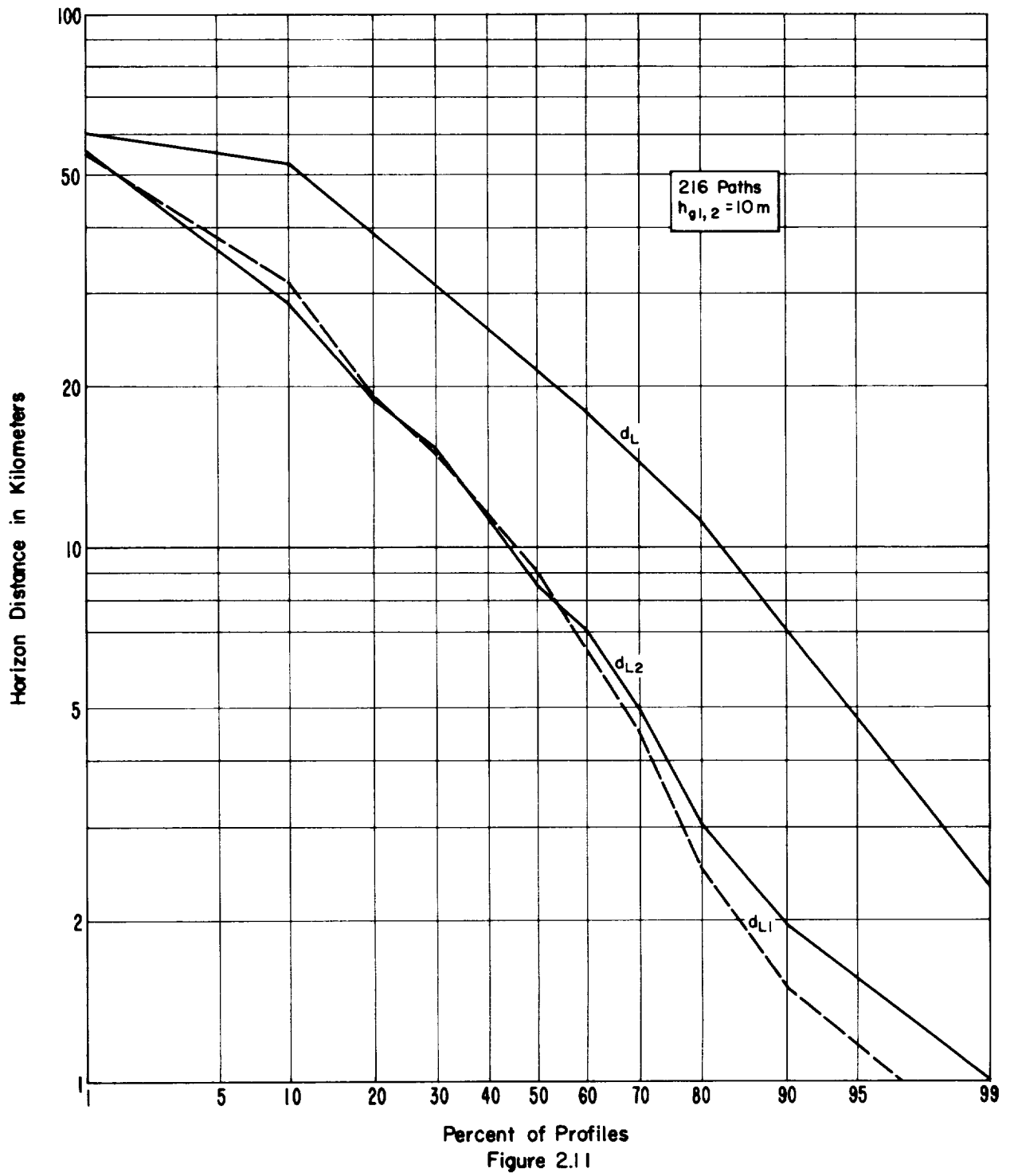
h_{g1}	h_{g2}	h_{g1}	h_{g2}	h_{g1}	h_{g2}
1	1	3	3	10	10
1	10	3	10	30	30
		3	30		

For paths of lengths 30, 40, 50, and 60 km, the horizon distances d_{L1} , d_{L2} , and the sum of the horizon distances d_L were obtained from each profile. Figures 2.10, 2.11, and 2.12 show cumulative distributions of d_{L1} , d_{L2} and d_L . As shown in table 2.1, these horizon distances are independent of path length, provided that the path length chosen is greater than d_L . Figure 2.10 shows cumulative distributions of d_{L1} , d_{L2} , and d_L for 101 random paths with $h_{g1} = h_{g2} = 1$ m. Figures 2.11 and 2.12 show similar distributions for 216 paths in the plains and in the rugged mountains with $h_{g1} = h_{g2} = 10$ m. Note that the median value of d_L is always greater than the sum of the medians of d_{L1} and d_{L2} .

CUMULATIVE DISTRIBUTIONS OF HORIZON DISTANCES U.S. Random Paths



CUMULATIVE DISTRIBUTIONS OF HORIZON DISTANCES U.S. Plains Paths



CUMULATIVE DISTRIBUTIONS OF HORIZON DISTANCES U. S. Mountain Paths

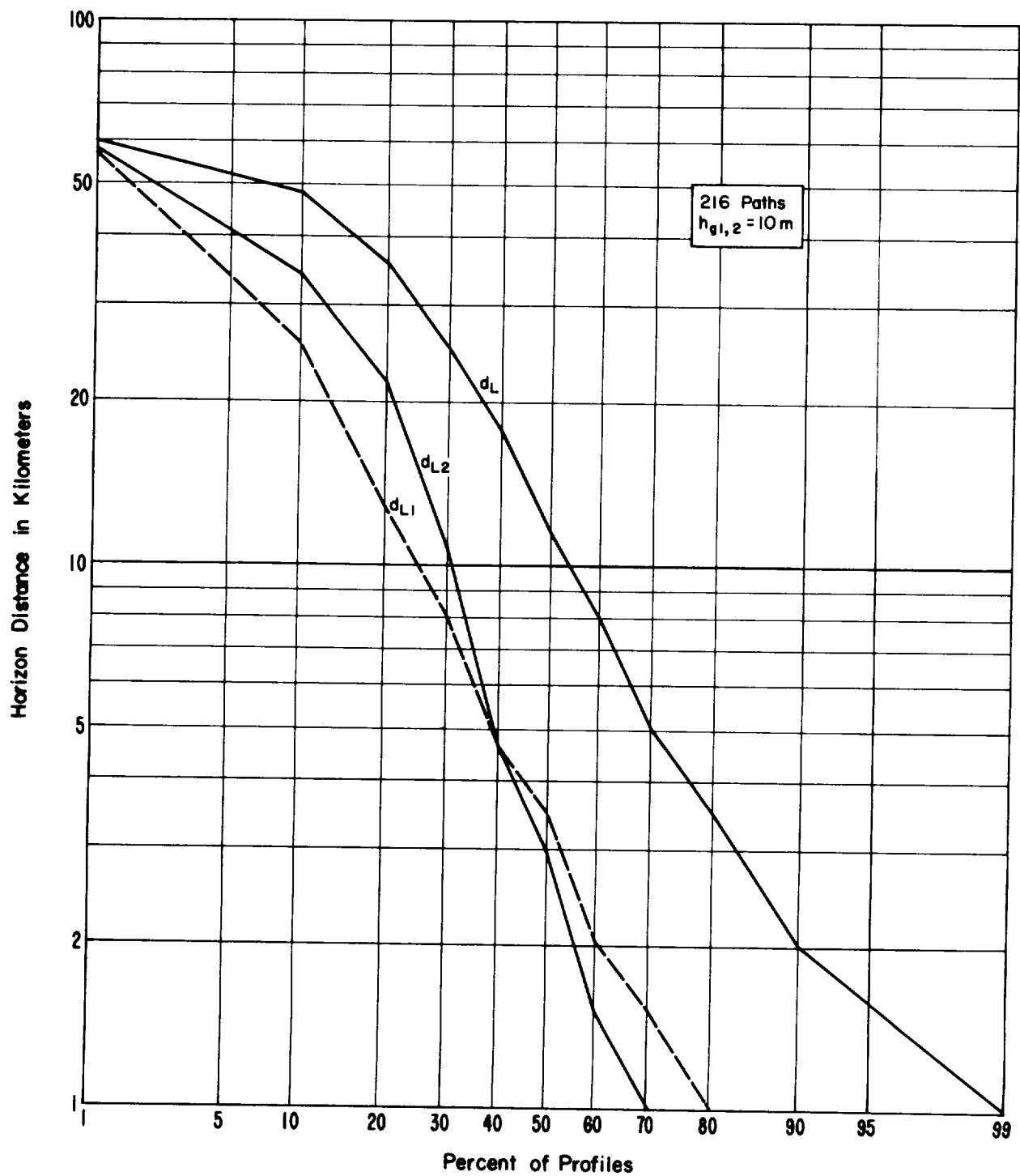


Figure 2.12

Table 2.2

Calculated values of d_{Ls1} and d_{L1}^*

h_{e1}	1	3	10	30 m.
Random Paths, $\Delta h = 90$ m, $N_s = 310$, $a = 8640$ km.				
d_{Ls1}	4.16	7.20	13.15	22.77
d_{L1}	3.1	5.6	10.7	20.2
Plains Paths, $\Delta h = 62$ m, $N_s = 290$, $a = 8330$ km.				
d_{Ls1}	4.08	7.07	12.91	22.36
d_{L1}	3.2	5.5	10.8	20.2
Mountain Paths, $\Delta h = 900$ m, $N_s = 250$, $a = 7850$ km.				
d_{Ls1}	3.96	6.86	12.53	21.70
d_{L1}	1.6	2.7	6.4	14.8

$$*d_{L1} = d_{Ls1} \exp(-0.07\sqrt{\Delta h/h_e})$$

The constant in (5c) was estimated by computing the smooth earth distances d_{Ls1} and d_{Ls2} that correspond to these median values of d_{L1} and d_{L2} and rewriting (5c) as

$$d_{L1,2} = d_{Ls1,2} \exp(-k_{1,2} \sqrt{\Delta h / h_e}) \quad (2.1a)$$

$$k_{1,2} = \log_e (d_{Ls1,2} / d_{L1,2}) (\Delta h / h_e)^{-1/2}. \quad (2.1b)$$

The median of all computed values was $k = 0.07$.

Table 2.2 shows calculated values of d_{Ls1} and d_{L1} for four antenna heights for the random, plains, and mountains paths. Table 2.3 shows a) median values of d_L from profiles and b) corresponding calculated values for seven antenna height combinations.

The values show rather good agreement in all areas for low to medium antenna heights, with a decided tendency to overestimate d_L when both antennas are as much as 30 m above ground, especially in the mountains. These comparisons are all made assuming effective antenna heights equal to structural heights.

2-4. The Elevation Angle θ_e

For each of the large number of terrain profiles available, the elevation angles θ_{e1} and θ_{e2} were computed using (3.1) of annex 3, and for each profile the sum of these angles θ_e was also computed. Figures 2.13, 2.14, and 2.15 show cumulative distributions of θ_{e1} , θ_{e2} , and θ_e given in milliradians. These are plotted on logarithmic probability paper, but it should be kept in mind that a small percentage of these angles are negative, especially in the group of plains paths. As previously observed for the horizon distances d_{L1} , d_{L2} , and d_L , these

Table 2.3

The Sum of the Horizon Distances d_L

$h_{e1,2}$	1, 1	3, 3	1, 10	3, 10	10, 10	3, 30	30, 30 m
Random Paths							
a)	11.2	13.5	15.2	17.5	19.7	24.2	35.2
b)	6.2	11.2	13.8	16.3	21.4	25.8	40.4
Plains Paths							
a)	12.5	15.2	17.2	18.7	21.4	25.5	35.4
b)	6.4	11.0	14.0	16.3	21.6	25.7	40.4
Mountain Paths							
a)	9.2	9.2	10.2	10.2	10.7	11.2	13.5
b)	3.2	5.4	8.0	9.1	12.8	17.5	29.6

a) Median value from profiles

b) Calculated using (5e)

elevation angles are independent of path length, provided that the path length chosen is greater than the sum of the horizon distances.

Figure 2.13 shows cumulative distributions θ_{e1} , θ_{e2} , and θ_e for 101 random paths with $h_{g1,2} = 1$ m, and figures 2.14 and 2.15 show similar distributions for 216 paths in the plains and in the mountains, with $h_{g1,2} = 10$ m. As with the horizon distances, the median value of θ_e is always greater than the sum of the median values of θ_{e1} and θ_{e2} . Table 2.4 shows median values of θ_{e1} , θ_{e2} and θ_e for several antenna height combinations.

Estimates of the elevation angles were made using the expression (6a) given in the main body of this report,

$$\theta_{e1,2} = \frac{0.0005}{d_{Ls1,2}} \left[1.3 \left(\frac{d_{Ls1,2}}{d_{L1,2}} - 1 \right) \Delta h - 4 h_{e1,2} \right] \text{ radians. (6a)}$$

Table 2.5 shows median values of θ_{e1} , θ_{e2} , and θ_e calculated using this expression and actual values of d_{L1} and d_{L2} as read from the profiles. Since no consistent distance dependence is observed, median values of θ_e for each antenna height combination are compared with the calculated values. For the random and plains paths, the median estimates of θ_e are approximately equal to the median values given in Table 2.4. For the mountain paths the estimated values of θ_e are almost twice as large as those obtained directly from profiles.

Considering the situation where predictions are based solely on estimates of terrain characteristics, without actual profiles for individual paths, values of θ_{e1} , θ_{e2} , and θ_e were calculated using equation (6a)

CUMULATIVE DISTRIBUTIONS OF ELEVATION ANGLES U.S. Random Paths

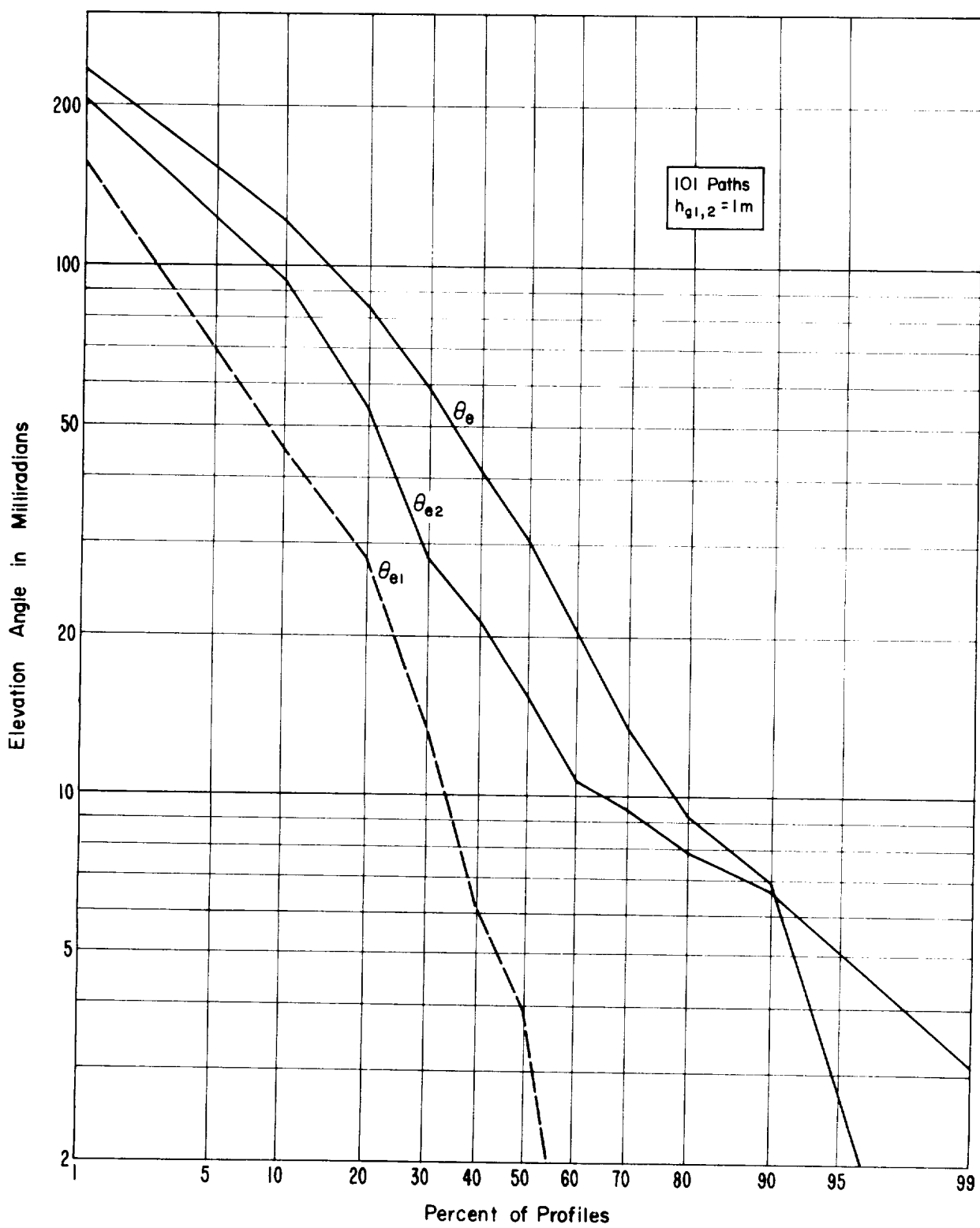
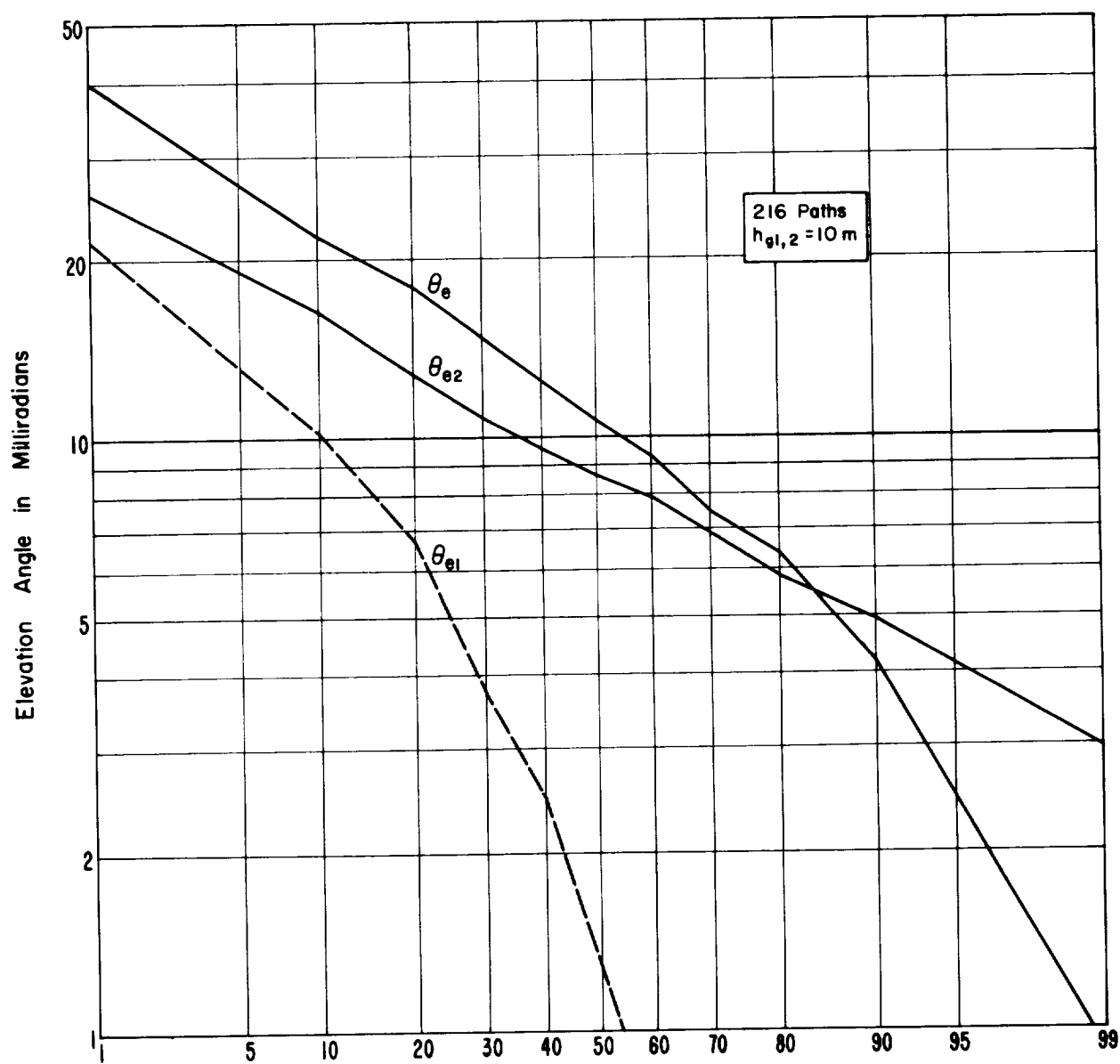


Figure 2.13

CUMULATIVE DISTRIBUTIONS OF ELEVATION ANGLES U.S. Plains Paths



Percent of Profiles
Figure 2.14

Table 2.4

Median Values of the Elevation Angles

 θ_{e1} , θ_{e2} , and θ_e in Milliradians

$h_{g1,2}$	1, 1			3, 3		m
d_{km}	θ_{e1}	θ_{e2}	θ_e	θ_{e1}	θ_{e2}	θ_e
Random						
30	2.95	10.72	19.73	2.59	9.33	17.63
40	3.84	12.64	25.10	2.85	11.00	21.38
50	3.98	13.11	22.52	3.25	12.78	19.34
60	3.96	15.36	30.38	3.30	13.71	29.73
Plains						
30	3.91	7.30	13.51	2.62	6.20	11.72
40	3.67	8.58	15.24	2.68	8.06	13.04
50	3.51	10.46	15.50	2.59	9.18	13.68
60	3.69	11.07	15.94	2.71	10.17	14.19
Mountains						
30	108.4	124.8	268.1	106.1	122.6	263.1
40	105.0	81.8	212.2	104.4	81.3	207.3
50	99.5	75.7	206.5	99.1	73.9	203.4
60	100.0	85.0	227.9	97.1	84.4	225.9

CUMULATIVE DISTRIBUTIONS OF ELEVATION ANGLES U. S. Mountain Paths

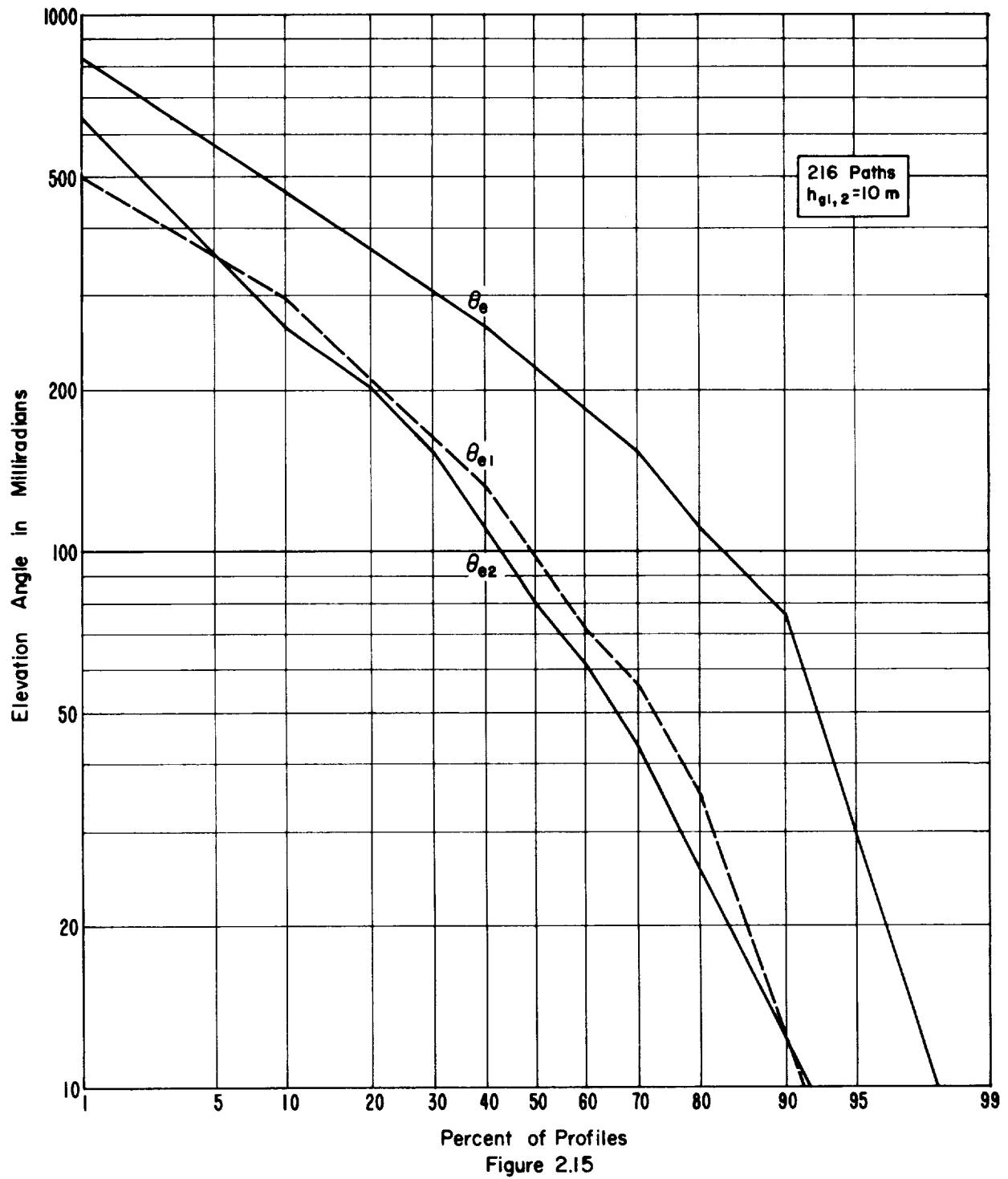


Table 2.4 (continued)

$h_{g1,2}$	3, 10			10, 10		m
	θ_{e1}	θ_{e2}	θ_e	θ_{e1}	θ_{e2}	θ_e
Random						
30	2.68	6.92	15.04	1.59	7.26	13.22
40	3.42	7.54	20.04	1.67	7.70	19.72
50	3.28	10.53	16.44	1.83	10.86	14.79
60	3.40	11.26	25.22	1.33	11.26	23.16
Plains						
30	2.70	4.40	9.86	1.37	4.44	8.47
40	2.70	6.25	10.90	1.47	6.26	9.75
50	2.59	7.78	11.88	1.58	7.78	9.80
60	2.71	8.62	12.22	1.28	8.62	10.62
Mountains						
30	106.1	117.1	255.8	100.9	117.1	249.0
40	104.4	77.1	201.7	102.2	77.1	197.9
50	99.1	68.3	199.3	94.9	68.3	192.1
60	97.3	79.0	220.1	93.2	79.0	215.4

Table 2.5

Median Values of the Elevation Angles Calculated
Using (6a), With d_{L1} , d_{L2} from Profiles

θ_{e1} , θ_{e2} , θ_e in milliradians

$h_{g1,2}$	1, 1			3, 3		m
	θ_{e1}	θ_{e2}	θ_e	θ_{e1}	θ_{e2}	θ_e
Random						
30	0.11	8.88	24.17	0.81	7.78	25.46
40	0	14.73	33.71	0.06	10.56	25.63
50	0	4.98	33.36	0.06	5.69	23.79
60	-2.17	8.88	30.01	0.06	7.78	26.54
Plains						
30	1.15	0	11.51	1.51	1.51	10.10
40	1.15	-0.14	20.09	0.78	1.51	8.78
50	1.15	0	17.65	0.17	0.78	9.93
60	1.15	-1.41	14.28	0.17	0	9.65
Mountains						
30	46.8	241.8	678.6	108.9	303.9	754.0
40	46.8	85.8	359.6	108.9	147.9	479.6
50	46.8	85.8	418.6	108.9	147.9	510.2
60	46.8	144.3	581.1	108.9	206.4	705.2

Table 2.5 (continued)

$h_{g1,2}$	3, 10			10, 10		m
d_{km}	θ_{e1}	θ_{e2}	θ_e	θ_{e1}	θ_{e2}	θ_e
Random						
30	1.26	1.36	15.20	0.54	1.36	17.99
40	0.44	3.04	23.36	0.20	3.04	20.68
50	0.06	3.79	15.85	0	3.79	14.55
60	0.06	4.68	15.59	0	4.68	14.74
Plains						
30	1.96	0	5.96	0.37	0	4.47
40	0.78	0	4.99	0.07	0	2.68
50	0.17	-0.19	4.77	-0.19	-0.19	3.12
60	0.17	0.07	5.72	-0.19	0.07	2.03
Mountains						
30	108.9	244.2	651.1	118.8	244.2	618.4
40	108.9	146.7	504.7	118.8	146.7	526.8
50	108.9	146.7	495.6	118.8	146.7	520.9
60	108.9	146.7	580.6	118.8	146.7	544.1

with values of d_{L1} and d_{L2} calculated as functions of Δh (5c). As one would expect, these estimates of θ_e do not correspond closely to median values from individual profiles.

Table 2.6 shows the comparison between (a) median values of θ_e obtained directly from terrain profiles, (b) those estimated using actual horizon distances in (6a), and (c) values calculated using (6a) and estimates of d_{L1} and d_{L2} computed using (5c). For the random and plains

Table 2.6

Elevation Angles θ_e in Milliradians				
$h_{g1,2}$	1, 1	3, 3	3, 10	10, 10
Random				
a)	23.8	20.5	18.2	17.2
b)	31.7	25.6	15.7	16.4
c)	8.7	3.9	1.5	-1.0
Plains				
a)	15.4	13.4	10.9	9.8
b)	16.0	9.8	5.4	2.9
c)	4.5	1.5	-0.2	-1.9
Mountains				
a)	220.0	218.6	210.9	206.6
b)	499.8	607.7	542.6	535.4
c)	459.2	264.0	174.4	84.8

- a) median values of θ_e from profiles
- b) median values of θ_e calculated using (6a) and values of d_{L1} , d_{L2} from profiles
- c) values of θ_e calculated using (6a) with values of $d_{L1,2}$ calculated using (5c)

paths, method (c) underestimates θ_e for all antenna height combinations tested, but for the mountain paths it provides a better estimate than method (b), which overestimates the elevation angle by a wide margin, yielding values more than twice as large as the median values from terrain profiles. Since the elevation angle θ_e is probably the single most important terrain parameter for predicting transmission loss, this wide range in estimates introduces considerable prediction error.

2-5 Terrain Parameters for Colorado Plains, Mountains, and Northeastern Ohio

Profiles of the paths in the foothills and plains of Colorado and in northeastern Ohio were used to obtain horizon distances and elevation angles. These are compared with values calculated as previously described in sections 2-3 and 2-4 for the U. S. random, plains, and mountain paths.

These paths represent much smaller samples than those previously discussed, so one would expect the terrain statistics to be less consistent. Table 2.7 shows median values of the horizon distances d_{L1} , d_{L2} , and d_L for the antenna height combinations used in the measurement program, at distances of 20, 30, 50 and 80 km. The total number of paths, N , in each group is also tabulated. The horizon distances do not appear to be independent of path length as they were for the U. S. random, plains, and mountain paths. This may be attributed in part to the small sample size, and in Colorado to the fact that all paths radiate from a single transmitter located in the plains, resulting in median values of d_{L1} much greater than those of d_{L2} , even with comparable antenna

Table 2.7
The Horizon Distances, Colorado Plains, Mountains, and Ohio
Median Values from Profiles

	h_{g1}	4	h_{g2}	0.6	1.7	3	6	9	m		
d_{km}	N	d_{L1}	d_{L2}	d_L	d_{L2}	d_L	d_{L2}	d_L	d_{L2}	d_L	km

Colorado Plains, $\Delta h = 90$ m, $N_s = 290$, $a = 8327$ km

20	14	11.2	2.0	19.1	2.7	18.1	4.7	19.2	7.2	19.4	7.2	19.4
30	33	12.6	2.0	21.6	2.0	21.6	2.0	21.6	2.0	20.4	4.4	23.4
50	43	14.4	5.0	28.9	6.0	29.0	6.0	29.6	9.2	32.3	18.0	33.7
80	52	21.0					4.5	28.5	10.8	33.3	16.5	35.8

Colorado Mountains, $\Delta h = 650$ m, $N_s = 290$, $a = 8327$ km

20	10	7.6	1.2	10.5	1.2	10.9	1.2	10.9	2.0	10.9	2.0	10.9
30	14	9.8	1.5	11.5	1.5	11.5	1.5	11.5	1.5	11.5	1.5	11.5
50	16	10.2	2.8	15.0	2.8	15.0	2.8	15.0	4.3	15.3	4.3	15.3

NE Ohio, $\Delta h = 90$ m, $N_s = 312$, $a = 8676$ km

20	42	5.0			2.2	14.1	2.8	12.3	3.0	12.6	5.0	15.0
30	62	7.0			2.5	18.0	2.8	18.0	5.5	23.2	6.0	23.5
50	92	8.6			3.8	22.3	4.4	23.1	5.3	25.3	7.9	26.3

heights. The median value of d_L is not always much greater than the sum of the medians of d_{L1} and d_{L2} especially with the higher receiver heights. The paths in Ohio radiate from six different antenna locations and show median values of d_L much greater than the sum of the medians of d_{L1} and d_{L2} .

The smooth-earth distances d_{Ls1} and d_{Ls2} were calculated for each antenna height and used in (5c) to calculate values of d_{L1} , d_{L2} , and d_L :

$$d_{L1,2} = d_{Ls1,2} \exp(-0.07 \sqrt{\Delta h/h_e}). \quad (5c)$$

Table 2.8 shows these calculated values compared with median values from the profiles. The calculated values of d_L are consistently less than the median values from terrain profiles, especially in the Colorado plains. The calculated values of d_{L2} , however, correspond quite well with those from the profiles. This better agreement with d_{L2} is to be expected as the receivers are much more randomly located than the transmitters. The calculated values of d_{L1} and d_{L2} , using (5c), never exceed the corresponding smooth-earth values, but for the Colorado plains paths the median d_L is always much greater than the corresponding value of d_{Ls} . This results from the fact that the transmitter is located in a bowl or depression with rising ground in all directions so the horizon is much farther away than it would be due to the normal fall-off of the earth.

For each of the terrain profiles in the Colorado plains and foothills and in northeastern Ohio, the elevation angles θ_{e1} , θ_{e2} , and their sum θ_e were computed using (3.1) from annex 3 of this report. Table 2.9 shows median values at each distance for the antenna heights used in the

Table 2.8
The Horizon Distances, Colorado Plains, Mountains, and Ohio
Median and Calculated Values

$h_{g1} = 4\text{m}, h_{g2} = 0.6$			1.7		3		6		9 m	
d_{L1}	d_{L2}	d_L	d_{L2}	d_L	d_{L2}	d_L	d_{L2}	d_L	d_{L2}	d_L km

Colorado Plains, $\Delta h = 90$ m, $N_s = 290$, $a = 8327$ km

a)	13.8	3.5	25.7	4.0	25.3	4.0	28.5	5.6	32.3	11.2	33.7
b)	6.1	2.4	8.5	4.0	10.1	5.2	11.3	7.6	13.7	9.8	15.9
c)	8.2	3.2	11.4	5.3	13.5	7.1	15.2	10.0	18.2	12.2	20.4

Colorado Mountains, $\Delta h = 650$ m, $N_s = 290$, $a = 8327$ km

a)	9.8	1.5	11.5	1.5	11.5	1.5	11.5	2.0	11.5	2.0	11.5
b)	3.7	1.4	5.1	2.4	6.1	3.2	6.9	5.0	8.7	6.8	10.5
c)	8.2	3.2	11.4	5.3	13.5	7.1	15.2	10.0	18.2	12.2	20.4

NE Ohio, $\Delta h = 90$ m, $N_s = 312$, $a = 8676$ km

a)	7.0			2.5	18.0	2.8	18.0	5.3	23.2	6.0	23.5
b)	6.2			3.2	9.4	5.4	11.6	7.8	14.0	10.0	16.2
c)	8.3			4.2	12.5	7.2	15.5	10.2	18.5	12.5	20.8

- a) Median values from profiles
- b) Calculated values using (5c)
- c) Smooth earth values, $d_{Ls1,2}$ and d_{Ls}

Table 2.9

The Elevation Angles, Colorado Plains, Mountains and Ohio
Median Values in Milliradians

d_{km}	$\frac{h}{g_1} \quad 4$	$\frac{h}{g_2} \quad 0.6$		1.7		3		6		9 \text{ m}	
	θ_{e1}	θ_{e2}	θ_e	θ_{e2}	θ_e	θ_{e2}	θ_e	θ_{e2}	θ_e	θ_{e2}	θ_e

Colorado Plains, $\Delta h = 90 \text{ m}$, $N_s = 290$, $a = 8327 \text{ km}$

20	1.3	5.5	10.4	6.5	10.3	6.1	10.1	5.1	9.3	4.3	8.2
30	0.5	16.8	16.9	14.5	14.6	11.9	12.1	8.8	7.4	7.1	6.9
50	0.9	2.5	5.7	2.0	5.6	1.8	5.0	1.0	4.6	0.4	3.4
80	-2.1					1.9	0.8	1.3	-0.9	0.4	-1.4

Colorado Mountains, $\Delta h = 650 \text{ m}$, $N_s = 290$, $a = 8327 \text{ km}$

20	25.4	77.4	99.8	76.6	98.6	75.7	97.3	73.7	94.2	71.5	91.2
30	33.7	112.9	135.2	111.2	134.3	109.2	133.3	104.7	129.4	100.1	124.9
50	47.2	105.4	158.8	104.2	158.6	102.8	158.5	99.8	158.3	98.6	158.0

NE Ohio, $\Delta h = 90 \text{ m}$, $N_s = 312$, $a = 8676 \text{ km}$

20	3.5			6.0	11.2	5.6	11.4	4.8	11.0	4.0	9.9
30	1.0			6.1	10.6	4.8	9.6	3.6	9.0	3.0	6.6
50	0.3			5.3	7.6	4.3	7.3	3.1	6.6	2.8	6.0

measurements. These values show no consistent dependence on distance, and θ_e decreases only slightly with increasing height of the receiving antenna. Table 2.10 shows values of θ_{e1} , θ_{e2} , and θ_e calculated using (6a), compared with median values of θ_e for each antenna height.

$$\theta_{e1,2} = \frac{0.0005}{d_{Ls1}} \left[1.3 \left(\frac{d_{Ls1}}{d_{L1}} - 1 \right) \Delta h - 4 h_{e1} \right] \text{ radians.} \quad (6a)$$

2-6 Location Variability

The path-to-path variation in available wanted signal power is discussed in annex 1. Such random variations from location to location are assumed to be normally distributed with a standard deviation σ_{La} dB. An estimate of σ_{La} is required to calculate the service probability Q.

Analysis of path-to-path variability of radio transmission loss for a given frequency and terrain variance assumes statistical homogeneity of the terrain. It has been noted that the plains and mountain areas show a predictable change in the variance of terrain from one direction to another, and that in the area studied in NE Ohio the greatest terrain irregularity occurs in the vicinity of the central transmitter.

Transmission loss data from the measurement program reported by Miles and Barsis (1966) were used to obtain an estimate of σ_{La} . The interdecile range, ΔL , of values of transmission loss recorded for each frequency, polarization, antenna height combination, and distance was tabulated for the Colorado plains and mountain areas, and the area studied in NE Ohio. These interdecile ranges, given in table 2.11, show no consistent dependence on antenna height combinations or on path length, but do increase quite consistently with frequency and terrain irregularity. The interdecile ranges of transmission loss ΔL were plotted versus the parameter $\Delta h(d)/\lambda$ and a smooth curve was drawn through overlapping median values. The analytic expression,

Table 2.10
The Elevation Angles, Colorado Plains, Mountains, and Ohio
Median and Calculated Values in Milliradians

h_{g1}	4	h_{g2}	0.6	1.7		3		6		9 m	
	θ_{e1}	θ_{e2}	θ_e	θ_{e2}	θ_e	θ_{e2}	θ_e	θ_{e2}	θ_e	θ_{e2}	θ_e

Colorado Plains

a)	0.9	5.5	10.4	6.5	10.3	6.1	10.1	5.1	7.4	4.3	6.9
b)	1.5	5.7	7.2	3.0	4.5	2.2	3.7	0.6	2.1	-0.3	1.2

Colorado Mountains

a)	33.7	105.4	135.2	104.2	134.3	102.8	133.3	99.8	129.4	98.6	124.9
b)	61.7	169.4	231.1	95.7	157.4	71.7	133.4	41.0	102.7	26.0	87.7

NE Ohio

a)	1.0			6.0	10.6	4.8	9.6	3.6	9.0	3.0	6.6
b)	1.4			3.5	4.9	1.9	3.3	0.6	2.0	-0.3	1.1

a) Median values from profiles

b) Calculated using (6a), with $d_{L1,2}$ calculated using (5e)

Table 2.11

Interdecile Ranges of Transmission Loss ΔL in dB

Frequency	100 MHz						50 MHz		20 MHz
Polarization	Vertical			Horizontal			Vertical		Vertical
$h_{g_1} = 4, h_{g_2} =$	3	6	9	3	6	9	0.6	1.7	1.3 m
Colorado Plains									
d = 10 km.	24.5	21.9	20.9	23.2	25.5	24.7	23.4	22.1	9.4
20	21.2	21.8	26.6	21.8	25.9	26.1	22.6	16.0	9.0
30	32.3	31.3	29.8	31.0	33.3	34.5	17.5	15.8	19.6
50	17.4	22.0	22.0	20.0	20.6	22.5	16.3	17.5	8.6
80	17.0	21.8	21.0	19.7	18.4	17.8			
Colorado Mountains									
d = 10 km.	25.4	31.6	27.0	39.1		67.3	20.0	36.0	38.3
20	26.3	28.3	29.2	40.6	46.9	43.4	27.2	27.3	29.6
30	30.5	26.1	27.3	35.1		36.1	22.3	24.2	21.6
50	19.6	26.6	28.3				18.8	12.7	16.7
NE Ohio									
d = 10 km.	34.6	26.7	27.3	22.5	27.3	27.5	21.2	20.1	19.9
20	25.6	23.4	23.5	24.8	24.6	24.2	16.3	19.4	15.3
30	33.5	27.5	22.0	26.6	21.1	20.3	16.6	23.1	16.7

$$\sigma_{La} = [0.1 + 0.2 \lambda / \Delta h(d)]^{-1} \text{ dB}, \quad (2.2)$$

was then fitted to these values, where $\sigma_{La} = 0.39 \Delta L$. This function increases rapidly to about 9 dB for $\Delta h(d)/\lambda = 20$ and then slowly increases further to a maximum value of 10 dB.

The presently available data indicate larger values of σ_{La} with horizontal than with vertical polarization at 100 MHz in the mountains, but no significant polarization effect is observed in the Colorado plains or in Ohio. Further studies of location variability should be made, especially at higher frequency ranges and with higher antennas. The estimate of σ_{La} given by (2.2) depends entirely on the examination of data at 20, 50, and 100 MHz in Colorado and Ohio.

2-7 The Terrain Roughness Factor σ_h

The terrain roughness factor, in (3.5) annex 3, for line-of-sight calculations represents the rms deviation of terrain and terrain clutter within the limits of the first Fresnel zone in the dominant reflecting plane. For this report the factor σ_h is defined by (3.6) as

$$\sigma_h(d) = 0.78 \Delta h(d) \exp\{-0.5 [\Delta h(d)]^{1/4}\} \text{ m, for } \Delta h(d) > 4 \text{ m,} \quad (3.6a)$$

$$\sigma_h(d) = 0.39 \Delta h(d) \text{ m, for } \Delta h(d) \leq 4 \text{ m.} \quad (3.6b)$$

These analytic expressions were developed from a study of about 70 line-of-sight radio paths where detailed terrain profiles were available. For each of these paths the interdecile range of terrain heights $\Delta h(d)$ was calculated, and σ_h was computed using the formulas given in section 5, volume 1, and annex III, volume 2, of the report by Rice et al. (1967).

These formulas define the points at which the first Fresnel ellipse cuts the great circle plane. The factor σ_h was then calculated as the rms deviation of modified terrain elevations relative to a smooth curve within these limits.

The computed value of σ_h was plotted versus the corresponding value of $\Delta h(d)$ for each path. Equation (3.6) defines a smooth curve fitted to these computed values.

ANNEX 3 EQUATIONS AND METHODS FOR COMPUTING THE REFERENCE ATTENUATION A_{cr}

The minimum input parameters required to compute the reference attenuation relative to free space are the radio frequency f in megahertz, the path distance d in kilometers, and antenna heights above ground h_{g1} and h_{g2} in meters. Estimates of surface refractivity N_s , terrain irregularity Δh , and the ground constants σ and ϵ may be selected as described in section 2, when measured values are not available.

When detailed profiles of individual paths are not available, equations (3) through (6), section 2, are used to estimate median values of the additional parameters $h_{e1,2}$, $d_{L1,2}$ and $\theta_{e1,2}$.

When detailed profile information is available for a specific path, the actual horizon distances d_{L1} and d_{L2} , horizon elevation angles θ_{e1} and θ_{e2} , and effective antenna heights h_{e1} and h_{e2} above the dominant reflecting plane are used in computing A_{cr} . The location of a horizon obstacle may be determined by testing all possible horizon elevations and selecting the one for which the horizon elevation angle θ_{e1} or θ_{e2} is a maximum:

$$\theta_{e1} = \frac{0.001 (h_{L1} - h_{s1})}{d_{L1}} - \frac{d_{L1}}{2a} \text{ radians} \quad (3.1a)$$

$$\theta_{e2} = \frac{0.001 (h_{L2} - h_{s2})}{d_{L2}} - \frac{d_{L2}}{2a} \text{ radians,} \quad (3.1b)$$

where $h_{s1,2}$ are the antenna heights above sea level in meters, a is the effective earth's radius in kilometers, $h_{L1,2}$ are the heights in meters above sea level of the horizon obstacles, and $d_{L1,2}$ are the great circle distances in kilometers from each antenna to its horizon. The prediction method is limited to values of $\theta_{e1,2} \leq 0.2$ radians. For larger

elevation angles the assumption of an effective earth's radius a , based on the surface refractivity N_s , is not applicable.

An alternative procedure is first to compute a least-squares fit of a straight line to terrain elevations above sea level. The heights $h_{s1,2}$ and $h_{L1,2}$ are then defined relative to this curve fit, rather than relative to sea level. This amounts to replacing sea level by an arc of radius " a " that is a least-squares fit to the great circle path terrain profile.

For line-of-sight paths, the effective antenna heights $h_{e1,2}$ are defined as the height of each antenna above the dominant reflecting plane between the antennas, or the structural height, whichever is greater. The effective heights may be calculated as heights above a smooth curve fitted to great circle profile terrain elevations that are intervisible to both antennas. A straight line is first fitted by least squares to equidistant heights h_i , and an amount $d_i^2/2a$ is then subtracted at each distance d_i to allow for the path curvature $1/a$. When terrain is so irregular that it cannot be reasonably well approximated by one or more such reflecting planes, the effective heights are estimated using (4a) or (4b) in the main body of this report.

The total input required to compute A_{cr} is then: f , d , h_{g1} , h_{g2} , polarization, and actual or estimated values of N_s , Δh , σ , and ϵ . When available for specific paths, the parameters $\Delta h(d)$, d_{L1} , d_{L2} , θ_{e1} , θ_{e2} , h_{e1} , and h_{e2} are also included as input.

3-1. Two-Ray Optics Formulas for Computing A_0 and A_1

At distances d_0 and d_1 , which are well within radio line of sight, but are so chosen that the difference between the direct and ground-reflected rays never exceeds one fourth of the wavelength, the following formula is used to compute the attenuation relative to free space:

$$A = -10 \log_{10} \left[1 + R_e^2 - 2 R_e \cos \left(\frac{2\pi \Delta r}{\lambda} - c \right) \right] + G_p - 10 \log_{10} (g_{o1} g_{o2}) \text{ dB.} \quad (3.2)$$

Here g_{o1} and g_{o2} represent the directive gain for each antenna in the direction of the other, while $2\pi \Delta r / \lambda$ is the path length difference between direct and ground-reflected rays, expressed in electrical radians and in degrees as

$$\frac{2\pi \Delta r}{\lambda} = 4.1917 \times 10^{-5} f h_{e1} h_{e2} / d \text{ radians,} \quad (3.3a)$$

$$= 2.4017 \times 10^{-3} f h_{e1} h_{e2} / d \text{ degrees,} \quad (3.3b)$$

with f in MHz, $h_{e1,2}$ in meters, and d in kilometers. R_e is the magnitude of an effective reflection coefficient and c is its phase relative to π radians. Assuming matched polarizations, the median path antenna gain may be approximated as

$$G_p = 10 \log_{10} (g_{o1} g_{o2}) \text{ dB,} \quad (3.4)$$

and these terms in (3.2) then cancel each other.

No divergence factor is included in the definition of R_e since its use will not add significantly to the accuracy of the method described for irregular terrain. (See the smooth-earth formulas for D , h_{te} , h_{re} in Rice et al. (1967).

Let g_{r1} and g_{r2} represent the directive antenna gains in the direction of a point of ground reflection. Then,

$$\hat{R}_e = R_{h,v} \left(\frac{g_{r1} g_{r2}}{g_{o1} g_{o2}} \right)^{1/2} \exp \left(- \frac{2\pi \sigma_h \sin \psi}{\lambda} \right). \quad (3.5)$$

Usually, $g_{r1} = g_{o1}$ and $g_{r2} = g_{o2}$, unless beams are very narrow or are directed away from the earth's surface to minimize reflection from the surface. $R_{h,v}$ is the magnitude of the theoretical plane earth reflection coefficient, the subscripts h and v referring to horizontal and vertical polarization respectively, and the factor σ_h in the exponent is the rms deviation of terrain and terrain clutter within the limits of the first Fresnel zone in the dominant reflecting plane. For this report the factor σ_h and the grazing angle ψ are defined as follows:

$$\sigma_h(d) = 0.78 \Delta h(d) \exp\{-0.5 [\Delta h(d)]^{1/4}\} \text{ m, for } \Delta h(d) > 4 \text{ m,} \quad (3.6a)$$

$$\sigma_h(d) = 0.39 \Delta h(d), \text{ for } \Delta h(d) \leq 4 \text{ m,} \quad (3.6b)$$

$$\psi = \tan^{-1} [(h_{e1} + h_{e2}) / (1000 d)]. \quad (3.7)$$

$$\text{If } R_{h,v} \exp[-(2\pi \sigma_h \sin \psi) / \lambda] > 0.5 \text{ and } > \sqrt{\sin \psi}, \quad (3.8a)$$

$$R_e = \hat{R}_e.$$

$$\text{Otherwise, } R_e = \left[\frac{g_{r1} g_{r2}}{g_{o1} g_{o2}} \sin \psi \right]^{1/2}. \quad (3.8b)$$

The theoretical plane earth reflection coefficients R_h , R_v and the phase angle c are functions of the radio frequency f , grazing angle ψ , and the ground constants σ and ϵ . Their magnitudes may be read from figures III. 1 through III. 8, volume 2 of the report by Rice et al. (1967), or computed as follows:

$$x = 18000 \sigma / f, \quad q = x / (2p) \quad (3.9a)$$

$$2 p^2 = [(\epsilon - \cos^2 \psi)^2 + x^2]^{1/2} + (\epsilon - \cos^2 \psi) \quad (3.9b)$$

$$b_v = \frac{\epsilon^2 + x^2}{p^2 + q^2}, \quad b_h = \frac{1}{p^2 + q^2} \text{ radians} \quad (3.10)$$

$$m_v = \frac{2(p\epsilon + qx)}{p^2 + q^2}, \quad m_h = \frac{2p}{p^2 + q^2}. \quad (3.11)$$

Then

$$R_v^2 = [1 + b_v \sin^2 \psi - m_v \sin \psi] / [1 + b_v \sin^2 \psi + m_v \sin \psi] \quad (3.12a)$$

$$R_h^2 = [1 + b_h \sin^2 \psi - m_h \sin \psi] / [1 + b_h \sin^2 \psi + m_h \sin \psi]. \quad (3.12b)$$

The phase angle c in (3.2) is defined below for both horizontal and vertical polarization, c_h and c_v . The angle c_h defined as

$$c_h = \tan^{-1} \left(\frac{q}{p + \sin \psi} \right) - \tan^{-1} \left(\frac{q}{p - \sin \psi} \right) \text{ radians} \quad (3.13)$$

is always negative and ranges in value from $0 \geq c_h \geq -0.1$ radians. The angle c_v changes suddenly from near zero to $\pi/2$ at the pseudo-Brewster angle, $\sin^{-1} \sqrt{1/b_v}$. To define c_v , let

$$y_1 = (x \sin \psi + q) / (\epsilon \sin \psi + p), \quad y_2 = (x \sin \psi - q) / (\epsilon \sin \psi - p). \quad (3.14)$$

If $\epsilon \sin \psi \geq p$:

$$c_v = \tan^{-1} y_1 - \tan^{-1} y_2 + \pi \text{ radians}. \quad (3.15a)$$

If $\epsilon \sin \psi < p$ and $p \sin \psi > 0.5$:

$$c_v = \tan^{-1} y_1 + \tan^{-1} y_2 \text{ radians}. \quad (3.15b)$$

If $\epsilon \sin \psi \leq p$ and $p \sin \psi \leq 0.5$:

$$c_v = \tan^{-1} y_1 - \tan^{-1} y_2 \text{ radians}. \quad (3.15c)$$

In the above formulas, $\tan^{-1} y$ is in the first quadrant if y is positive and in the fourth quadrant if y is negative.

The two-ray optics formulas (3.2) to (3.15) are used to compute values of attenuation A_{ot} and A_{1t} at distances d_o and d_1 , respectively.

For $A_{ed} \geq 0$, define

$$d_o = 4 \times 10^{-5} h_{e1} h_{e2} f \text{ km, or } 0.5 d_L, \text{ whichever is smaller, (3.16a)}$$

For $A_{ed} < 0$, define

$$d_{o1} = -A_{ed} / m_d \text{ km, or } (d_L - 2) \text{ km, whichever is smaller, (3.16b)}$$

$$d_o = \begin{cases} d_{o1} & \text{for } d_{o1} \geq 0.5 d_L \\ 0.5 d_L & \text{otherwise} \end{cases} \quad (3.16c)$$

$$d_1 = d_o + 0.25 (d_L - d_o) \text{ km.} \quad (3.16d)$$

In (3.16) the radio frequency f is in MHz, the effective antenna heights $h_{e1,2}$ are in meters, d_L is the sum of the horizon distances in kilometers and the attenuation A_{ed} and slope m_d are defined in the next subsection (3.38).

In addition to the two-ray-theory estimates A_{ot} and A_{1t} of attenuation at the distances d_o and d_1 , estimates of diffraction attenuation A_{od} , A_{1d} , and A_{Ls} are also computed at d_o , d_1 , and d_{Ls} :

$$A_{od} = A_{ed} + m_d d_o \quad (3.17a)$$

$$A_{1d} = A_{ed} + m_d d_1 \quad (3.17b)$$

$$A_{Ls} = A_{ed} + m_d d_{Ls}, \quad (3.17c)$$

where A_{ed} and m_d are defined in the next subsection by (3.38).

The estimates of attenuation A_o and A_1 at the distances d_o and d_1 are then computed as weighted averages of the two-ray theory and the diffraction estimates

$$A_o = w_o A_{ot} + (1 - w_o) A_{od} \quad \text{or} \quad A_{od}, \text{ whichever is smaller,} \quad (3.18a)$$

$$A_1 = w_o A_{1t} + (1 - w_o) A_{1d} \quad \text{or} \quad A_{1d}, \text{ whichever is smaller,} \quad (3.18b)$$

$$w_o = (1 + f \Delta h 10^{-4})^{-1}. \quad (3.18c)$$

For distances less than the smooth-earth horizon distance d_{Ls} , the calculated reference value A_{cr} is defined by a smooth curve fitted to the three values of attenuation below free space, A_o , A_1 , and A_{Ls} , at the distances d_o , d_1 , and d_{Ls} .

For $0 < d \leq d_{Ls}$:

$$A_{cr} = A_o + k_1 (d - d_o) + k_2 \log_{10} (d/d_o) \quad \text{dB.} \quad (3.19)$$

The constants k_1 and k_2 in (3.19) are evaluated as follows. First estimates \hat{k}_1 , \hat{k}_2 of the slopes k_1 , k_2 in (3.19) are computed as

$$\hat{k}_2 = \frac{(A_{Ls} - A_o)(d_1 - d_o) - (A_1 - A_o)(d_{Ls} - d_o)}{(d_1 - d_o) \log_{10} (d_{Ls}/d_o) - (d_{Ls} - d_o) \log_{10} (d_1/d_o)} \quad \text{dB,}$$

or 0, whichever is larger algebraically, (3.20)

$$\hat{k}_1 = [(A_{Ls} - A_o) - \hat{k}_2 \log_{10} (d_{Ls}/d_o)] / (d_{Ls} - d_o) \quad \text{dB/km.} \quad (3.21)$$

If $\hat{k}_1 < 0$ set $k_1 = 0$ and

$$k_2 = (A_{Ls} - A_o) / \log_{10} (d_{Ls} / d_o). \quad (3.22)$$

If the reference attenuation A_{cr} computed from (3.19) is less than zero at any distance $0 \leq d \leq d_{Ls}$, let $A_{cr} = 0$ for that distance.

3-2. Formulas for Computing Diffraction Attenuation A_d

In the far diffraction region, the attenuation A_d is computed as a weighted average of two estimates, A_r for smooth terrain and A_k for highly irregular terrain. In general, A_d is defined by (13) as

$$A_d = (1 - w) A_k + w A_r \text{ dB},$$

where the empirically determined weighting factor w is defined as

$$w = \left\{ 1 + 0.1 \left[\frac{\Delta h(d)}{\lambda} \left(\sqrt{\frac{h_{e1} h_{e2} + C}{h_{g1} h_{g2} + C}} + \frac{a \theta_e + d_L}{d} \right) \right]^{\frac{1}{2}} - 1 \right\}, \quad (3.23)$$

with $\frac{\Delta h(d)}{\lambda} \leq 1000$. In the accompanying computer program and output $C = 0$. For low antennas with known path parameters $C \approx 10$.

In (3.23) the radio wavelength λ , terrain irregularity $\Delta h(d)$, and effective and structural antenna heights $h_{e1,2}$, $h_{g1,2}$ are in meters; the effective earth's radius a , the horizon distance d_L , and the distance d , at which A_k and A_r are computed are in kilometers; and the sum of the elevation angles θ_e is in radians. For very smooth terrain, the weight $w \approx 1$ and $A_d \approx A_r$, and for highly irregular terrain, the

weight $w \approx 0$ and $A_d \approx A_k$. The prediction approaches A_k when either the frequency or the terrain irregularity are very large; therefore, a limit is placed on this ratio.

The diffraction attenuation is computed at distances d_3 and d_4 , chosen well beyond the horizon:

$$d_3 = d_L + 0.5 (a^2 / f)^{\frac{1}{3}} \text{ km}, \quad d_4 = d_3 + (a^2 / f)^{\frac{1}{3}} \text{ km}. \quad (3.24)$$

If $d_3 < d_{Ls}$ set $d_3 = d_{Ls}$.

At these distances, d_3 and d_4 , the attenuations A_3 and A_4 are computed using the following formulas, substituting d_3 and d_4 for d in (3.23) to obtain w_3 and w_4 :

$$A_3 = (1 - w_3) A_{k3} + w_3 A_{r3} \quad (3.25a)$$

$$A_4 = (1 - w_4) A_{k4} + w_4 A_{r4} \quad (3.25b)$$

$$\theta_3 = \theta_e + d_3 / a, \quad \theta_4 = \theta_e + d_4 / a. \quad (3.25c)$$

The estimates A_{k3} and A_{k4} for highly irregular terrain are computed as though the horizon obstacles were sharp ridges or hills, and the attenuation is computed for a double knife-edge path.

$$v_{1.3} = 1.2915 \theta_3 \sqrt{f d_{L1} (d_3 - d_L) / (d_3 - d_{L2})} \quad (3.26a)$$

$$v_{2.3} = 1.2915 \theta_3 \sqrt{f d_{L2} (d_3 - d_L) / (d_3 - d_{L1})} \quad (3.26b)$$

$$v_{1.4} = 1.2915 \theta_4 \sqrt{f d_{L1} (d_4 - d_L) / (d_4 - d_{L2})} \quad (3.26c)$$

$$v_{2.4} = 1.2915 \theta_4 \sqrt{f d_{L2} (d_4 - d_L) / (d_4 - d_{L1})} \quad (3.26d)$$

$$\begin{cases} A(v) = 6.02 + 9.11 v - 1.27 v^2 & \text{for } 0 \leq v \leq 2.4 \\ A(v) = 12.953 + 20 \log_{10} v & \text{for } v > 2.4 \end{cases} \quad (3.27a)$$

$$(3.27b)$$

$$A_{k3} = A(v_{1.3}) + A(v_{2.3}), \quad A_{k4} = A(v_{1.4}) + A(v_{2.4}). \quad (3.27c)$$

The rounded earth attenuations A_{r3} and A_{r4} are defined as

$$A_{r3,4} = G(x_{3,4}) - F(x_1) - F(x_2) - 20 \text{ dB}, \quad (3.28)$$

where the functions $F(x_{1,2})$ and $G(x_{3,4})$ depend on the radio frequency, polarization, and ground constants σ and ϵ , the distances $d_{L1,2}$, $d_{3,4}$, and the effective earth's radii $a_{1,2}$ for the terrain between the antennas and their horizons and $a_{3,4}$ for the terrain between horizons. The latter are defined as

$$a_1 = d_{L1}^2 / (0.002 h_{e1}) \text{ km}, \quad a_2 = d_{L2}^2 / (0.002 h_{e2}) \text{ km} \quad (3.29a)$$

$$a_3 = (d_3 - d_L) / \theta_3 \text{ km}, \quad a_4 = (d_4 - d_L) / \theta_4 \text{ km}. \quad (3.29b)$$

Then the distances $x_{1,2,3,4}$ are defined as

$$x_1 = B_1 a_1^{-\frac{2}{3}} d_{L1} \text{ km}, \quad x_2 = B_2 a_2^{-\frac{2}{3}} d_{L2} \text{ km} \quad (3.30)$$

$$x_3 = B_3 a_3^{-\frac{2}{3}} (d_3 - d_L) + x_1 + x_2 \text{ km} \quad (3.31a)$$

$$x_4 = B_4 a_4^{-\frac{2}{3}} (d_4 - d_L) + x_1 + x_2 \text{ km}, \quad (3.31b)$$

where the parameter $B_{1,2,3,4}$ is defined for both vertical and horizontal polarization as

$$B_{1,2,3,4} = 416.4 f^{\frac{1}{3}} [1.607 - K_{h,v}(a_{1,2,3,4})] . \quad (3.32)$$

The parameters $K_h(a)$ for horizontal and $K_v(a)$ for vertical polarization are defined as

$$K_h(a) = 0.36278 (a f)^{-\frac{1}{3}} [(\epsilon - 1)^2 + x^2]^{-\frac{1}{4}} \quad (3.33a)$$

$$K_v(a) = K_h(a) [\epsilon^2 + x^2]^{\frac{1}{2}} , \quad (3.33b)$$

where x is defined by (3.9a) as $x = 18000 \sigma / f$, and the ground constants σ and ϵ are included in the input.

The functions $F(x_1)$ and $F(x_2)$ may be read from figures 8.5 or 8.6 of the report by Rice et al. (1967) or may be computed using the following formulas.

1. For $0 < x_{1,2} \leq 200$ and $0 \leq K_{h,v}(a_{1,2}) \leq 10^{-5}$:

$$F(x_{1,2}) = 40 \log_{10} x_{1,2} - 117, \text{ or} \quad (3.34a)$$

$$F(x_{1,2}) = -117 \text{ dB}, \quad (3.34b)$$

whichever yields the smaller absolute value.

2. For $0 < x_{1,2} \leq 200$ and $10^{-5} \leq K_{h,v}(a_{1,2}) < 1$,

$$\text{and } x \geq -450 / \{ \log_{10} [K_{h,v}(a_{1,2})] \}^3 ,$$

$F(x_{1,2})$ is calculated using (3.34a). Otherwise,

$$F(x_{1,2}) = 20 \log_{10} K_{h,v}(a_{1,2}) + 2.5 \times 10^{-5} x_{1,2}^2 / K_{h,v}(a_{1,2}) - 15 \text{ dB} .$$

(3.34c)

Note that when $K_{h,v}(a_{1,2}) > 0.1$ no test on x is required and (3.34c) is always used.

3. For $200 < x_{1,2} \leq 2000$, define

$$w_{1,2} = 0.0134 x_{1,2} \exp(-0.005 x_{1,2}). \quad (3.35a)$$

Then

$$F(x_{1,2}) = w_{1,2} (40 \log_{10} x_{1,2} - 117) + (1 - w_{1,2}) (0.05751 x_{1,2} - 10 \log_{10} x_{1,2}) \text{ dB}. \quad (3.35b)$$

4. For $x_{1,2} > 2000$,

$$F(x_{1,2}) = 0.05751 x_{1,2} - 10 \log_{10} x_{1,2} \text{ dB}. \quad (3.36)$$

The parameter $G(x_{3,4})$ is defined as

$$G(x_{3,4}) = 0.05751 x_{3,4} - 10 \log_{10} x_{3,4} \text{ dB}. \quad (3.37)$$

Values of $A_{k3,4}$ as given by (3.27) and of $A_{r3,4}$ as given by (3.28) are substituted in (3.24a,b) to obtain A_3 and A_4 . These computed values of A_3 at d_3 , and A_4 at d_4 are used to compute the slope m_d and intercept A_{ed} that define a straight line. The reference attenuation A_{cr} at any distance $d_{Ls} \leq d \leq d_x$ is then

$$A_{cr} = A_d = A_{ed} + m_d d \text{ dB}, \quad (3.38a)$$

$$A_{ed} = A_{fo} + A_4 - m_d d_4, \text{ and } m_d = (A_4 - A_3) / (d_4 - d_3), \quad (3.38b)$$

where A_{fo} is a "clutter factor", defined as

$$A_{fo} = 5 \log_{10} [1 + h_{g1} h_{g2} f \sigma_h (d_{Ls}) 10^{-5}] \text{ dB},$$

$$\text{or } 15 \text{ dB, whichever is smaller,} \quad (3.38c)$$

and the terrain roughness term $\sigma_h (d_{Ls})$ is obtained by substituting d_{Ls} for d in (3.6) and (3).

3-3. Formulas for Computing Scatter Attenuation A_s

At distances d_5 and d_6 , defined below, the following formulas are used to obtain initial estimates \hat{A}_5 and \hat{A}_6 of forward scatter attenuation relative to free space:

$$d_5 = d_L + 200 \text{ km}, \quad d_6 = d_L + 400 \text{ km} \quad (3.39)$$

$$\theta_5 = \theta_e + d_5/a, \quad \theta_6 = \theta_e + d_6/a \text{ radians} \quad (3.40)$$

$$\left. \begin{aligned} H_{5,6} &= \left(\frac{1}{h_{e1}} + \frac{1}{h_{e2}} \right) / (\theta_{5,6} f | 0.007 - 0.058 \theta_{5,6} |) \text{ dB} \\ \text{or } 15 \text{ dB, whichever is smaller.} \end{aligned} \right\} \quad (3.41)$$

$$S_5 = H_5 + 10 \log_{10} (f \theta_5^4) - 0.1 (N_s - 301) \exp(-\theta_5 d_5/40) \text{ dB} \quad (3.42a)$$

$$S_6 = H_6 + 10 \log_{10} (f \theta_6^4) - 0.1 (N_s - 301) \exp(-\theta_6 d_6/40) \text{ dB.} \quad (3.42b)$$

Substitute d_5 , θ_5 , S_5 , and d_6 , θ_6 , S_6 in the following expressions to obtain $\hat{A}_5 = \hat{A}_s$ at d_5 , and $\hat{A}_6 = \hat{A}_s$ at d_6 .

For $\theta d \leq 10$:

$$\hat{A}_s = S + 103.4 + 0.332 \theta d - 10 \log_{10} (\theta d) \text{ dB.} \quad (3.43a)$$

For $10 \leq \theta d \leq 70$:

$$\hat{A}_s = S + 97.1 + 0.212 \theta d - 2.5 \log_{10} (\theta d) \text{ dB.} \quad (3.43b)$$

For $\theta d \geq 70$:

$$\hat{A}_s = S + 86.8 + 0.157 \theta d + 5 \log_{10} (\theta d) \text{ dB} . \quad (3.43c)$$

3-3.1. For $H_5 \leq 10 \text{ dB}$

When the frequency gain function, H_5 , computed at d_5 is less than or equal to 10 dB, formulas (3.39) through (3.43) give the actual predicted scatter loss at the distances d_5 and d_6 , and

$$A_5 = \hat{A}_5 \text{ dB}, \text{ and } A_6 = \hat{A}_6 \text{ dB}.$$

The scatter attenuation A_s , at any distance d , is then given by (17) and (18) as

$$A_s = A_{es} + m_s d \text{ dB},$$

where

$$A_{es} = A_5 - m_s d_5, \text{ and } m_s = (A_6 - A_5) / (d_6 - d_5).$$

The distance d_x , where diffraction and scatter attenuations are equal, is

$$d_x = (A_{es} - A_{ed}) / (m_d - m_s) \text{ km}, \quad (3.44a)$$

$$\text{or } \underline{d_L} + 0.25 (a^2 / f)^{\frac{1}{3}} \log_{10} f, \text{ whichever is greater}, \quad (3.44b)$$

where A_{ed} and m_d are defined by (15), and (3.38b). When (3.44b) is used to define d_x , redefine A_{es} as

$$A_{es} = A_{ed} + (m_d - m_s) d_x \quad (3.44c)$$

The reference attenuation A_{cr} for transhorizon paths is then

$$\left. \begin{array}{l} \text{for } d_{Ls} \leq d \leq d_x, A_{cr} = A_d = A_{ed} + m_d d \text{ dB} \\ \text{for } d_x \leq d \leq 1500 \text{ km}, A_{cr} = A_s = A_{es} + m_s d \text{ dB} \end{array} \right\} . \quad (3.45)$$

3-3.2. For $H_5 > 10$ dB and ≤ 15 dB

When the frequency gain function H_5 computed at d_5 is greater than 10 dB, the estimates \hat{A}_5 and \hat{A}_6 are modified by comparison with the scatter loss expected over a smooth earth, $\Delta h = 0$. To determine the distance d_{xo} , where diffraction and scatter losses would be equal over a smooth earth, the diffraction loss, with $\Delta h = 0$, is also computed.

For the special case, $\Delta h = 0$, let $A_{do} = A_{ed}$, $m_{do} = m_d$, and \hat{A}_{50} be the preliminary estimate of scatter attenuation at d_5 . Assume that the slope m_s is not changed. Then one estimate of d_{xo} is obtained by substituting in (3.44):

$$d_{x1} = \hat{d}_{xo} = (\hat{A}_{50} - m_s d_5 - A_{do}) / (m_{do} - m_s) \text{ km.} \quad (3.46a)$$

When H_5 is large, a good estimate of d_{xo} is

$$d_{x2} = \hat{d}_{xo} = d_L + 0.25 (a^2/f)^{\frac{1}{3}} \log_{10} f \text{ km.} \quad (3.46b)$$

For smaller values of H_5 , d_{x1} is the better estimate of d_{xo} , and for larger values d_{x2} is the better estimate. Therefore, a weighted function is used to compute d_{xo} as follows:

$$d_{xo} = d_{x1} (3 - 0.2 H_5) + d_{x2} (0.2 H_5 - 2) \text{ km.} \quad (3.46c)$$

For $\Delta h = 0$, scatter and diffraction losses are equal at d_{xo} . The diffraction attenuation A_{xo} at d_{xo} is

$$A_{xo} = A_{do} + m_{do} d_{xo} \text{ dB.} \quad (3.47)$$

It is assumed that, in general, the forward scatter attenuation A_{sx} at $d = d_{xo}$ for any value of Δh is

$$A_{sx} = A_{xo} + (\hat{A}_5 - \hat{A}_{50}) \text{ dB.} \quad (3.48)$$

The intercept at $d = 0$ would then be

$$A_{es} = A_{sx} - m_s d_{xo} \text{ dB.} \quad (3.49)$$

Substituting this value of A_{es} in (3.44a or b) determines the distance d_x , and for any distance $d \geq d_x$,

$$A_{cr} = A_s = A_{es} + m_s d \text{ dB.}$$

3-4. List of Symbols and Abbreviations

In the following list the English alphabet precedes the Greek alphabet and lower case letters precede upper case letters. In general, upper case letters are used for quantities expressed in decibels.

- a an effective earth's radius that allows for average refraction of radio rays near the surface of the earth, (1) and (3.1).
- a_1, a_2 effective earth's radii for the terrain between the transmitting or receiving antennas, respectively, and the corresponding horizon, (3.29a).
- a_3, a_4 effective earth's radii for the terrain between horizons at distances d_3 and d_4 respectively, (3.29b).
- A attenuation relative to free space, expressed in decibels. Attenuation below free space is written as positive values of A .
- A_{cr} a predicted reference value of attenuation below free space, expressed in decibels.
- A_d the diffraction attenuation in dB, (13), (16), and section 3-2.
- A_{do} the diffraction attenuation in dB equivalent to A_{ed} , but computed assuming a smooth spherical earth, (3.47).
- A_e attenuation below free space in dB defined by (11), to simplify (10).
- A_{ed} estimated diffraction attenuation below free space in dB, extrapolated to zero distance, (15) and (3.38).
- A_{es} estimated scatter attenuation below free space in dB, extrapolated to zero distance, (17) and (3.49).
- A_{fo} an estimate of attenuation due to surface clutter, (3.38c).
- A_k an estimate of knife-edge diffraction attenuation, (13).
- A_{k3}, A_{k4} an estimate of knife-edge attenuation computed at distances d_3 and d_4 , respectively, (3.27).

A_L diffraction attenuation in dB, computed at the distance d_L .
 A_{Ls} diffraction attenuation in dB, computed at the distance d_{Ls} ,
 (3.17c).
 A_r an estimate of the diffraction attenuation over the bulge of
 the earth, (13), and subsection 3-2.
 A_{r3}, A_{r4} the diffraction attenuation A_r computed at distances d_3
 and d_4 , respectively, (3.28).
 A_s forward scatter attenuation in dB, (18).
 A_{sx} forward scatter attenuation computed at $d = d_{xo}$, (3.48).
 \hat{A}_s an estimate of the forward scatter attenuation, (3.43).
 A_{xo} an estimate of the diffraction attenuation over a smooth earth,
 computed at d_{xo} , (3.47).
 $A(v)$ an estimate of knife-edge diffraction as a function of the
 parameter v , (3.26).
 A_o, A_l attenuation below free space computed at the distances d_o
 and d_l , respectively, (10) and (3.18).
 A_{ot}, A_{lt} estimates of attenuation below free space computed at the
 distances d_o and d_l , respectively, using two-ray optics,
 (3.18).
 A_3, A_4 predicted diffraction attenuation computed at distances d_3
 and d_4 , respectively, (3.25).
 A_5, A_6 predicted scatter attenuation computed at distances d_5 and
 d_6 , respectively.
 \hat{A}_5, \hat{A}_6 estimates of scatter attenuation computed at distances d_5
 and d_6 , respectively, (3.43).
 \hat{A}_{50} a preliminary estimate of scatter attenuation computed over
 a smooth earth at the distance d_5 , (3.46).

- $A(0.5)$ a long-term median estimate of attenuation relative to free space for any particular set of data.
- b_h, b_v parameters used in computing the theoretical plane earth reflection coefficients for horizontal and vertical polarization, respectively, (3.10).
- $B_{1,2,3,4}$ parameters used in computing the modified distances $x_{1,2,3,4}$, (3.32).
- c phase angle relative to π radians of an effective reflection coefficient, (3.2).
- c_h, c_v the phase angle c for horizontal and vertical polarization, respectively, (3.13) to (3.15).
- d great circle path distance in kilometers.
- dB decibels, $10 \log_{10}$ (power ratio).
- d_i one of a series of equal distances at which terrain heights h_i are read, p. 3-2.
- d_L sum of the distances d_{L1} and d_{L2} from each antenna to the corresponding horizon, (5d).
- d_{L1}, d_{L2} the distances from the transmitting and receiving antenna, respectively, to their corresponding horizons, (5c).
- d_{Ls} the sum of the smooth-earth horizon distances d_{Ls1} and d_{Ls2} .
- d_{Ls1}, d_{Ls2} distances from the transmitting and receiving antennas, respectively, to their corresponding horizons over a smooth earth, (5a).
- d_x the distance at which diffraction and scatter attenuations are equal, (3.44).
- d_{xo} the distance at which diffraction and scatter attenuation would be equal over a smooth earth, (3.46c).

d_{x1}, d_{x2} estimates of the distance d_{x0} , defined by (3.46a) and (3.46b).
 \hat{d}_{x0} a preliminary estimate of the distance d_{x0} , (3.46a) and (3.46b).
 d_o a distance chosen to approximate the greatest distance at which the attenuation below free space is zero dB, (3.16).
 d_{o1} one estimate of the distance d_o , (3.16).
 d_1 a distance greater than d_o but less than d_L , defined by (3.16d).
 d_3, d_4 distances defined by (3.24) at which diffraction attenuation is calculated.
 d_5, d_6 distances defined by (3.39) at which scatter attenuation is calculated.
 e the base for natural or Napierian logarithms, $e \approx 2.7183$, (3.21).
 f radio wave frequency, expressed in megahertz (MHz) in this report.
 $F(x_1), F(x_2)$ a function used in computing diffraction attenuation, (3.34).
 g_{o1}, g_{o2} directive gain of each antenna in the direction of the other, (3.2) and (3.5).
 g_{r1}, g_{r2} directive gain of each antenna in the direction of a point of ground reflection, (3.5).
 G_p path antenna gain expressed in decibels above the unit gain of an isotropic radiator, (3.3).
 $G(x_3, x_4)$ a function used in computing the diffraction attenuation at the distances d_3 and d_4 , (3.37).

h subscript referring to horizontal polarization.
 h_i any one of a series of equidistant heights of terrain above sea level.
 h_e a height in meters used in computing the horizon distances, (5c).
 h_{e1}, h_{e2} effective antenna heights of the transmitting and receiving antennas, respectively, (4) and (3.3).
 h_{g1}, h_{g2} structural antenna heights above ground, (4).
 h_{L1}, h_{L2} height above sea level of the horizon obstacle for the transmitter and receiver, respectively, (3.1).
 h_s height of the surface of the ground above sea level, (2).
 h_{s1}, h_{s2} height above sea level of the transmitting and receiving antennas, respectively, (3.1).
 H_5, H_6 frequency gain function computed at the distances d_5 and d_6 , respectively, (3.41).
 k a coefficient used in defining effective antenna heights, (4).
 k_1, k_2 coefficients that define the slope of a smooth curve of A_{cr} versus distance for distances $0 \leq d \leq d_{Ls}$, (10) and (3.19).
 \hat{k}_1, \hat{k}_2 estimates of the coefficients k_1 and k_2 , (3.20).
 $K_h(a), K_v(a)$ parameters for horizontal and vertical polarization, respectively, used in computing diffraction attenuation, (3.33).
 \log_{10} logarithm to the base 10.
 L_{bf} basic transmission loss in free space, (9).
 L_{cr} median reference value of transmission loss (8).
 m_d slope of the curve of diffraction attenuation A_d versus distance, (15b) and (3.38).

m_{do} slope of diffraction attenuation in dB/km for $\Delta h = 0$, (3.46a).
 m_s slope of the curve of scatter attenuation A_s versus distance, (17b) and (3.45).
 m_h, m_v parameters used in computing the magnitudes of the theoretical plane earth reflection coefficients R_h and R_v , (3.11).
 N_s the surface refractivity, (2).
 N_o surface refractivity reduced to sea level, fig. 1.
 p parameter used in computing the theoretical plane earth reflection coefficient, (3.9b).
 q parameter used in computing the theoretical plane earth reflection coefficient, (3.9a).
 R_e the magnitude of an "effective" reflection coefficient, (3.5) and (3.8).
 R_h, R_v the magnitude of the "theoretical" plane earth reflection coefficient for horizontal and vertical polarization, respectively, (3.12a) and (3.12b).
 \hat{R}_e estimate of an effective reflection coefficient, (3.5).
 S_5, S_6 terms defined by (3.42) that are used in estimating the forward scatter attenuation A_s , (3.43).
 v subscript referring to vertical polarization.
 $v_{1.3}, v_{2.3}$ parameters used to compute the double knife-edge attenuation, (3.25) through (3.27).
 $v_{1.4}, v_{2.4}$ parameters used to compute the double knife-edge attenuation, (3.25) through (3.27).
 w weighting factor, determined empirically as a function of radio frequency and terrain parameters, (3.23).
 $w_{1,2}$ parameters used in computing rounded earth attenuations, defined by (3.35a).

w_3, w_4 estimates of w corresponding to $d = d_3, d = d_4$, (3.25).
 x a parameter used in computing the theoretical plane earth reflection coefficient, (3.9a).
 $x_{1, 2, 3, 4}$ distances defined by (3.30) through (3.31b).
 y_1, y_2 parameters used in computing the theoretical plane earth reflection coefficient, (3.14).

Δh an asymptotic value of $\Delta h(d)$ which is used to characterize the terrain, table 1, and (3).
 $\Delta h(d)$ interdecile range of terrain heights above and below a straight line fitted to elevations above sea level, (3).
 Δr the difference in path length of the direct and reflected ray, (3.2) and (3.3).
 ϵ the permittivity or relative dielectric constant of the ground, (3.9) through (3.15).
 θ angular distance for a transhorizon path, (7).
 θ_e the sum of the elevation angles θ_{e1} and θ_{e2} , (6b).
 θ_{e1}, θ_{e2} the angles by which the horizon rays are elevated or depressed relative to the horizontal at each antenna, (6a) and fig. 2.
 θ_3, θ_4 angular distances corresponding to d_3, d_4, d_5, d_6 in (3.26), (3.29), (3.40), (3.41) and (3.42).
 θ_5, θ_6
 λ radio wave length, used for example in (3.23).
 σ the conductivity of the earth's surface, (3.9) and following.
 σ_h the rms deviation of terrain and terrain clutter within the limits of the first Fresnel zone in the dominant reflecting plane, (3.6).
 ψ the grazing angle of a ray reflected from a point on the surface of a smooth earth, (3.7).

3-5. Computer Program Listing and Sample Output

A computer program listing and a sample of the output are given in this section. The program is written in Fortran IV for a digital computer.* A list that relates program symbols to corresponding terms and equations in the report is provided as well as a brief flow chart of the program. Attenuation is computed at fixed distances in addition to the parameters required to obtain curves of A_{cr} versus d .

The sample output shows computations for paths in northeastern Ohio and in the Colorado plains and mountains that correspond to those where measurements were made. The curves of A_{cr} versus d shown in figures 3 through 8 were plotted from this output. Calculations were made at frequencies of 100, 50 and 20 MHz, for appropriate antenna heights above ground. The terrain of the area in Ohio and the Colorado plains is characterized by $\Delta h = 90$ m, while for the mountain paths $\Delta h = 650$ m. Values of surface refractivity used are $N_s = 312$ in Ohio and $N_s = 290$ in Colorado. For the longer mountain paths a somewhat lower value of N_s would be appropriate. The terrain parameters d_{L1} , d_{L2} , θ_{e1} and θ_{e2} were calculated using equations (5) and (6), and for these low, randomly located antennas we assumed $h_{e1,2} = h_{g1,2}$. In each area the first three sets at 100 MHz are for vertical polarization and the second three sets are for horizontal polarization. At frequencies of 50 and 20 MHz only vertical polarization is shown. The smooth-earth horizon distances d_{Ls} , and corresponding attenuation A_{Ls} are listed. Similarly, the distance d_x , at which diffraction and scatter attenuation are equal, and the corresponding attenuation A_{dx} are given.

*The program was written for a Control Data Corporation CDC-3600 computer and may require slight modification for use with other computers.

From this output the calculated reference attenuation A_{cr} may be obtained at any desired distance d :

$$\text{For } 0 \leq d \leq d_{Ls} \quad A_{cr} = A_e + k_1 d + k_2 \log_{10} d \text{ dB.}$$

$$\text{For } d_{Ls} \leq d \leq d_x \quad A_{cr} = A_{ed} + m_d d \text{ dB.}$$

$$\text{For } d \geq d_x \quad A_{cr} = A_{es} + m_s d \text{ dB.}$$

Reference List of Program Symbols

Program	Report	Equation	Program	Report	Equation
A	a	(1)	AOG	A_o	
ACR	A_{cr}	(8)	A1	A_1	(3.18b)
AD	A_d	(13)	A1, 2	$a_{1,2}$	(3.29a)
ADO	A_{do}		A3, 4	$a_{3,4}$	(3.29b)
ADX	A_{dx}		A3, 4	$A_{3,4}$	(3.25)
AED	A_{ed}	(3.38b)	B	b	(3.10)
AES	A_{es}	(18)	B1, 2	$B_{1,2}$	(3.32)
AFO	A_{fo}	(3.38c)	B3, 4	$B_{3,4}$	(3.32)
AG	A	(3.2)	C	c	(3.13) to (3.15)
AH5, 6	$\hat{A}_{5,6}$	(3.48)	D	d	
AH50	\hat{A}_{50}	(3.48)	DEDO	A_{od}	(3.17a)
AK3, 4	$A_{k3,4}$	(3.27c)	DED1	A_{1d}	(3.17b)
ALS	A_{Ls}	(3.17c)	DH	Δh	(3)
AR3, 4	$A_{r3,4}$	(3.28)	DHD	$\Delta h(d)$	(3)
AS	A_s	(17)	DHD3, 4	$\Delta h(d_{3,4})$	(3)
ASX	A_{sx}	(3.48)	DL	d_L	(5d)
AV13, 23	$A(v_{1.3,2.3})$	(3.27)	DLS	d_{Ls}	(5b)
AV14, 24	$A(v_{1.4,2.4})$	(3.27)	DL1, 2	$d_{L1,2}$	(5c)
AXO	A_{xo}	(3.47)	DLS1, 2	$d_{Ls1,2}$	(5a)
AO	A_o	(3.18a)	DX	d_x	(3.44)

Reference List of Program Symbols (continued)

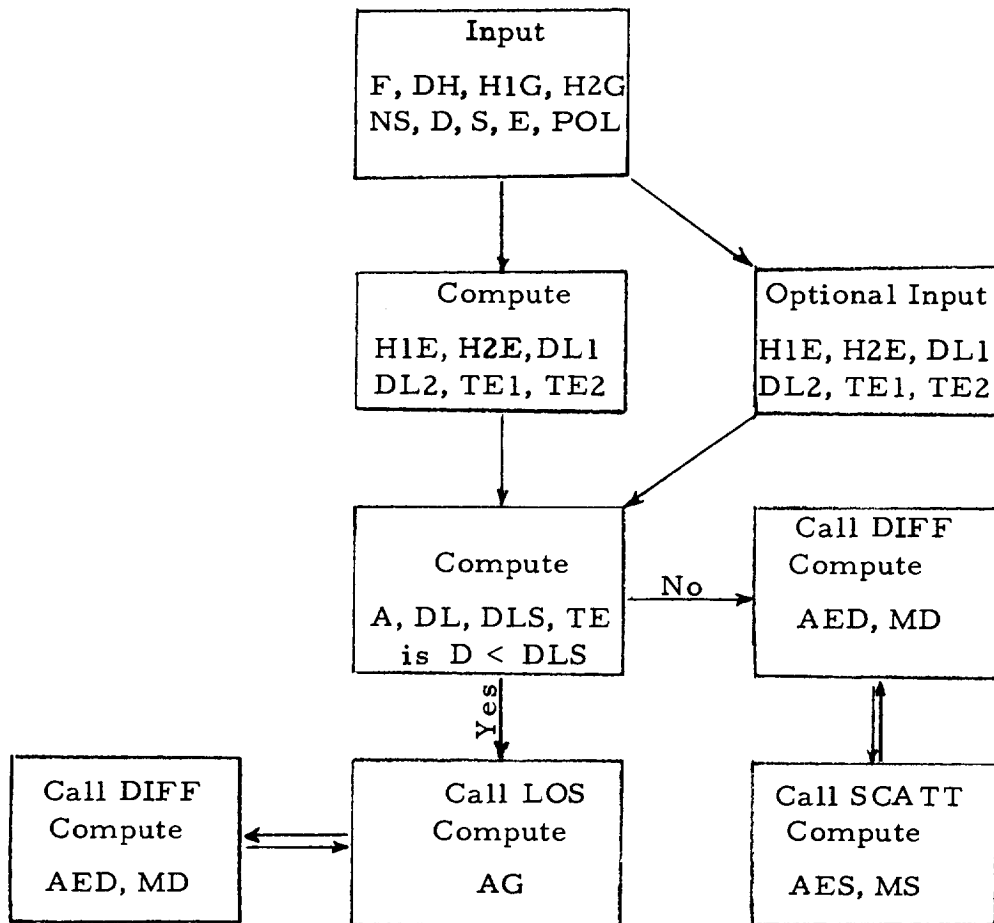
Program	Report	Equation	Program	Report	Equation
DXO	d_{xo}	(3.46)	MS	m_s	(18)
DX1, 2	$d_{x1, 2}$	(3.46)	NS	N_s	(2)
DO	d_o	(3.16c)	P	p	(3.9b)
DO1, 2	$d_{o1, 2}$	(3.16b)	POL	polarization	
D1	d_1	(3.16d)	PSI	ψ	(3.7)
D3, 4	$d_{3, 4}$	(3.24)	Q	q	(3.9a)
D5, 6	$d_{5, 6}$	(3.39)	RE	R_e	(3.5) & (3.8)
E	ϵ	(3.9) to (3.15)	S	σ	(3.9)
F	f in MHz		SH	σ_h	(3.6)
FX1, 2	$F(x_{1, 2})$	(3.34)	SHDLS	$\sigma_h(d_{Ls})$	(3.38)
GX3, 4	$G(x_{3, 4})$	(3.37)	SP	$\sin \psi$	(3.8a)
H1E, 2E	$h_{e1, 2}$	(4b)	S5, 6	$S_{5, 6}$	(3.42)
H1G, 2G	$h_{g1, 2}$	figure 2	TD	θ_d	(3.43)
H5, 6	$h_{5, 6}$	(3.41)	TE	θ_e	(6b)
K1, 2	$k_{1, 2}$	(3.10) to (3.22)	TE1, 2	$\theta_{e1, 2}$	(6a)
K1, 2	$K(a_{1, 2})$	(3.33)	T3, 4	$\theta_{3, 4}$	(3.25c)
K3, 4	$K(a_{3, 4})$	(3.33)	T5, 6	$\theta_{5, 6}$	(3.40)
M	m	(3.11)	V13, 23	$V_{1.3, 2.3}$	(3.26)
MD	m_d	(3.38b)	V14, 24	$V_{1.4, 2.4}$	(3.26)
MDO	m_{do}	(3.47)	W	w_o	(3.18)

Reference List of Program Symbols (continued)

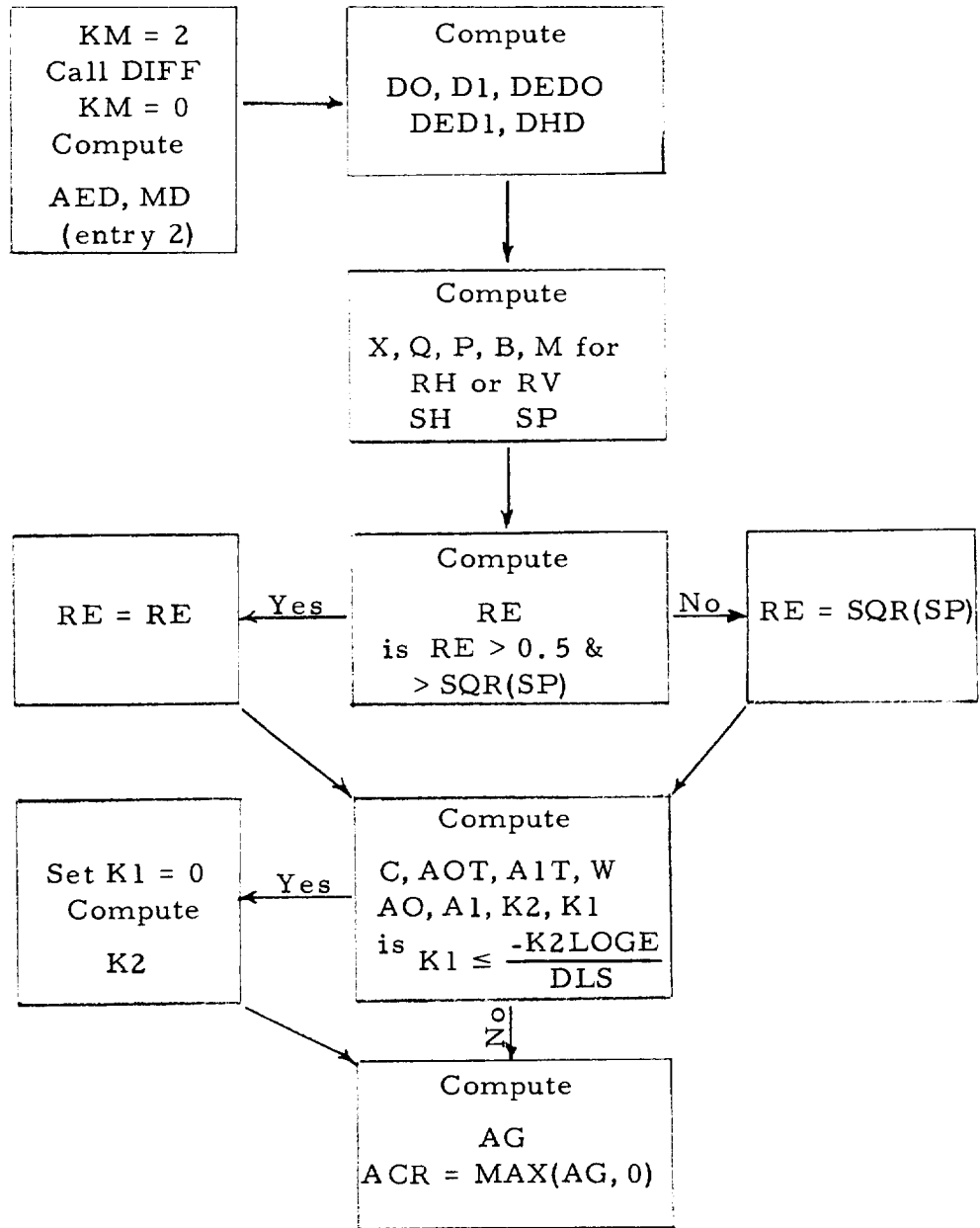
Program	Report	Equation
$W_{1,2}$	$w_{1,2}$	(3.35)
$W_{3,4}$	$w_{3,4}$	(3.23)
X	x	(3.9a)
$X_{1,2}$	$x_{1,2}$	(3.30)
$X_{3,4}$	$x_{3,4}$	(3.31)
$Y_{1,2}$	$y_{1,2}$	(3.14)

Flow Charts

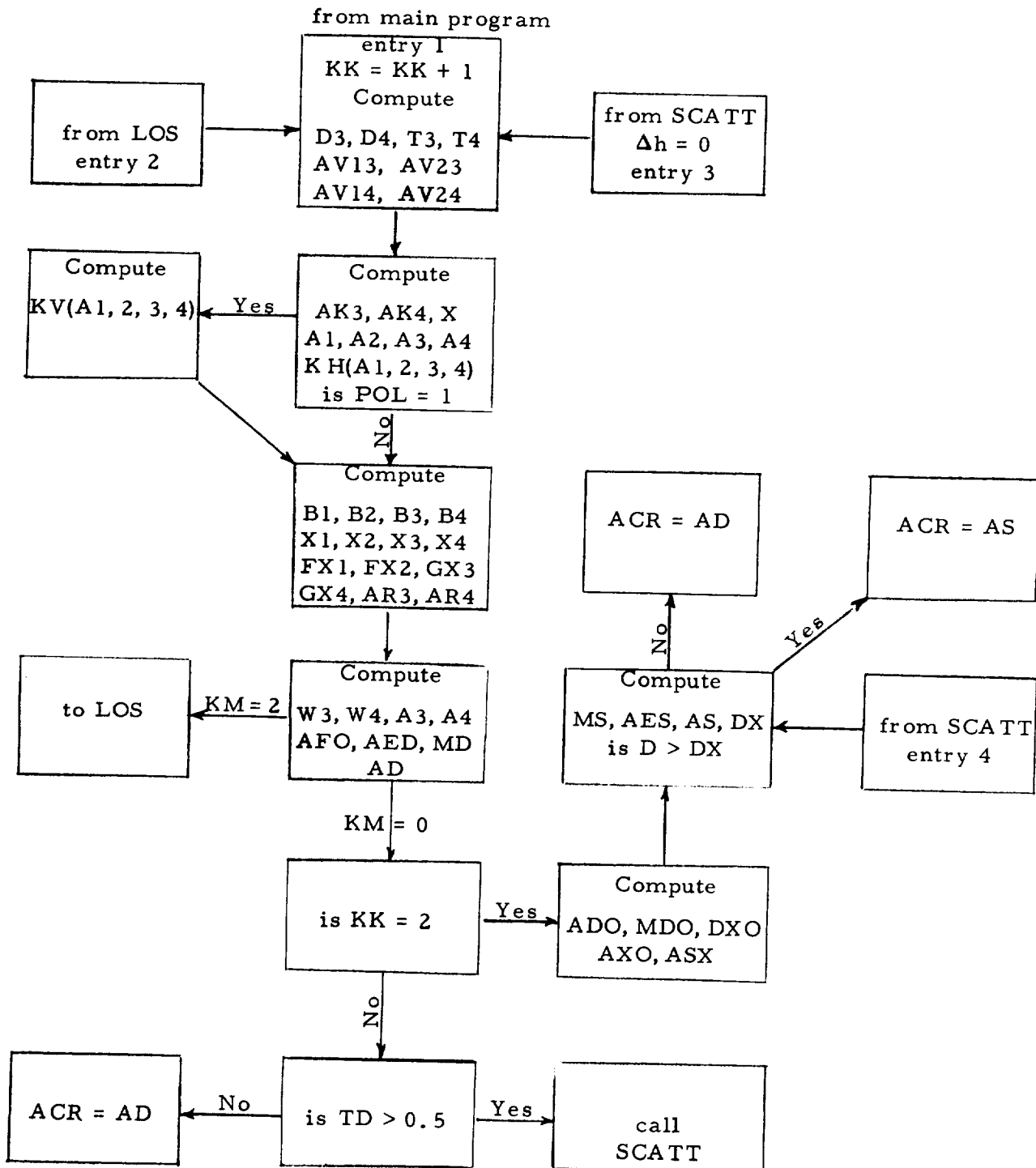
Main Program



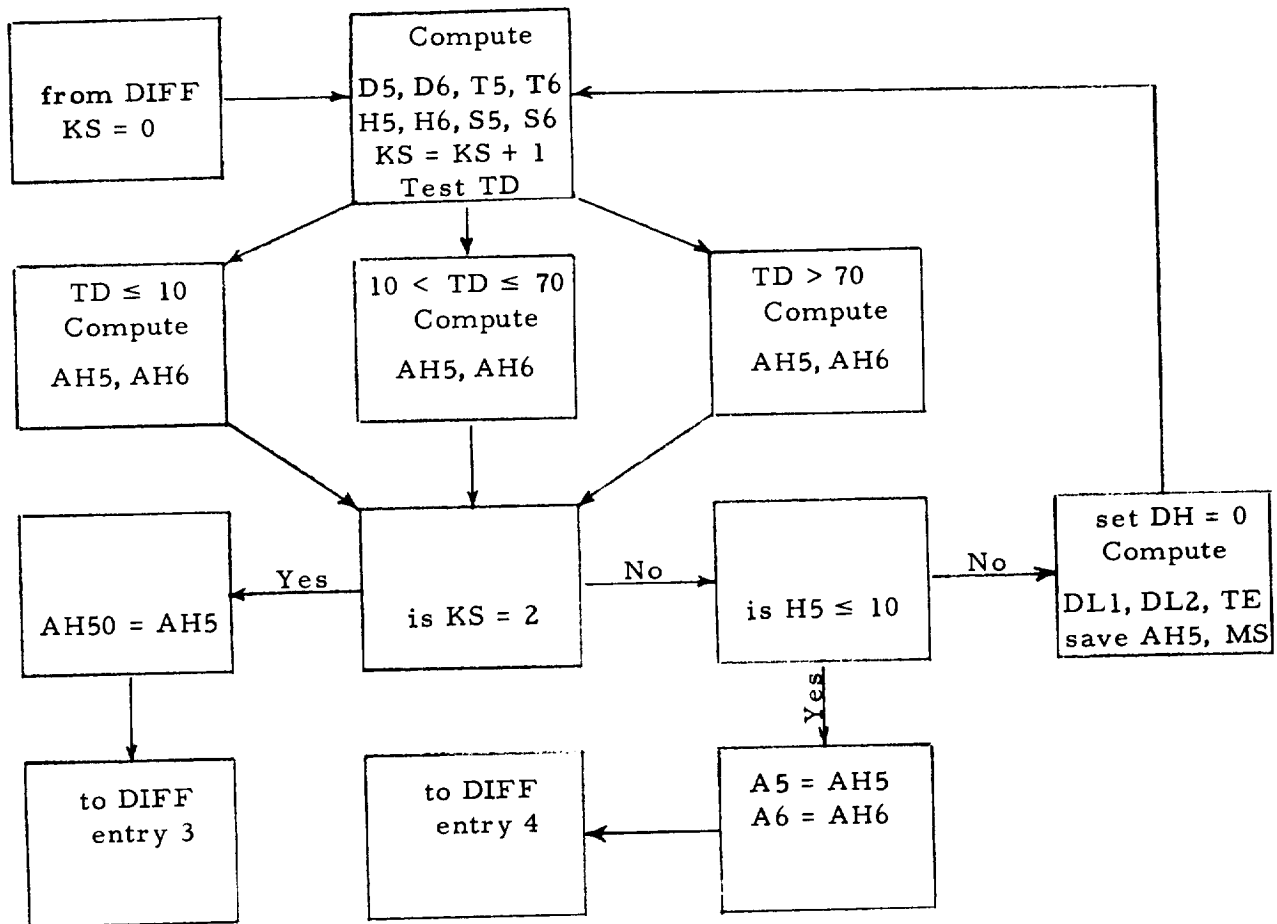
Line-of-Sight Subroutine, LOS



Diffraction Subroutine, DIFF



Scatter Subroutine, SCATT



Computer Program Listing

```

PROGRAM COMTE
C PROGRAM TO DETERMINE PARAMETERS AND WRITE OUTPUT
C
COMMON /M/F,D,NS,A,DH,DHS,S,E,POL,KM
COMMON /MP/ H1E,H2E,H1G,H2G,DLS1,DLS2,DL1,DL2,DL,DLS,TE1,TE2,TE,KL
COMMON /MLDS/ AG,AD,AS,ACR,AED,MD,AH50,AH5,D5,MS,AES,DX,H5
COMMON /ML/ D0,D1,D01,D02,A0,A1,K1,K2,AL,ALS,A0G
DIMENSION ANS(3),DKM(6),DELH(6),SD(6),SA(6)
REAL NS,MD,MDO,MS,MSS,MDS,K1,K2,K3,K4,LBF
DATA (ANS=290.,290.,312.)
DATA (DKM=5.,10.,20.,30.,50.,80.)
DATA (DELH=105.,165.,234.,315.,575.)

C
C CALCULATION OF INPUT PARAMETERS
C
S=.005 $ E=15.
DO 500 IX=1,3
NS=ANS(IX)
A=6370./(1.-.04665*EXPF(.005577*NS))
WRITE ( 2,56)1
56 FORMAT (R1)
IF (IX .EQ. 1) WRITE ( 2,57)
IF (IX .EQ. 2) WRITE ( 2,58)
IF (IX .EQ. 3) WRITE ( 2,59)
57 FORMAT (2X,*COLORADO PLAINS NS=290.*//)
58 FORMAT (2X,*COLORADO MOUNTAINS NS=290.*//)
59 FORMAT (2X,*OHIO NS=312.*//)
DO 400 I=1,9
KK=0
DO 300 IZ=1,6
IF (IX .EQ. 2 .AND. IZ .EQ. 6) GO TO 300
IF (IX .EQ. 3 .AND. (IZ .EQ. 1 .OR. IZ .EQ. 6)) GO TO 300
D=DKM(IZ)
DH=DHS=90.
IF (IX .EQ. 2) DH=DHS=650.
F=100.
IF (I .GT. 6) F=50.
IF (I .EQ. 9) F=20.
POL=+1.
IF (I .GT. 3 .AND. I .LT. 7) POL=-1.
H1G=H1E=4.
IF (IX .NE. 3 .AND. I .EQ. 9) H1G=H1E=3.3
IF (IX .EQ. 3 .AND. I .GT. 6) H1G=H1E=4.24
IF (IX .EQ. 3 .AND. I .EQ. 9) H1G=H1E=3.68
H2G=H2E=3.
IF (I .EQ. 2 .OR. I .EQ. 5) H2G=H2E=6.
IF (I .EQ. 3 .OR. I .EQ. 6) H2G=H2E=9.
IF (IX .EQ. 3 .AND. I .EQ. 7) H2G=H2E=1.
IF (IX .NE. 3 .AND. I .EQ. 7) H2G=H2E=.55
IF (IX .NE. 3 .AND. I .EQ. 8) H2G=H2E=1.7
IF (IX .NE. 3 .AND. I .EQ. 9) H2G=H2E=1.3
DLS1=SQRTF(.002*A*H1E)
DLS2=SQRTF(.002*A*H2E)
DLS=DLS1+DLS2

```

Computer Program Listing (continued)

```

DL1=DLS1*EXP(-.07*SQRT(DH/H1E))
DL2=DLS2*EXP(-.07*SQRT(DH/H2E))
DL=DL1+DL2
TE1=(.00065/DLS1)*((DLS1/DL1-1.)*DH-3.077*H1E)
TE2=(.00065/DLS2)*((DLS2/DL2-1.)*DH-3.077*H2E)
TE=MAX1((TE1+TE2),(-DL/A))
KK=KK+1
IF (D .GT. DLS) GO TO 40
CALL LOS
SD(KK)=D
SA(KK)=ACR
GO TO 300
40 CALL DIFF
SD(KK)=D
SA(KK)=ACR
IF (IX .EQ. 1 .AND. KK .NE. 6) GO TO 300
IF (IX .EQ. 2 .AND. KK .NE. 5) GO TO 300
IF (IX .EQ. 3 .AND. KK .NE. 4) GO TO 300
AE=A0G-K1*D0-K2*ALOG10(D0)
C
C WRITE OUTPUT
C
WRITE ( 2,60) F,DH,H1G,H2G,TE,DX
60 FORMAT (4X,*F=*F6.1,* DH=*F6.2,* H1G=*F6.2,* H2G=*F6.2,
C* TE=*F10.6,* DX=*F8.2)
WRITE ( 2,61) AE,K1,K2,DLS,ALS
61 FORMAT (4X,*AE=*F8.2,* K1=*F10.5,* K2=*F10.5,* DLS=*F8.2,
C* ALS=*F8.2)
ADX=AED+MD*DX
WRITE ( 2,62) AED,MD,AES,MS,ADX
62 FORMAT (4X,*AED=*F8.2,* MD=*F10.5,* AES=*F8.2,* MS=*F10.5,
C* ADX=*F8.2)
WRITE ( 2,63) (SD(JZ), JZ=1,KK)
WRITE ( 2,64) (SA(JZ), JZ=1,KK)
63 FORMAT (4X,*D*6F10.2)
64 FORMAT (4X,*A*6F10.2)
WRITE ( 2,56)
300 CONTINUE
400 CONTINUE
500 CONTINUE
CALL EXIT
END

SUBROUTINE DIFF
C SUBROUTINE TO COMPUTE DIFFRACTION ATTENUATION
C
COMMON /NR/ JZ,W,SW3,SW4,SA3,SA4,SAF0
COMMON /MAR14/D3,D4,T5
COMMON /M/F,D,NS,A,DH,DHS,S,E,POL,KM
COMMON /MP/ H1E,H2E,H1G,H2G,DLS1,DLS2,DL1,DL2,DL,DLS,TE1,TE2,TE,KL
COMMON /MLDS/ AG,AD,AS,ACR,AED,MD,AH50,AH5,D5,MS,AES,DX,H5
REAL NS,MD,MDO,MS,MSS,MDS,K1,K2,K3,K4
FNA(C)=6.02+9.11*C-1.27*C*C

```

Computer Program Listing (continued)

```

FNB(C)=12.953+20.*ALOG10(C)
FNC(C)=416.4*F**.3333333333*(1.607-C)
FND(C)=(.36278/(C*F)**.3333333333)*1./((E-1.):**2+X*X)**.25
FNE(C)=C*SQRTF(E*E+X*X)
RDL=DL
KK=0
10 KK=KK+1
D3=DL+.5*(A*A/F)**.3333333333
IF (D3 .LT. DLS) D3=DLS
D4=D3+(A*A/F)**.3333333333
T3=TE+D3/A
T4=TE+D4/A
C
C CALCULATION OF KNIFE EDGE DIFFRACTION
C
V13=1.2915*T3*SQRTF(F*DL1*(D3-DL)/(D3-DL2))
V23=1.2915*T3*SQRTF(F*DL2*(D3-DL)/(D3-DL1))
V14=1.2915*T4*SQRTF(F*DL1*(D4-DL)/(D4-DL2))
V24=1.2915*T4*SQRTF(F*DL2*(D4-DL)/(D4-DL1))
AV13=FNA(V13)
IF (V13 .GT. 2.4) AV13=FNB(V13)
AV23=FNA(V23)
IF (V23 .GT. 2.4) AV23=FNB(V23)
AV14=FNA(V14)
IF (V14 .GT. 2.4) AV14=FNB(V14)
AV24=FNA(V24)
IF (V24 .GT. 2.4) AV24=FNB(V24)
AK3=AV13+AV23
AK4=AV14+AV24
C
C CALCULATION OF ROUNDED EARTH DIFFRACTION
C
A1=DL1*DL1/(.002*H1E)
A2=DL2*DL2/(.002*H2E)
A3=(D3-DL)/T3
A4=(D4-DL)/T4
X=18000.*S/F
K1=FND(A1)
K2=FND(A2)
K3=FND(A3)
K4=FND(A4)
IF (POL .EQ. -1.) GO TO 15
K1=FNE(K1)
K2=FNE(K2)
K3=FNE(K3)
K4=FNE(K4)
15 B1=FNC(K1)
B2=FNC(K2)
B3=FNC(K3)
B4=FNC(K4)
X1=B1*DL1/A1**.6666666666
X2=B2*DL2/A2**.6666666666
X3=B3*(D3-DL)/A3**.6666666666+X1+X2
X4=B4*(D4-DL)/A4**.6666666666+X1+X2

```

Computer Program Listing (continued)

```

XL1=450./ABSF(ALOG10(K1)**3)
XL2=450./ABSF(ALOG10(K2)**3)
IF(X1.GT.0..AND.X1.LE. 200. .AND.K1 .GE. 0..AND. K1.LE. .00001)
C16,17
16  T=40.*ALOG10(X1)-117.
    T1=-117.
    T2=MIN1F((ABSF(T)),(ABSF(T1)))
    FX1=T
    IF (T2 .EQ. ABSF(T1)) FX1=T1
17  IF(X2.GT.0..AND. X2.LE.200. .AND. K2 .GE.0..AND. K2.LE. .00001)
C18,19
18  T=40.*ALOG10(X2)-117.
    T1=-117.
    T2=MIN1F((ABSF(T)),(ABSF(T1)))
    FX2=T
    IF (T2 .EQ. ABSF(T1)) FX2=T1
19  IF(X1.GT.0. .AND.X1 .LE.200. .AND.K1 .GT. .00001 .AND. K1 .LT. 1.
C) 21,22
21  FX1=40.*ALOG10(X1)-117.
    IF (X1 .LE. XL1) FX1=20.*ALOG10(K1)+2.5*1. E-5*X1*X1/K1-15.
22  IF(X2 .GT.0. .AND.X2 .LE.200. .AND.K2 .GT. .00001 .AND. K1 .LT. 1.
C) 23,24
23  FX2=40.*ALOG10(X2)-117.
    IF (X2 .LE. XL2) FX2=20.*ALOG10(K2)+2.5*1. E-5*X2*X2/K2-15.
24  W1=.0134*X1*EXPF(-.005*X1) $ W2=.0134*X2*EXPF(-.005*X2)
    IF(X1.GT.200. .AND. X1.LE.2000.)
C FX1=W1*(40.*ALOG10(X1)-117.)+(1.-W1)*(.05751*X1-10.*ALOG10(X1))
    IF(X2 .GT. 200. .AND. X2 .LE. 2000.)
C FX2=W2*(40.*ALOG10(X2)-117.)+(1.-W2)*(.05751*X2-10.*ALOG10(X2))
    IF(X1.GT. 2000.) FX1=.05751*X1-10.*ALOG10(X1)
    IF(X2 .GT. 2000.) FX2=.05751*X2-10.*ALOG10(X2)
    GX3=.05751*X3-10.*ALOG10(X3)
    GX4=.05751*X4-10.*ALOG10(X4)
    AR3=GX3-FX1-FX2-20.
    AR4=GX4-FX1-FX2-20.
C
C COMBINATION OF ROUNDED EARTH AND KNIFE EDGE DIFFRACTION
C
28  DHD3=DH*(1.-.8 *EXPF(-.02*D3))
    DHD4=DH*(1.-.8 *EXPF(-.02*D4))
    P13=SQRTF((H1E*H2E)/(H1G*H2G))+(A*TE+DL)/D3
    P14=SQRTF((H1E*H2E)/(H1G*H2G))+(A*TE+DL)/D4
    DOL3=MIN1F(1000.,(DHD3*F/299.7925))
    DOL4=MIN1F(1000.,(DHD4*F/299.7925))
63  W3=1./(1+.1 *SQRTF(DOL3*P13))
    W4=1./(1+.1 *SQRTF(DOL4*P14))
31  A3=(1.-W3)*AK3+W3*AR3
    A4=(1.-W4)*AK4+W4*AR4
    MD=(A4-A3)/(D4-D3)
    AED=A4-MD*D4
    DHDLS=DH*(1.-.8*EXPF(-.02*DLS))
    SHDLS=.78*DHDLS*EXPF(-.5*(DHDLS**.25))
    AFO=5.*ALOG10(1.+H1G*H2G*F*SHDLS*.00001)
    AFO=MIN1F(AFO,15.)

```

Computer Program Listing (continued)

```

91  AED=AED+AF0
    IF (KM .EQ. 2) GO TO 40
    IF (KK.EQ. 2) GO TO 20
    SAFO=AF0
    SW3=W3 $ SW4=W4 $ SA3=A3 $ SA4=A4
29  AD=AED+MD*D
32  TD=(TE+D/A)*D
    SDL1=DL1 $ SDL2=DL2 $ SDL=DL $ STE1=TE1 $ STE2=TE2
    STE=TE
C
C  CALCULATION OF SCATTER ATTENUATION
C
    CALL SCATT
    IF (H5 .LE. 10.) AES=AH5 -MS*D5
    IF (H5 .LE. 10.) AS=AES+MS*D
    IF (H5 .LE. 10.) GO TO 30
    MDS=MD
    AEDS=AED
    DH=0.
    GO TO 10
20  ADO=AED
    MDO=MD
    MD=MDS
    AED=AEDS
    DX1=(AH50-MS*D5-ADO)/(MDO-MS)
    DX2=(RDL+.25*(A*A/F)**.3333333333*ALOG10(F))
    DXO=DX1*(3.-.2*H5)+DX2*(.2*H5-2.)
    AXO=ADO+MDO*DXO
    ASX=AXO+(AH5-AH50)
    AES=ASX-MS*DXO
    AS=AES+MS*D
30  DX=(AES-AED)/(MD-MS)
    DXN=DL+.25*(A*A/F)**.3333333333*ALOG10(F)
    IF (DXN .GT. DX) AES=AED+(MD-MS)*DX
    IF (DXN .GT. DX) DX=DXN
    ACR=AD
    IF (D .GT. DX) ACR=AS
    DL1=SDL1 $ DL2=SDL2 $ DL=SDL $ TE1=STE1 $ TE2=STE2
    TE=STE
    DH=DHS
41  CONTINUE
40  RETURN
    END

SUBROUTINE SCATT
C  SUBROUTINE TO COMPUTE SCATTER PARAMETERS
C
COMMON /M/F,D,NS,A,DH,DHS,S,E,POL,KM
COMMON /MP/ H1E,H2E,H1G,H2G,DLS1,DLS2,DL1,DL2,DL,DLS,TE1,TE2,TE,KL
COMMON /MAR14/D3,D4,T5
COMMON /MLDS/ AG,AD,AS,ACR,AED,MD,AH50,AH5,D5,MS,AES,DX,H5
REAL NS,MD,MDO,MS,MSS,MDS,K1,K2,K3,K4
KK=0

```

Computer Program Listing (continued)

```

10  KK=KK+1
    D5=DL+ 200.
    D6=DL+ 400.
11  T5=TE+D5/A
    T6=TE+ D6/A
    H5=MIN1F(((1./H1E +1./H2E)/(T5*F*ABSF(.007-.058*T5))), (15.))
    H6=MIN1F(((1./H1E+1./H2E)/(T6*F*ABSF(.007-.058*T6))), (15.))
    S5=H5+10.*ALOG10(F*T5**4)-.1*(NS-301.)*EXP(-T5*D5/40.)
    S6=H6+10.*ALOG10(F*T6**4)-.1*(NS-301.)*EXP(-T6*D6/40.)
    IF(T5*D5 .LE.10.) AH5=S5+103.4+.332*T5*D5-10.*ALOG10(T5*D5)
    IF(T6*D6 .LE.10.) AH6=S6+103.4+.332*T6*D6-10.*ALOG10(T6*D6)
    IF(T5*D5 .GT. 10. .AND.T5*D5.LE. 70.) AH5=S5+97.1+.212*T5*D5-2.5*
C    ALOG10(T5*D5)
    IF(T6*D6 .GT. 10. .AND.T6*D6 .LE. 70.) AH6=S6+97.1+.212*T6*D6-2.5
C    ALOG10(T6*D6)
    IF(T5*D5 .GT. 70.) AH5=S5+86.8+.157*T5*D5+5.*ALOG10(T5*D5)
    IF(T6*D6 .GT. 70.) AH6=S6+86.8+.157*T6*D6+5.*ALOG10(T6*D6)
    MS=(AH6-AH5)/(D6-D5)
    IF (KK .EQ. 2) GO TO 25
    IF (H5 .LE. 10.) GO TO 30
    IF (KK .EQ. 1) GO TO 20
25  MS=MSS
    AH50=AH5
    AH5=AH5S
    D5=D5S
    GO TO 30
20  DH=0.
    DL1=DLS1*EXP(-.07*SQRTE(DH/H1E))
    DL2=DLS2*EXP(-.07*SQRTE(DH/H2E))
    DL=DL1+DL2
    TE1=(.00065/DLS1)*((DLS1/DL1-1.)*DH-3.077*H1G)
    TE2=(.00065/DLS2)*((DLS2/DL2-1.)*DH-3.077*H2G)
    TE=MAX1F((TE1+TE2),(-DL/A))
    T=TE+D/A
    AH5S=AH5
    MSS=MS
    D5S=D5
    GO TO 10
30  CONTINUE
    RETURN
    END

SUBROUTINE LOS
C  SUBROUTINE TO COMPUTE LINE OF SIGHT ATTENUATION
C
COMMON /M/F,D,NS,A,DH,DHS,S,E,POL,KM
COMMON /NR/ JZ,W,SW3,SW4,SA3,SA4,SAF0
COMMON /MP/ H1E,H2E,H1G,H2G,DLS1,DLS2,DL1,DL2,DL,DLS,TE1,TE2,TE,KL
COMMON /MLDS/ AG,AD,AS,ACR,AED,MD,AH50,AH5,D5,MS,AES,DX,H5
COMMON /ML/ D0,D1,D01,D02,A0,A1,K1,K2,AL,ALS,A0G
REAL NS,MD,MDO,MS,MSS,MDS,K1,K2,K3,K4,M
KM=2
CALL DIFF

```

Computer Program Listing (continued)

```

      KM=0
C
C      CALCULATION OF TWO RAY THEORY
C
      D01=.00004*H1E*H2E*F
      D02=MIN1F((-AED/MD),(DL-2.))
      IF (AED .GE. 0.) D0=MIN1F(D01,(.5*DL))
      IF (AED .LT. 0.) D0=.5*DL
      IF (AED .LT. 0. .AND. D02 .GE. D0) D0=D02
      D1=D0+.25*(DL-D0)
      IF (D1 .LE. D0) D1=D0+.25*(DLS-D0)
      J=0 $ DS=D
      IF (J.EQ. 0) D=D0
22     DIV=1. $ PSI=ATANF((H1E+H2E)/(1000.*D))
2     DHD=DH*(1.-.8 *EXP(-.02*D))
      SH=.78*DHD*EXP(-.5*DHD**.25)
      SP=SINF(PHI)
      X=18000.*S/F
      P2=(SQRTF((E-COSF(PHI)*COSF(PHI))**2+X*X)+E-COSF(PHI)*COSF(PHI))/2
C
      P=SQRTF(P2)
      Q=X/(2.*P)
      IF (POL .EQ. 1.)B=(E*E+X*X)/(P2+Q*Q)
      IF (POL .EQ. -1.)B=1./(P2+Q*Q)
      IF (POL .EQ. 1.)M=2.*(P*E+Q*X)/(P2+Q*Q)
      IF (POL .EQ. -1.)M=2.*P/(P2+Q*Q)
      R2=(1.+B*SP*SP-M*SP)/(1.+B*SP*SP+M*SP)
      RE=SQRTF(SP)
      SQEXF=SQRTF(R2)*EXP(-.0209584473*F*SH*SP)*DIV
      IF (SQEXF .GT. .5 .AND. SQEXF .GT. RE) RE=SQEXF
      C=ATANF(Q/(P+SP))-ATANF(Q/(P-SP))
      IF (POL .EQ. -1.)GO TO 40
      Y1=(X*SP+Q)/(E*SP+P)
      Y2=(X*SP-Q)/(E*SP-P)
      IF (E*SP .GE. P) C=ATANF(Y1)-ATANF(Y2)+3.141592654
      IF (E*SP .LT. P .AND. P*SP .GT. .5) C=ATANF(Y1)+ATANF(Y2)
      IF (E*SP .LT. P .AND. P*SP .LE. .5) C=ATANF(Y1)-ATANF(Y2)
40     IF (J .EQ. 0)
      CA0=-10.*ALOG10(1.+RE*RE-2.*RE*COSF(.000041917*F*H1E*H2E/D0-C))
      IF (J .EQ. 1) GO TO 3
      D=D1 $ J=1
      GO TO 22
3     CONTINUE
      D=DS
      IF (J .EQ. 1)
      CA1=-10.*ALOG10(1.+RE*RE-2.*RE*COSF(.000041917*F*H1E*H2E/D1-C))
C
C      COMBINATION OF TWO RAY THEORY AND DIFFRACTION
C
      ALS=AED+MD*DLS
      AL=AED+MD*DL
      DED0=AED+MD*D0
      DED1=AED+MD*D1
      SA0=A0 $ SA1=A1

```

Computer Program Listing (continued)

```

W=(MIN1F(H1E,H2E)/MAX1F(H1E,H2E))/(1.+F*DH*.0001)
W=1./(1.+F*DH*.0001)
A0=MIN1F((W*A0+(1.-W)*DED0),DED0)
A1=MIN1F((W*A1+(1.-W)*DED1),DED1)
10 K2=((ALS-A0)*(D1-D0)-(A1-A0)*(DLS-D0))/((D1-D0)*ALOG10(DLS/D0)-
C(DLS-D0)*ALOG10(D1/D0))
K2=MAX1F(K2,0.)
K1=((ALS-A0)-K2*ALOG10(DLS/D0))/(DLS-D0)
IF (K1 .GE. 0.) GO TO 50
K1=0.
K2=(ALS-A0)/(ALOG10(DLS/D0))
50 AG=A0+K1*(D-D0)+K2*ALOG10(D/D0)
IF (AG .LT. 0.) AG=0.
51 AOG=A0
53 ACR=AG
RETURN
END

```


Computer Program Output

COLORADO PLAINS NS=290.

F= 100.0 DH= 90.00 H1G= 4.00 H2G= 3.00 TE= 0.004861 DX= 133.88
 AE= 28.09 K1= 0.49356 K2= 6.69918 DLS= 15.23 ALS= 43.53
 AED= 39.24 MD= 0.28151 AES= 69.68 MS= 0.05418 ADX= 76.93
 D 5.00 10.00 20.00 30.00 50.00 80.00
 A 35.24 39.72 44.87 47.69 53.32 61.76

F= 100.0 DH= 90.00 H1G= 4.00 H2G= 6.00 TE= 0.002464 DX= 130.11
 AE= 24.93 K1= 0.40159 K2= 7.10267 DLS= 18.16 ALS= 41.17
 AED= 36.15 MD= 0.27636 AES= 64.85 MS= 0.05575 ADX= 72.11
 D 5.00 10.00 20.00 30.00 50.00 80.00
 A 31.91 36.05 41.68 44.44 49.97 58.26

F= 100.0 DH= 90.00 H1G= 4.00 H2G= 9.00 TE= 0.001556 DX= 126.02
 AE= 22.62 K1= 0.36162 K2= 7.20867 DLS= 20.41 ALS= 39.44
 AED= 33.81 MD= 0.27609 AES= 61.49 MS= 0.05641 ADX= 68.60
 D 5.00 10.00 20.00 30.00 50.00 80.00
 A 29.47 33.44 39.23 42.09 47.61 55.89

F= 100.0 DH= 90.00 H1G= 4.00 H2G= 3.00 TE= 0.004861 DX= 135.25
 AE= 30.15 K1= 0.32410 K2= 7.97226 DLS= 15.23 ALS= 44.51
 AED= 40.18 MD= 0.28417 AES= 71.29 MS= 0.05418 ADX= 78.62
 D 5.00 10.00 20.00 30.00 50.00 80.00
 A 37.34 41.36 45.87 48.71 54.39 62.92

F= 100.0 DH= 90.00 H1G= 4.00 H2G= 6.00 TE= 0.002464 DX= 129.21
 AE= 26.22 K1= 0.24421 K2= 8.39353 DLS= 18.16 ALS= 41.22
 AED= 36.16 MD= 0.27885 AES= 64.98 MS= 0.05575 ADX= 72.19
 D 5.00 10.00 20.00 30.00 50.00 80.00
 A 33.30 37.05 41.73 44.52 50.10 58.46

F= 100.0 DH= 90.00 H1G= 4.00 H2G= 9.00 TE= 0.001556 DX= 125.44
 AE= 23.70 K1= 0.23397 K2= 8.47052 DLS= 20.41 ALS= 39.57
 AED= 33.88 MD= 0.27858 AES= 61.75 MS= 0.05641 ADX= 68.83
 D 5.00 10.00 20.00 30.00 50.00 80.00
 A 30.79 34.51 39.40 42.24 47.81 56.17

F= 50.0 DH= 90.00 H1G= 4.00 H2G= 0.55 TE= 0.029474 DX= 121.70
 AE= 31.31 K1= 1.01536 K2= 8.14286 DLS= 11.19 ALS= 51.21
 AED= 47.89 MD= 0.29676 AES= 78.36 MS= 0.04634 ADX= 84.00
 D 5.00 10.00 20.00 30.00 50.00 80.00
 A 42.07 49.60 53.82 56.79 62.72 71.63

F= 50.0 DH= 90.00 H1G= 4.00 H2G= 1.70 TE= 0.008505 DX= 136.42
 AE= 29.15 K1= 0.47486 K2= 9.49046 DLS= 13.48 ALS= 46.28
 AED= 42.92 MD= 0.24920 AES= 69.78 MS= 0.05227 ADX= 76.91
 D 5.00 10.00 20.00 30.00 50.00 80.00
 A 38.16 43.39 47.90 50.40 55.32 62.86

F= 20.0 DH= 90.00 H1G= 3.30 H2G= 1.30 TE= 0.011970 DX= 139.21
 AE= 30.25 K1= 0.31408 K2= 10.97428 DLS= 12.07 ALS= 45.91
 AED= 43.48 MD= 0.20074 AES= 64.35 MS= 0.05084 ADX= 71.43
 D 5.00 10.00 20.00 30.00 50.00 80.00
 A 39.49 44.36 47.50 49.51 53.52 59.54

Computer Program Output (continued)

COLORADO MOUNTAINS NS=290.

F= 100.0 DH=650.00 H1G= 4.00 H2G= 3.00 TE= 0.180463 DX= 131.08
 AE= 52.42 K1= 0.68866 K2= 0.66909 DLS= 15.23 ALS= 63.70
 AED= 59.29 MD= 0.28955 AES= 91.24 MS= 0.04574 ADX= 97.24
 D 5.00 10.00 20.00 30.00 50.00
 A 56.33 59.97 65.08 67.97 73.76

F= 100.0 DH=650.00 H1G= 4.00 H2G= 6.00 TE= 0.117712 DX= 164.84
 AE= 47.62 K1= 0.57113 K2= 0.69038 DLS= 18.16 ALS= 58.86
 AED= 53.99 MD= 0.26795 AES= 94.89 MS= 0.01984 ADX= 98.16
 D 5.00 10.00 20.00 30.00 50.00
 A 50.95 54.02 59.35 62.03 67.39

F= 100.0 DH=650.00 H1G= 4.00 H2G= 9.00 TE= 0.100178 DX= 164.32
 AE= 45.85 K1= 0.52997 K2= 0.63153 DLS= 20.41 ALS= 57.49
 AED= 52.17 MD= 0.26061 AES= 87.84 MS= 0.04351 ADX= 94.99
 D 5.00 10.00 20.00 30.00 50.00
 A 48.94 51.78 57.27 59.99 65.20

F= 100.0 DH=650.00 H1G= 4.00 H2G= 3.00 TE= 0.180463 DX= 125.95
 AE= 53.20 K1= 0.67804 K2= 0.80520 DLS= 15.23 ALS= 64.48
 AED= 60.01 MD= 0.29374 AES= 91.24 MS= 0.04574 ADX= 97.00
 D 5.00 10.00 20.00 30.00 50.00
 A 57.16 60.79 65.88 68.82 74.70

F= 100.0 DH=650.00 H1G= 4.00 H2G= 6.00 TE= 0.117712 DX= 161.69
 AE= 48.13 K1= 0.55941 K2= 0.83653 DLS= 18.16 ALS= 59.34
 AED= 54.43 MD= 0.27074 AES= 95.00 MS= 0.01984 ADX= 98.20
 D 5.00 10.00 20.00 30.00 50.00
 A 51.51 54.56 59.84 62.55 67.96

F= 100.0 DH=650.00 H1G= 4.00 H2G= 9.00 TE= 0.100178 DX= 161.52
 AE= 46.33 K1= 0.51989 K2= 0.78175 DLS= 20.41 ALS= 57.96
 AED= 52.59 MD= 0.26327 AES= 88.08 MS= 0.04351 ADX= 95.11
 D 5.00 10.00 20.00 30.00 50.00
 A 49.47 52.31 57.74 60.49 65.75

F= 50.0 DH=650.00 H1G= 4.00 H2G= 0.55 TE= 1.482328 DX= 163.97
 AE= 68.73 K1= 1.87381 K2= 1.59156 DLS= 11.19 ALS= 91.37
 AED= 86.21 MD= 0.46115 AES= 120.32 MS= 0.25309 ADX= 161.82
 D 5.00 10.00 20.00 30.00 50.00
 A 79.21 89.06 95.43 100.04 109.27

F= 50.0 DH=650.00 H1G= 4.00 H2G= 1.70 TE= 0.305643 DX= 128.35
 AE= 51.08 K1= 1.01365 K2= 2.02007 DLS= 13.48 ALS= 67.03
 AED= 62.71 MD= 0.32004 AES= 95.06 MS= 0.06799 ADX= 103.79
 D 5.00 10.00 20.00 30.00 50.00
 A 57.56 63.23 69.11 72.31 78.71

F= 20.0 DH=650.00 H1G= 3.30 H2G= 1.30 TE= 0.437338 DX= 146.37
 AE= 44.25 K1= 1.52346 K2= 4.18953 DLS= 12.07 ALS= 67.17
 AED= 63.15 MD= 0.33315 AES= 98.92 MS= 0.08873 ADX= 111.91
 D 5.00 10.00 20.00 30.00 50.00
 A 54.80 63.68 69.81 73.14 79.80

Computer Program Output (continued)

OHIO NS=312.

F= 100.0 DH= 90.00 H1G= 4.00 H2G= 3.00 TE= 0.004762 DX= 140.04
 AE= 28.13 K1= 0.47405 K2= 6.72692 DLS= 15.55 ALS= 43.52
 AED= 39.26 MD= 0.27418 AES= 69.81 MS= 0.05598 ADX= 77.65
 D 10.00 20.00 30.00 50.00
 A 39.60 44.74 47.48 52.97

F= 100.0 DH= 90.00 H1G= 4.00 H2G= 6.00 TE= 0.002414 DX= 135.88
 AE= 24.98 K1= 0.38606 K2= 7.13023 DLS= 18.53 ALS= 41.18
 AED= 36.19 MD= 0.26912 AES= 64.94 MS= 0.05754 ADX= 72.76
 D 10.00 20.00 30.00 50.00
 A 35.97 41.57 44.26 49.65

F= 100.0 DH= 90.00 H1G= 4.00 H2G= 9.00 TE= 0.001524 DX= 131.49
 AE= 22.67 K1= 0.34787 K2= 7.23686 DLS= 20.83 ALS= 39.46
 AED= 33.86 MD= 0.26883 AES= 61.55 MS= 0.05821 ADX= 69.21
 D 10.00 20.00 30.00 50.00
 A 33.39 39.04 41.92 47.30

F= 100.0 DH= 90.00 H1G= 4.00 H2G= 3.00 TE= 0.004762 DX= 141.46
 AE= 30.18 K1= 0.30841 K2= 7.99234 DLS= 15.55 ALS= 44.50
 AED= 40.19 MD= 0.27675 AES= 71.43 MS= 0.05598 ADX= 79.34
 D 10.00 20.00 30.00 50.00
 A 41.26 45.73 48.50 54.03

F= 100.0 DH= 90.00 H1G= 4.00 H2G= 6.00 TE= 0.002414 DX= 134.94
 AE= 26.26 K1= 0.23228 K2= 8.41271 DLS= 18.53 ALS= 41.23
 AED= 36.20 MD= 0.27151 AES= 65.07 MS= 0.05754 ADX= 72.83
 D 10.00 20.00 30.00 50.00
 A 36.99 41.63 44.34 49.77

F= 100.0 DH= 90.00 H1G= 4.00 H2G= 9.00 TE= 0.001524 DX= 130.88
 AE= 23.74 K1= 0.22313 K2= 8.49031 DLS= 20.83 ALS= 39.59
 AED= 33.94 MD= 0.27121 AES= 61.81 MS= 0.05821 ADX= 69.43
 D 10.00 20.00 30.00 50.00
 A 34.46 39.25 42.07 47.50

F= 50.0 DH= 90.00 H1G= 4.24 H2G= 1.00 TE= 0.014366 DX= 138.42
 AE= 30.00 K1= 0.61595 K2= 8.93820 DLS= 12.74 ALS= 47.73
 AED= 44.45 MD= 0.25734 AES= 72.89 MS= 0.05189 ADX= 80.07
 D 10.00 20.00 30.00 50.00
 A 45.10 49.60 52.17 57.32

F= 50.0 DH= 90.00 H1G= 4.24 H2G= 3.00 TE= 0.004564 DX= 144.92
 AE= 27.49 K1= 0.39565 K2= 9.59105 DLS= 15.79 ALS= 45.23
 AED= 41.53 MD= 0.23414 AES= 67.33 MS= 0.05610 ADX= 75.46
 D 10.00 20.00 30.00 50.00
 A 41.04 46.22 48.56 53.24

F= 20.0 DH= 90.00 H1G= 3.68 H2G= 3.00 TE= 0.005064 DX= 148.33
 AE= 27.77 K1= 0.19176 K2= 11.81777 DLS= 15.21 ALS= 44.65
 AED= 41.83 MD= 0.18600 AES= 61.14 MS= 0.05580 ADX= 69.41
 D 10.00 20.00 30.00 50.00
 A 41.50 45.55 47.41 51.13

